ENERGY AND SPECTRAL EFFICIENCY AUGMENTATION IN MASSIVE MIMO SYSTEMS

SUPERIOR UNIVERSITY

PH.D. ELECTRICAL ENGINEERING

By:

RAO MUHAMMAD ASIF

ROLL NO: PHEE-S16-003

SESSION: 2016-2019

DEPARTMENT OF ELECTRICAL ENGINEERING

SUPERIOR UNIVERSITY

LAHORE, PAKISTAN

ENERGY AND SPECTRAL EFFICIENCIES AUGMENTATION IN MASSIVE MIMO SYSTEMS

SUPERIOR UNIVERSITY

thesis submitted in partial fulfilment for

the degree of Doctor of Philosophy in

Electrical Engineering

by

RAO MUHAMMAD ASIF

ROLL NO: PHEE-S16-003

SESSION: 2016-2019

SUPERVISOR:

DR. MUSTAFA SHAKIR

DEPARTMENT OF ELECTRICAL ENGINEERING

SUPERIOR UNIVERSITY

LAHORE, PAKISTAN

Copyright © 2021 by Author

Rao Muhammad Asif

Date:

DEDICATION

This thesis is proudly dedicated to……

To our last prophet Muhammad (Peace be upon him), my great hero and messenger of Allah Almighty. One of the most influential men that humanity has ever witnessed.

To my beloved father, Rao Munawar Ali Khan, who has been my source of inspiration and gave me strength, especially when I thought of giving up. My father is the most enthusiastic about supporting all the decisions which I made. He provides me their moral, spiritual, emotional, and financial support throughout my education career.

Rao Muhammad Asif

Date:

RESEARCH COMPLETION CERTIFICATE

It is certified that the research work contained in this thesis report titled **"Energy and Spectral Efficiency Augmentation in Massive MIMO Systems"** has been carried out and completed by **Rao Muhammad Asif** Roll No. **PHEE-S16-003** under my supervision. Therefore, the undersigned hereby certify that they have read and recommended the thesis entitled for the degree of **Doctor of Philosophy in Electrical Engineering**.

EXAMINATION JURY/BOARD APPROVAL:

Sr. No	Name	Role	Signature
1	Dr. Arfan Jaffar	Chair	
2	Dr. Mustafa Shakir	Thesis Supervisor	
3	Dr. Intesar Ahmed	External Examiner-1	
4	Dr. Haroon Farooq	External Examiner-2	
5	Dr. Saif Ur Rehman	Internal Examiner-1	

AUTHOR'S DECLARATION

I, **Rao Muhammad Asif** Roll No. **PHEE-S16-003** student of Department of Electrical Engineering, Superior University, Lahore in the subject of Ph.D. Electrical Engineering Session 2016-2019, hereby declare that the matter printed in the thesis as **"Energy and spectral efficiency augmentation in massive MIMO systems"** is my work and has not been printed, published, and submitted as research work, thesis, or publication in any form in any university, research institutions, etc. in Pakistan or aboard. Wherever contributions of others are involved, every effort is made to indicate this clearly, with due reference to the literature and acknowledgment of collaborative research and discussions. I also declare that this work is the result of my investigations, except where identified by references and free from plagiarism of the work of others.

Signature:

Date: _____

_____
Rao Muhammad Asif

PLAGIARISM UNDERTAKING

I solemnly declare that the research work presented in this thesis titled "Performance evaluation of Energy and spectral efficiencies augmentation in massive MIMO systems" is solely my research work with no significant contribution from any other person. However, small contribution/help wherever taken has been duly acknowledged, and I have written that complete thesis.

I understand the zero-tolerance policy of the HEC and Superior University, Lahore, towards plagiarism. Therefore, as an author of the above-titled thesis, I declare that no portion of my thesis has been plagiarized and any material used as reference is properly referred/cited.

I undertake that if I am found guilty of any formal plagiarism in the above-titled thesis even after awarding of Ph.D. Degree, the University reserves the right to draw/revoke my Ph.D. degree and that HEC and the University have the right to publish my name on the HEC/University website on which names of students are placed who submitted plagiarized work.

Rao Muhammad Asif

Date:

LIST OF PUBLICATIONS

It is certified that following publication(s) have been made out of the research work that has been carried out for this thesis:

Journal Articles:

1. "Energy Efficiency Augmentation in Massive MIMO Systems Through Linear Precoding Schemes and Power Consumption Modeling", *Wireless Communications and Mobile Computing*, Volume 2020, pp: 1-13. DOI: 10.1155/2020/8839088 **(IF: 2.336) (Category: W)**

2. "Performance evaluation of Spectral Efficiency for Uplink and Downlink Multi-Cell Massive MIMO Systems", submitted in *International Journal of Communication, Systems*, **(IF: 2.047) (Category: W, *Under Review*)**

3. "Energy Efficiency Trade-off with Spectral Efficiency in MIMO Systems", *Computers, Materials & Continua*, DOI:10.32604/cmc.2022.020777 **(IF: 3.772) (Category: W)**

Rao Muhammad Asif

Date:

ACKNOWLEDGEMENTS

In the name of Allah Almighty, the Most Beneficent, the Most Merciful. Thanks to Allah Almighty, who is the source of all the information and knowledge in this world, for the strengths and assistance in finishing this research work. I would like to thank all people who assisted me in compiling and completing this research. I express my sincere gratitude to **Prof. Dr. Chaudhary Abdur Rehman** (Chairman Superior Group) and **Dr. Sumaira Rehman** (Rector Superior University) for their invaluable leadership and inspiration throughout my educational tenure at Superior University.

I heartedly thank my supervisor, **Dr. Mustafa Shakir,** for his precious discussions, encouragement, and guidance through all phases of this work. I gained tremendous experience in research work with him. His supervision was always a great privilege and honor for me.

I am also obliged to my mentors, Pirzada Sami Ullah Sabri, Capt. Sajjad Mehmood and Mr. Adnan Yousaf, whose motivation and inspiration boosted me towards adopting the accurate route. During the Ph.D. Studies, I cannot thank them enough for their support and motivation verbally.

I want to acknowledge all faculty and staff members of Superior University, Lahore, to provide a supportive and working environment. I am very thankful for my teachers, especially Mr. Muhammad Aslam Ahsan (LATE), who have inspired me with their insightful guidance and comments. All my teachers provided me a carefree environment to help me maintain the focus on my study. In the end, I am very grateful to Ateeq Ur Rehman for their motivation throughout my research work.

In the end, I am so grateful to my mother for her prayers and loving heart to me. Even though she does not know what is research writing is and what my area of research. May Allah Almighty give them good health and keep them safe. Finally, to my elder brother Rao Saqib, my wife, younger brothers, sisters, and relatives who directly or indirectly encouraged me to this work, their kindness means a lot to me. Thank you all very much.

Rao Muhammad Asif

Date:

ABSTRACT

The first section of the thesis is based on realistic and technically implementable energy efficiency (EE) model for massive MIMO systems. Linear processing approaches such as zero-forcing (ZF), minimum means squared error (MMSE), and maximal-ratio-transmission (MRT) are utilized for detection and precoding. In addition, a power dissipation model that takes account of overall power usage in uplink (UL) and downlink (DL) communications is also modelled. The proposed model includes the general power consumed by the power amplifier (PA) and circuit components at the base station (BS) and single-antenna user equipment (UEs). The optimal number of BS antennas to support the total number of UEs is also calculated. The simulation findings confirm significant gains in area throughput and EE. It also indicates that the optimum area throughput and EE may be obtained when more antenna arrays at BS are built to support a more significant number of UEs.

The second portion of the thesis presents a practical model that augmented the Spectral Efficiency (SE) of massive MIMO systems using a multi-cell model scenario. First, channel estimation is performed at BSs using UL transmission. Simultaneously, the minimum mean-squared error (MMSE), element-wise MMSE, and least-square (LS) estimators are used. The feasible SE of the UL is next examined using the MMSE channel estimator with various received combining techniques. Moreover, the DL transmission model is also modelled with different precoding schemes using the same vectors used in combining schemes. The simulation results show a significant improvement in SE by developing UL and DL transmission models. It is also realized that the average sum of SE per cell is improved by optimized MMSE channel estimation, installing multiple BS antennas, and serving multiple UEs per cell.

In 3rd part of the thesis, an optimal solution for tradeoffs of SE and throughput with EE has been presented. The research work is based on the Wyner models of UL and DL transmission models, where a multi-cell model scenario is considered. The tradeoff of SE-EE is carried out by optimizing the selection of antenna and UEs, while the logarithm function-based approximation method is used for the optimization. The author analyzes the combining and precoding schemes for the UL and DL power consumption modeling with all realistic circuit power consumption models to optimize

the tradeoff between EE and throughput. The findings of the simulation demonstrate a significant improvement in SE-EE trade-offs by establishing suitable UL and DL transmission models and logarithm-function based approaches. The trade-off between performance and EE can also be strengthened by knowing the entire realistic energy utilized by the network.

TABLE OF CONTENTS

LIST OF TABLES

LIST OF FIGURES

LIST OF ABBREVIATIONS

ADC	Analog to Digital Conversion
AF	Amplify & Forward
AWGN	Additive white Gaussian noise
AQNM	Additive Quantization Noise Model
B5G	Beyond 5G
BBU	Base-Band unit
BER	Bit Error rate
BS	Base Station
BMAA	Building-Mounted Antenna Array
CPU	Central Processing Unit
CSI	Channel State Information
C-RAN	Cloud- RAN
D2D	Device 2 Device
DRAA	Distributed Resource Allocation Algorithm
DL	Downlink
DoF	Degree of Freedom
EE	Energy Efficiency
EELCA	Energy-Efficient Low-Complexity Algorithm
GASEE	Global Average Secrecy EE
Gbps	Giga Bytes per Second
GP	Geometric Programming
Het Nets	Heterogenous Networks

HPN	High Power Nodes
IAP	Indoor Access Point
ITU	International Telecommunication Unit
IoT	Internet of Things
LED	Light Emitting Diode
LS	Least square
LOS	Line of Sight
MAC	Multiple Access Channels
MIMO	Multiple-Input & Multiple-Output
ML	Maximum Likelihood
MMSE	Minimum Mean Squared Error
MRT	Maximum Ratio Transmission
MBSALA	Micro-based Station Antenna Array
NSE	Neumann Series Expansion
OMP	Orthogonal Matching Pursuit
PA	Power Amplifier
QoS	Quality of Service
RAN	Radio Access Network
RF	Radio Frequency
RR	Round Robin
RRHs	Remote Radio Heads
SCA	Successive Convex Approximation
SE	Spectral Efficiency
(SM)	Spatial Modulation

STBC’s	Space Time Block Codes
SKEE	Secret Key EE
SWIPT	Simultaneously Wireless Information and Power transfer
TDD	Time Division duplexing
UC	User Centric
UE’s	User Equipment’s
UL	Uplink
ZF	Zero Forcing

LIST OF SYMBOLS

$\|.\|$ *and* $\|\|.\|\|$	*Absolute values and Euclidean norm*
I_K	K × K identity matrix
0_K and 1_K	K-dimensional null and unit column vectors
$\mathcal{CN}(.,.)$	Multi-variant circularly symmetric complex Gaussian distribution
T_{coh} & B_{coh}	Coherence Time & Coherence Bandwidth
S_{CB}	Coherence time-frequency ($S_{CB} = T_{coh} * B_{coh}$)
$\gamma^{(UL)}$ and $\gamma^{(DL)}$	Constant transmission ratio symbols (UL & DL)
S_{CB}* $\gamma^{(UL)}$	UL transmission
S_{CB}* $\gamma^{(DL)}$	DL transmission
$\mathbb{E}(.)$	Expectation
$\boldsymbol{I}_K$	K × K identity matrix
Ψ	Pilot signal sequence
n_j^{dl}	additive receiver noise
B	Bandwidth
T_{coh} & B_{coh}	Coherence Time & Coherence Bandwidth
$w_{lr} \in C^{M_l}$	Assigned as transmit precoding vector
$y_j^{UL} \epsilon \mathbb{C}$ and $y_j^{DL} \epsilon \mathbb{C}$	Transmission symbols (UL & DL)
$\frac{\tau_{UL}}{\tau_{coh}}$& $\frac{\tau_{DL}}{\tau_{coh}}$	UL transmission & DL transmission pre log factor
β_r	Ratio of Inert cell and Intra cell channels gain
$H_l^l \in \mathbb{C}$	Channel Response
n_l^{UL}	Noise in UL
O_{M_j} and σ_{UL}^2	zero means and variance

n_j^{dl}	Additive receiver noise in DL
B	Bandwidth
ρ_{UL}	Transmit power
σ_{UL}^2	Noise power
$p_{UL}\beta_l^l$, $p_{UL}\beta_j^l$	Signal power and interference power
CP_l	Circuit power
μ	Power amplifier efficiency
P_{fix}	Fix power consumed
P_{tran}	Transceiver power consumed
P_{ch}	Channel estimator power
$P_{c,d}$	Consumed power by coder/decoder
$P_{L,bH}$	Load dependent consumption
P_{DSP}	Digital signal processing power

CHAPTER 1

INTRODUCTION

Massive MIMO systems offer the viable potential for mobile communication systems of the 5th generation (5G) since they can improve the area throughput and energy efficiency (EE) [1]. Massive MIMO systems have become the most persuasive technology for 5G as it increased the EE gigantically compared to other wireless communication systems. Wireless networks are fully occupied with high traffic demands as the cellular systems are installed within a few meters to raise needs [2]. Machine-to-machine communication and the internet of things (IoT) are promising concepts of the high data demand, while smartphone applications are also reasons for elevation in enormous wireless traffic. More facilities like live games, video calls, Facebook, Twitter, WhatsApp, and many other social media services have dramatically changed the scenario. It is causing transitions from third-generation (3G) to 5G since low latency is required with a high data rate. As reported in [3], the data needed for smartphone services are ten times increased in the latest five years. Figure 1.1 shows the annual growth of mobile data and the number of devices used for this purpose.

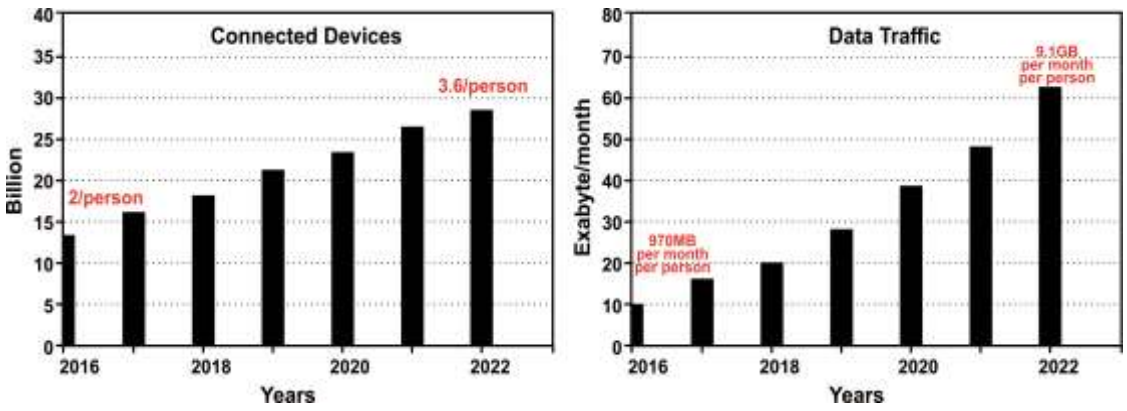

Figure 1.1 *Annually growth of mobile data and numbers of devices from 2016-21 [3].*

The immense volume of data traffic has become a challenge for the already installed infrastructure. Massive MIMO is an extension of MIMO systems. It becomes a fascinating technology to fulfil the current rising needs by providing thousands of antennas to Base stations (BSs) since it contributes towards augmenting Spectral Efficiency (SE), EE, and throughput. This technology caters to all the necessities

required for ultra-high capacity and speed for 5G through carrying multiple antennas, radios, and greater spectrum at the same time [4]. Massive MIMO is distinguished by the enormous array gain attained by an enormous number of antennas. Mobile networks have famed marvellous evolution in the last few years as they advanced from 1G to 5G and beyond, as shown in Figure 1.2. It is an impressive growth in mobile technology, while the era started in the early 80s.

These wireless networks are developed with the BS and User Equipment (UE), whereas both are rapidly advanced in technology, as seen in Fig 1.3. The 5G mobile technology will be implemented 100 times faster than the existing 4G technology since it offers high data rates up to 10 Giga bytes per second (Gbps) [3]. It enables IOTs networks, smart vehicles, and many other smart applications.

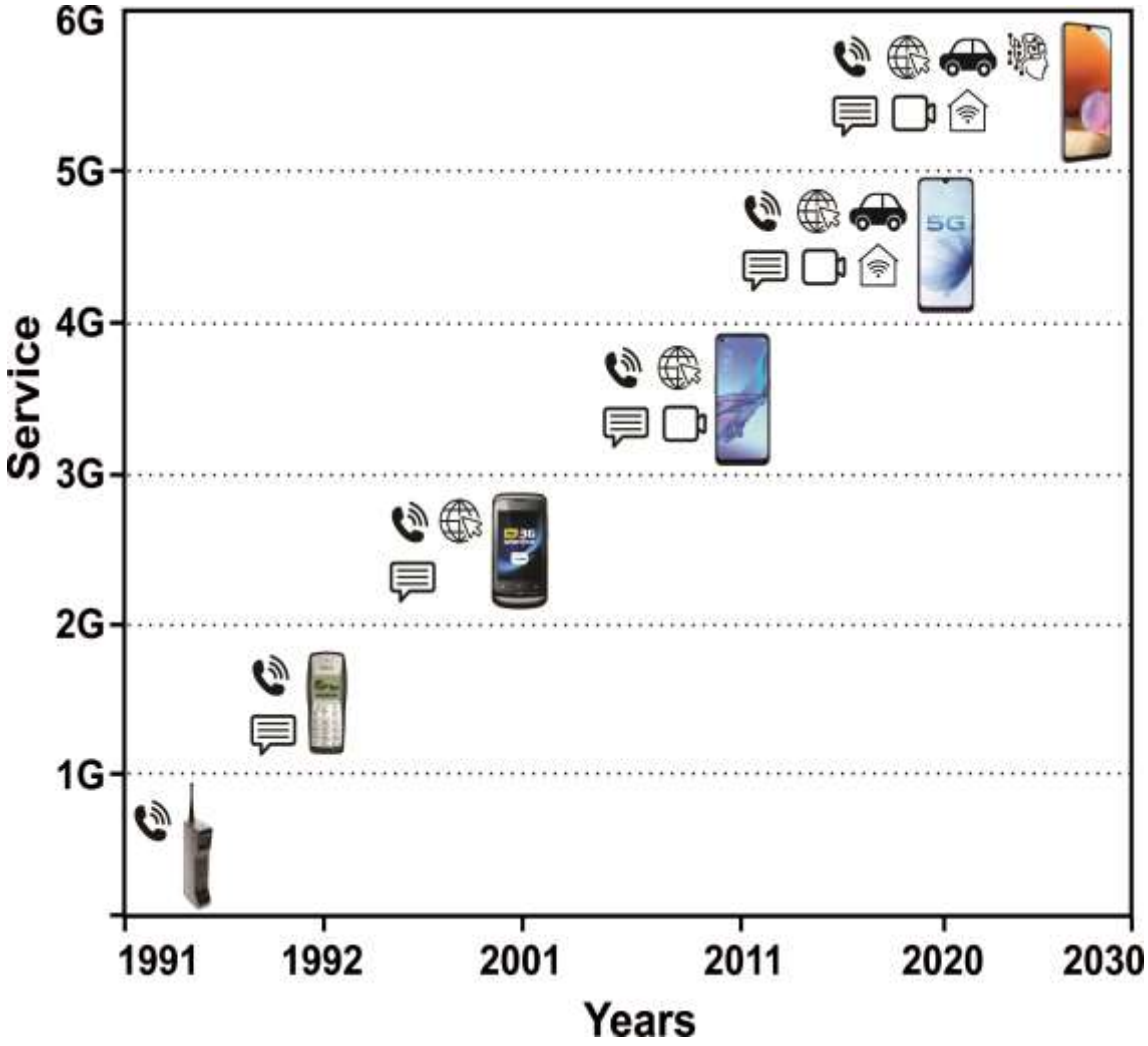

Figure 1.2 *Rapid advancement in mobile communication from 1G to 5G and beyond.*

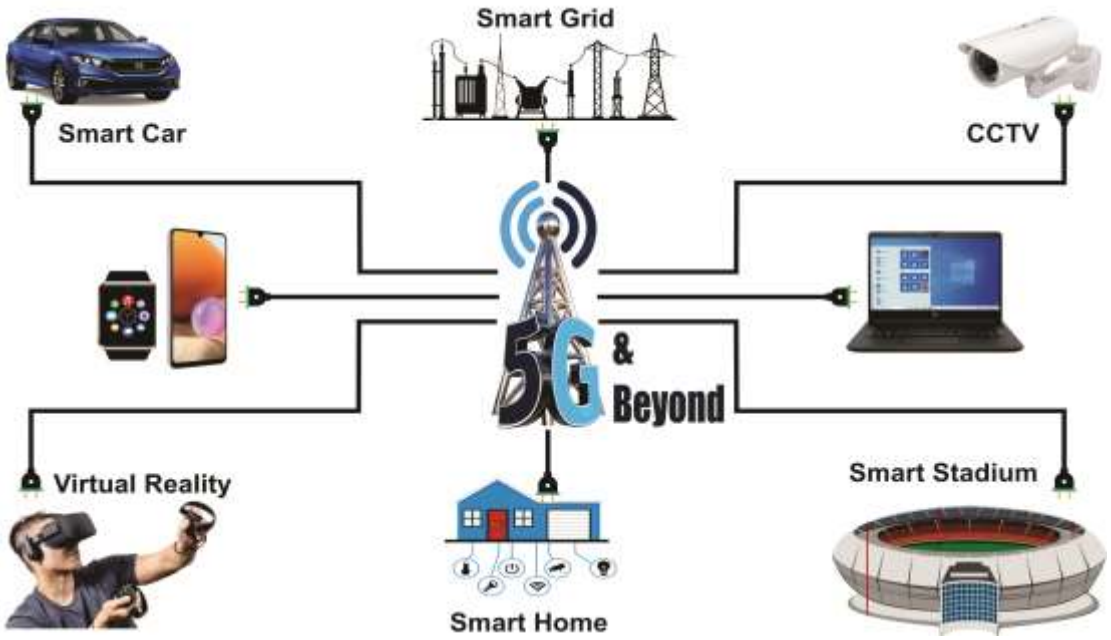

Figure 1.3 *Illustration of factors reasoning to rapid growth in data traffic.*

5G technology becomes an efficient wireless network with massive throughput at the same bandwidth to cater to high traffic demand. The primary concern with the existing wireless networks is optimizing the bandwidth or densifying the cells to achieve the required throughput [5]. Meanwhile, the EE is also becoming primary since the SE) and throughput reaches their maximum limits. On the other hand, optimizing SE and throughput increases the latency and cost of the hardware setup. Unfortunately, these are unchanged even with the rapid growth of wireless networks [6]. Therefore, 5G communication networks have created wonders in the progress of wireless communication technology, as shown in Figure 1.3. The reason is that it increases the SE and throughput enormously compared to the other technologies [7]. This research work is based on the optimal model development of energy-efficient massive MIMO systems as the most vibrant research technology. In this regard, massive MIMO technology becomes the most influential technology for 5G due to enormous antennas and UEs. Ultimately, it raises the circuit power consumption and reduces the EE [8].

1.1 Background

In 5G, BS of a massive MIMO system is equipped with many antennas to provide the advantage of SE and EE, but it leads to increases in cost and energy consumption of

UEs [9], [10], [11]. The selection of multiple antennas is the latest need of a massive MIMO system. The example of massive MIMO systems is shown in Figure 1.4. The BS of MIMO systems consists of M numbers of antennas as M>>1 having a single UE antenna. The received vector y is denoted as [12] :

$$y = Hx + n \tag{1.1}$$

Where y is used for $[y_1, y_2, y_3, y_4 \dots\dots\dots\dots\dots y_M]$ is the signal vector as shown in Figure 1.4. The channel matrix is $H \in \mathbb{C}^{M\times K}$, and $x \in \mathbb{C}^K$ is a transmitted symbol for K users. Additive white Gaussian noise (AWGN) denotes as $n \in \mathbb{C}^M$ followed by $n \sim \mathcal{CN}(0, \sigma^2 I)$

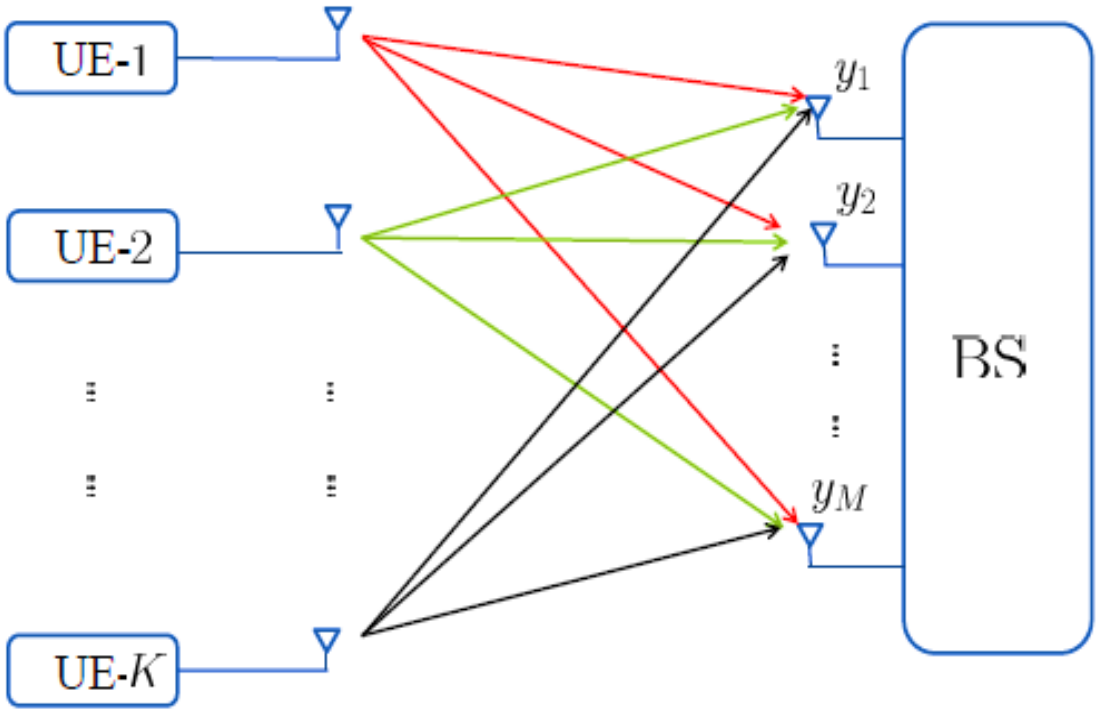

Figure 1.4 *Illustration of massive MIMO systems [12].*

Massive MIMO is a multi-user MIMO technology, serves the users with K single-antenna on the same time-frequency resource through BS. This BS is usually equipped with a large no. of M antennas, i.e., M >> K, as shown in Figure 1.5. Generally, in a massive- MIMO scheme, UEs are supported with many antennas. But, in [13], a simple analysis with one antenna UEs is done. The installation of too many antennas at BS

causes favourable propagation, and the channel becomes more deterministic. The reason is that the radio link between BS and the user~~'s~~ equipment becomes orthogonal to each other. It happens because the impact of small-scale fading disappears asymptotically in an enormous M system. Essential EE gain can be attained in favourable propagation as realizing multi-order multiplexing and array gain. In this regard, both uplink (UL) and downlink (DL) transmission are considered in a multi-cell massive MIMO.

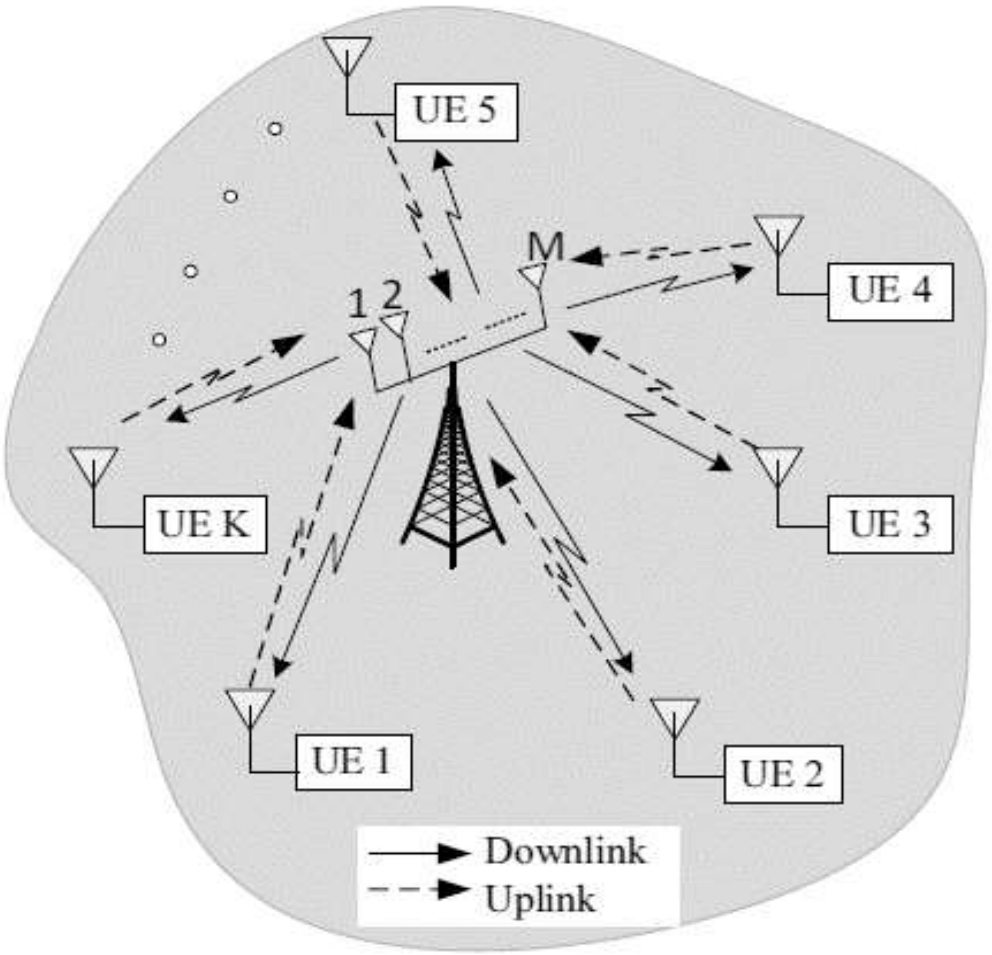

Figure 1.5 *A multi-user MIMO scenario where K as single-antenna and UEs are served by a BS with M >> K antennas [14].*

The equation below shows the asymptotic Shannon capacity for UL and DL by taking multiple user MIMO channels in favorable propagation [14].

$$C_{UL} = \sum_{k=1}^{k} \log_2(1 + p_{u,k} M \beta_k) \tag{1.2}$$

$$C_{DL} = \sum_{k=1}^{k} \log_2(1 + p_{D,k} M_{ak} \beta_k) \tag{1.3}$$

Where: $p_{u,k}$and $p_{u,k}$ Notifies SNR of UL and DL for kth UE. $\beta_k$signifies large scale fading coefficients for K^{th} equipment, and a_k Shows an optimal vector to find DL. For more simplification, the effect of β_k can be neglected. Now, assume that each user equipment transfers average SNR PU; therefore, Shannon capacity simplifies into equation [14].:

$$C_{UL} = Klog_2\,(1 + M_{pu}) \tag{1.4}$$

The same equation can be obtained for DL transmission as above. Equation (1.4) has led us to the following observations

- The system's input and output can be enhanced by raising the K or by multiplexing parallel creeks of data to many UEs at the same time-frequency response.
- Power of transmission per UE can be lower down by increasing M or increasing BS antennas.

The definitions of basic terms are:

Definition 1: "The total number of bits successfully sent per kilometre travelled in 1 second is referred to as area throughput, which is measured in bits-per-Joule". [15].

$$Area\ throughput = \frac{(Available\ data\ rate)}{(Area\ of\ cell)} = \frac{\left(\frac{bits}{sec}\right)}{km^2} \tag{1.5}$$

$$T_{Put}(\gamma) = T_{put}, \frac{max}{N_T} \sum_{i=1}^{N_T} (1 - \mathrm{P}(\gamma_i)) \tag{1.6}$$

$T_{Put}(\gamma) = T_{put}$ defines as maximum throughput that has to be achieved.

Definition 2: "The total bits sent successfully by the consumption of an energy joule is known as Energy Efficiency measured in bits/per/joule [15]. EE depends on numerous massive MIMO systems parameters, i.e. SE, network architecture, power consumption, and transmission protocol. [16]".

The definition of SE is [15].

"The average numbers of bits containing information per complex sample which a channel can reliably transmit under given considerations is called SE".

BS and UE architecture, the power is consumed by power source, cooling network, backhaul connection, and other control equipment that have a viable impact on the characterization of EE for the next-generation 5G network.

1.2 Objectives

This thesis has the following three objectives:

- Linear Precoding Schemes and Power Consumption Modeling are computed for EE enhancement in Massive MIMO Systems. The power amplifier and analogue circuit consumption are also computed.
- Performance evaluation of SE for UL and DL in Multi-Cell Massive MIMO Systems is evaluated. In addition, the SE is enhanced by using combing schemes and precoding schemes for UL and DL transmission, respectively.
- EE trade-off with SE and throughput is optimized based on the Wyner models of UL and DL transmission models where a multi-cell model scenario is considered. Power consumption models, optimal numbers of antenna and user equipment are also computed.

1.3 Main Contributions

The significant contributions of the thesis are given below:

In the first part, mathematical models of linear precoding schemes and power consumption are optimized for EE augmentation. In this regard, a canonical system is considered for the single cell scenarios.

A realistic model is proposed in the second part that augmented the SE of massive MIMO systems where a multi-cell model scenario is considered. Furthermore, the DL transmission model is also modelled with different precoding schemes by taking the same vectors used in combining schemes for the UL transmission.

In the third part, optimal EE Trade-Off with SE and throughput for Massive MIMO systems are evaluated. The trade-off of EE with SE is obtained from the optimal selection of BS antennas and UE. Throughput is optimized through the computation of power consumption modelling.

1.4 Used Environment

This thesis model is simulated in a MATLAB simulation environment on a research workstation with Intel Core i5-6100U, 8GB RAM, 64-bit operating system, and 2.50 GHz Processor.

1.5 Structure of the Dissertation

In this chapter, a general overview of massive MIMO systems, the latest trends of wireless networks, EE, SE, and throughput in massive MIMO are briefly introduced. In addition, the thesis contribution and highlights of each chapter are also elaborated.

In the 2nd chapter, a survey of related work is explained. The key feature of the previous work is summarized in tabular form. The latest trends and approximation methods used for the augmentation of EE are particularized while combing and precoding schemes with power consumption models used by researchers are also considered. The SE enhancement schemes are deeply analyzed, and key factors are elaborated as well. The latest articles related to the tradeoff of EE with SE and throughout are summarized in the end.

This thesis's third chapter depicts the standard of massive MIMO networks for both UL and DL transmission. It also discusses the user distribution and linear precoding techniques. Linear processing approaches, as earlier mentioned in the chapter, are employed for detection and precoding. It later contains all essential mathematical modelling and computations of the data rate and power utilization model. M, N, power, area throughput, and EE optimization are all articulated. Furthermore, the results are described in order to validate the theoretical analysis and draw comparisons between the proposed model and current studies using predefined linear processing approaches.

In the 4th chapter, the computed results of proposed models are appropriate to endorse the massive MIMO systems that can enhance SE in a 5G cellular network. It illustrates the proposed model for both UL and DL communication while the UL SE with the MMSE estimator is compared with EW-MMSE and LS. In the end, the maximum-ratio (MR) precoding scheme is modeled for the augmentation of DL SE.

In the 5th chapter, the model for a tradeoff between EE and SE for UL and DL where the Wyner model is considered for the approximation and logarithm function-based approximation methods is used for the optimized tradeoff. It investigates EE-SE tradeoff by keeping in view the Wyner model for two cell scenarios and computed optimized relation to select multiple antennas and UEs. The chapter also includes the computational model to compute the complete realistic power and examined the combining and precoding schemes for UL and DL networks ultimately. Finally, it refers to the optimized tradeoff between EE and throughput. In the end. The results discussion with model validation and conclusion are briefly particularized.

In the 6th chapter, a discussion of the conclusion is drawn from this research. The extension of future work is also examined.

CHAPTER 2
LITERATURE REVIEW

2.1 Introduction

As earlier mentioned, Massive MIMO is a system in which the transmitter utilizes many antennas and serves multiple users at one time under the same frequency resource. It is considered a favourable technology for addressing challenges in next-generation networks, i.e.,5G.[67]. The framework and analytical study of a massive MIMO system is an innovative area of research [68]. However, its practical implementation faces many challenges which still need to be solved. Higher data rates can be achieved if BSs communicate under the same frequency or time resources with the end-users. The data transmission in the DL network of massive-MIMO causes inter-user interference and needs high transmission power. Therefore, interference cancellation at every BS is necessary [19]. EE and ES massive MIMO systems and the system model used in this thesis are introduced to review the corresponding EE issues in massive MIMO design. The representative EE and SE studies relevant to channel fading, signal processing, and power consumption are reviewed in Sections 2.4, 2.5, and 2.6, respectively. The trade-off of EE with SE and throughput is explained in section 2.8. The summary of this chapter is highlighted in the last section.

2.2 Energy-Efficient Massive MIMO Systems

5G communication networks have a high EE, smooth connectivity, and lower latency, and it helps us create a bridge and secure point-to-point communication. Heterogeneous networks (HetNet) have multiple BS, which establishes a mother network that depends upon the coverage network, ultimately expanding the capacity and providing a cost-effective way for users [20]. In recent years, these networks have saved energy consumption for a future wireless system by consisting of nodes with different parameters like coverage size and transmission power. High power nodes (HPN) are installed in urban and semi-urban areas due to their extensive coverage size, while there is a low power node is deployed in small coverage areas. It is also used to improve the

EE of the system as compared to HPN. Two ways are reported to increase the system capacity with the same EE, the first one is the different cell sizes, and the second one is the user density of the system. EE can be improved by increasing the density of the BS, but small cells are the best solution for EE formation [21].

MIMO technology is used for outdoor and indoor communication using 6 GHz frequencies for long-distance high data rates. Beyond 5G (B5G) technology is deployed to separate indoor and outdoor communication in ultra-dense networks. Meanwhile, it becomes a network architecture that separates indoor and outdoor transmission and supports a high data rate for less energy consumption than the non-separate scenario [22]. 5G systems are designed to improve system capacity, SE whereas, 5G and B5G networks combine macro, Pico, and small cell for the efficient wireless ultra-dense networks. Alongside, loss of mm-wave and small coverage of LiFi reduce the efficiency of an indoor access point (IAP) fixed in the neighbour rooms and buildings. A-line of sight (LOS) path with a sub-6 GHz frequency band is used for communication between a micro-based station antenna array (MBSALA) and a building-mounted antenna array (BMAA). Besides that, LiFi technology balance the data through a light-emitting diode (LED) and supports high-speed wireless communication using illumination [23].

5G utilizes high bandwidth and has a greater capacity than 4G, but maximum EE is achieved by increasing and decreasing the system's power consumption. Maximum EE is accomplished by combining the small cell access points to a massive MIMO system. Moreover, the BS and a small cell access point are combined for designing of EE system. Meanwhile, 5G have a data rate of 100 Mbps for billions of users in which user have equal access of data with an increment of SE. In this way, power consumption can also be minimized by supporting quality of service (QoS) [24]. The system proposed in [25] provides a high data rate at the same power per subcarrier under the consideration of two path loss models. The total power consumption of the BS and small cell access points is also erratic according to the number of antennas at the BS.

2.3 Energy and Spectral Efficienc Augmentation

In the MIMO system, the number of antennas equipped with multiple radio frequencies is impractical for EE. Therefore, hybrid precoding techniques instead of full digital precoding are installed more energy-efficient and achieve better SE. Moreover, it has a point-to-point transmission to minimize the Euclidean distance between the hybrid and fully digital precoder [26]. Researchers used orthogonal matching pursuit (OMP) system to get a hybrid precoder and fully connected structure to resolve hybrid beamforming design. The alternating minimization (MO-AltMin) scheme was used for the matrix factorization problem. Furthermore, the category of hybrid precoding involved joint iterative and non-uniform quantization schemes to get a low-resolution shifter [27]. On the other hand, hybrid precoding with high resolution provides a solution using the additive quantization noise model (AQNM). The expression SE for point-to-point mm-wave using Buss-gang theorem and AQNM are computed, and hybrid precoding gets maximum adjustment between the SE and EE [28]. In device-to-device (D2D) MIMO wireless communication, the distributed access point uses small cells in the DL and is established by UEs. It can transfer data with or without the involvement of the BS [29]. As earlier mentioned in the chapter. 1, the SE is known as efficiently transmits the number of bits, and spectrum information ultimately improves the EE and SNR. In the contest of wireless D2D communication, the distributed resource allocation algorithm (DRAA) is more suitable than a centralized resource allocation algorithm used in drone communication and self-driving vehicles [30].

An energy-efficient two-way MIMO amplifier and forward Amplify and Forward (AF) relay system is designed [31]. It used the precoding method to improve the energy loss MIMO systems. The precoding matrix was in closed form, and the numerical method confirmed these matrices' efficiency. The energy-efficient 5G antenna is designed, which is set by the international telecommunication union (ITU) [31]. The relay-based communication methods have been further proposed by [32], where multiple proposals like amplified and forward (AF), decode and forward, or compress and forward are discussed. AF provides a break for the development interval on a one-way MIMO-AF system from a single relay by using precoding techniques that have been spread to many other matrices and other scenarios [32]. Basically, in one-way communication, the relay

is used for two nodes in one direction, and in two-way communication, SE is twice larger as one-way communication.

Researcher studies in [33] about EE, physical layer security of multi-user massive MIMO systems is discussed. Secure information transmission is based on an increment of secrecy rate by increasing transmit power. Secret key energy efficiency (SKEE) combines cryptographic and physical layer security, defined as the ratio of secret-key capacity and consumed power [34]. The co-located and distributed massive MIMO are primarily used for physical security systems and improve the secrecy rate by transmitting artificial noise (AN) when the number of a user is much less than the number of the antenna. Global average secrecy energy efficiency (GASEE) measures EE performance in a multi-user wiretap system [35]. 5G communication is the tool of multiple antennas to improve SE, robustness, and reliability while it increases power consumption. It raises the problem of designing wireless network systems. Nakagami-m fading channel is used to minimize the conflict in different distributions and classified as hybrid and co-located distribution [36].

The conversion of channel conditions develops an efficient MIMO wireless communication system for a BS according to their user and QoS requirement. Moreover, power consumption and EE of the BS can be improved by using an effective strategy including zero-forcing, beamforming, and perfect channel [37]. Although unimodal and user data rates increase for maximum EE, unimodal is average EE per BS. Still, it increases the data rate that leads toward the loss of average EE. Moreover, the linear precoding schemes of channels must be efficient with DL and UL pre-coders due to the effect of inter-user and improper noise.

Furthermore, large array and multiplexing gain also enhanced the SE and EE, where a BS is equipped with a large antenna array to develop the orthogonal channel pairwise among users. Besides that, a massive MIMO system reduces the transmitted power of the BS and terminal. However, most power is consumed at DL used by the cooling system and PA at the BS [38]. Therefore, it can be reduced by decreasing the radio frequency (RF) of transmitted power. Therefore, data rate and maximum outage are two main factors for user QoS demand. Moreover, power consumption increases traffic load for that power consumption that could be managed in green communication.

Cell-free Massive MIMO uses the access point with the central processing unit (CPU) using wireless microwave links. Work proposed in [39], SE is analyzed by estimating and quantizing channel error where internal problems are divided into two sub-domains: receiver filter coefficient design and power allocation. The first sub-domain problem is developed as an eigenvalue problem. Still, the second one is converted into geometric programming (GP) problem by using successive convex approximation (SCA) and sub-optimal scheme [40]. Moreover, the 5G radio access network (RAN) has a wide range for users to meet SE and EE's improvements [41]. Although, MIMO and Cloud- radio access network (C-RAN) is the key factor of the 5G system. At the same time, the C-RAN distributes remote radio heads (RRHs) across the coverage area and processing the baseband at the base-band unit (BBU) [42]. Besides that, C-RAN helps the networks to implement the RANs without inter-cell interference and combine MIMO and C-RAN technology using a coordinated multiprocessing point. Newton and Lagrange's decomposition methods solve the power allocation problem in closed form to decrease the power involvement in EE and data rates. Meanwhile, maximum EE expression is computed for many antennas at the BS using an energy-efficient low-complexity algorithm (EELCA). In another scenario, the power consumption cost is increased by loss in the RF chain [43]. However, the communication system demand has solved channel variations and inter-user interference for a large number of antennas to get strength. Although, a large number of the antenna increases system capacity at the transmitter side with a restricted number of active users. The BSs allow the user to get channel state information (CSI) according to channel gain, where maximum EE is dependent on BS. The study shows the BS in the MIMO system consists of many antenna arrays due to a high range of radiofrequency chains, which increases the power consumption that consists of the circuit and transmitting power consumption. In the research, RF chain power consumption increases in digital to analogue conversion, power amplification, multiplexing, and signal filter [44]. EE becomes a more significant concern for any communication system in this era. This study gives the solution to maximize the EE of DL using power allocation with perfect channel state information (CSI). Furthermore, the author improves energy and SE using power amplification, and the power allocation algorithm depends on zero-forcing (ZF) by turning off the RF of sedentary antennas [45].

A model of low quality and cheap hardware with analog to digital converter is proposed based on the low resolution [46]. The models are dependent on the implementation of hardware and parametric analysis as a function of analogue to digital conversion (ADC) resolution for UL-EE. The range of 4-8 bits by scaling antennas and decreasing ADC resolution, the EE is increased with deduction of bit resolution by coupling antennas scaling and degrading ADC resolution [47], [48]. The use of linear processing in UL and DL indicates that the performance and power consumption are strongly connected with an inverse relationship between hardware quality and the number of antennas. Therefore, the power dissipation of ADC is enhanced in linearity due to the sampling rate, but it has the concern of cheaper BS. However, the low average bit resolution with low SNR is used at a large number of antennas and EE. Although, it is maximized by the value of ADC resolution depend on the energy consumption block on the receiver side. The ADC resolution is determined by the number of a user when the number of antennas is increasing.

If the numbers of users are kept constant, the optimal resolution decreases if the user has linearly increased the optimal resolution. The modulation schemes use UL and DL data transmission at both sides of the novel transmitter and receiver, depending on the user terminal's energy-efficient hybrid architecture. The analogue circuit has divided into two stages: phase shifter and analogue switches, respectively. Phase shifter stages overcome the path loss of outdoor mm-wave. Using high gain and analogue switches smartly allows the antenna and combine the spatial correlation using a phase shifter. In addition, it increases the EE by reducing the complex algorithm of beamforming and combining UL and DL [49].

As earlier mentioned in [3], the number of connected devices is reached in tens of billion in 2030 where it increases the demand of average data rate up to 1000 times compared to the present network. The existing networks have a bandwidth shortage in a low-frequency band, which moves towards the high frequency (mm-wave) band such as massive MIMO systems. Therefore, MIMO technology provides a solution to the challenges of several path losses and sensitivity of blockage by increasing the number of antennas [50]. IT encourages the trade-off between antenna gain (AG) and degree of freedom (DoF). Meanwhile, the large number of antennas increases the complexity and bandwidth usage required by the precise CSI problem [51]. It is solved by the channel-

based estimation and low complexity-based algorithm. Besides that, a large number of antennas with digital architecture cannot be implemented due to space limitations and power consumption. On the other hand, hybrid beamforming achieves a high data rate than analogue beamforming [52]. The spatial modulation (SM) technique is developed to reduce the cost, power consumption, and several RF chains [53].

2.4 Power Consumption Modeling

Researchers have developed an interest in low-cost and energy-efficient MIMO systems with low-resolution (ADCs) in massive MIMO systems. The low-cost hardware brings signal distortion and quantization error and reduces the communication quality. Meanwhile, a maximum ratio combining receiver schemes is derived by [56] for accurate approximation of UL SE where all ADC is considered to have the same resolution. Although, AQNM is used for additive and independent noise to close the ADC quantization error [57]. In the future, UEs could serve simultaneously using a massive antenna at the BS for a cellular communication system.

With the rapid increase of world technology, with the same aspects, the MIMO technique becomes an exciting technology with minimum cost and better efficiency with low-resolution ADC [58]. Communication quality decreases due to low cost, and the number of antennas enhances the quality of signals. High frequency reduced the signal-to-noise ratio (SINRs) [59]. Many signal distortions decrease the date rate for UL and DL transmissions. To remove the noise in analogue to digital converter, ADC and AQNM are adopted that provide better results in communication networks [60].

The drawback of a high SE system is the complexity and power consumption. In this regard, SM reduces the complexity of the transmission system while EE is improved by CSI [61]. The transmitter end has multiple antennas to enhance system reliability using automatic repeat request (ARQ) feedback. This system has a single RF chain, PA, and multiple antennas to transmit data efficiently. Meanwhile, ARQ, chase combining hybrid automatic repeat query (CC-HARQ), and incremental redundancy(IR)-HARQ techniques are used to transmit information with their positive and negative acknowledgement (ACK), respectively [62]. Although, exponential growth in wireless data traffic can’t be secure by using a current cellular network. 5G network with uniform coverage, high reliability, and low latency can improve the system capacity.

Massive MIMO provides significant gain multiplexing by the channel estimation of single and multiple users. BS with numbers of antennas send pilot signals using MRT or ZF precoding techniques to simultaneously serve tens of users [63]. Therefore, the power consumption of the circuit increases in hardware size, and EE optimization can't be obtained by time diversity for the power consumption model and specific model parameters [64].

Massive MIMO technology faces difficulties by rapid growth in the number of users and demand. In wireless technology mobile phones, the user increases the multimedia needs, requiring more data rates and a better network. For that case, the CSI method used in [65], the Time-division duplexing (TDD) mode, is also deployed for better spectral and EE. To overcome the noise and protection of system losses, the signal strength space-time block codes (STBCs) are used to secure the system by reducing the SINRs [66]. The pilot contamination method is also introduced in cellular networks to improve the data traffic management system in terms of social and economic [67]. The power consumption in UL and DL transmission is model in [68].

$$P = P_{PA} + P_C + P_{sys} \tag{2.1}$$

Where P_{PA} Implies total power consumed by P_{PA} and UE's at BS for UL and DL. P_c is the total circuit power consumed by various analogue and digital signal processing signals for UL and DL at the BS and user's equipment [68]. P_{sys} involves rest of system's dependent component P.

P_{PA} Rationalizes the total sum of power expense on RF transmission and Pc contains total consuming power from RF chain component es, e.g. filters, mixers, synthesizers, and baseband operations, named digital up/down conversion, precoding/receiver combination, channel coding/decoding, and channel estimation. It is to be noted here that a P_C It cannot be modelled as common practice or as a fixed-term free of M, K. This is because the hardware deployment and its operational circuitry demands grow with growing values of M, K. For example, taking unit RF chain per antenna employed in the existing LTE system increases the numbers of RF chains at BS and UE. Moreover, the mathematical calculation necessity for different base band operation is taken as a function of M and K [69].: such as M, K operation are needed for ZF pre-coding, M, K for MRC detection, M, K for minimum mean squared error (MMSE) channel

estimation, and O(K) for channel coding, respectively. That is why the practical model may take power consumption as a function of M, K and change in PC with M, K might be analyzed in the middle of designing the energy-efficient massive-MIMO system. Finally, P_{sys} Justifies consumed power by site-specific and architecture-specific parameters, e.g. BS and UE architecture, Power source, cooling network, backhaul connection, and other control equipment. P_{sys} will have an viable impact on characterization of EE for the next-generation 5G network as many BS and UE types will exist in multiple frames of work with various cell sizes and power levels [18].

2.5 Pre-Coding and Combine Vector Schemes

Pre-coding techniques play an essential role in subtracting the interferences before transmitting them through the channel from end-users on the transmitter side [70]. The pre-coding technique is a practical and straightforward approach and is represented by Linear Precoding [71]. In this technique, suitable signal processing is done at the transmitter side to isolate users present in that space by enabling CSI at the transmitter (CSIT) [72]. Obtaining a faultless CSIT is difficult in a severely faded channel. The author in [73] articulates different challenges of implementing massive MIMO in 5G systems, particularly transmitting antennas. Among them, precoding is considered an active and more suitable research topic for massive-MIMO.

The estimation errors in CSI are studied in [74]. The article [75] investigated linear and nonlinear pre-coding methods, which showed how using the pre-coding technique can improve bit error rate (BER) by utilizing faultless CSI. Upon investigation, it has been concluded that the nonlinear pre-coding approach needs complex computations at both BSs and UEs. The author [76] analyzed the performance of massive-MIMO in a uni-cell DL with various precoding techniques under faultless CSI. The authors took the same SINR for pre-coders that were supposed to be ignored for better analysis. It is done because each pre-coding has a different SINR.

In [77], a matrix and vector normalization for ZF and MRT pre-coding are compared. The performance of these pre-coding techniques was investigated using CSI in a unit cell boundary scenario. The article [28], a brief investigation based on the performance of DL massive-MIMO along with ZF pre-coding, is done in terms of outage probability and BER using faultless CSI. The system's efficiency is tested using faultless CSI with

ZF, and MRT is evaluated in [78]. The power capacity on UL of massive-MIMO following perfect and imperfect CSI using a minimum value of mean square error, ZF, and maximum ratio combining receivers is investigated [79]. The authors in [25], examined and compared the efficacy of Eigen beamforming (BF) and RZF based on feasible data rates alongside channel estimation errors in multi-cell DL systems [80]. To achieve the UL data rate of massive-MIMO, it incorporates the ZF and MRC receiver, and a Ricean fading channel is analyzed using both perfect and imperfect CSI [81].

The majority of work explained above has discussed the use of perfect CSI, but it is practically difficult to obtain such a scenario. This work studied the effect of estimation error, which is abandoned in [82]. Upon considering error estimation, it is analyzed that this study is novel and more suitable for practical scenarios. However, channel estimation was taken into account in [83], which examined the performance of UL channel, and in BF and RZF, pre-coding was analyzed along with imperfect CSI. Still, here in this research work, the DL channel is incorporated with ZF, where Pre-coding is considered.

2.6 Related Work to Pre-coding Schemes in Energy Efficiency Augmentation

Existing literature describes mathematical modelling of the characteristics mentioned above to improve area throughput and EE. The authors of [84] have presented a comprehensive power consumption modelling for the modelling of EE optimization. Furthermore, the total circuit power consumption on the transmission of an antenna is considered by authors in [18], [85], [86], [87]. The author in [88] emphasizes UL communication and the total power consumption considered in the massive MIMO network. The authors also determined the models of EE optimization by taking the antennas of UEs as turned off. At the same time, the DL communication is examined of a system and concluded EE by considering the concave function of multiple antennas [85]. In [89], [90], the results for the optimal value of M to optimize EE is observed, and a multi-cell scenario for a fixed number of UEs is taken into account. In addition, the EE is enhanced by power consumption models for UL and DL in processing schemes [91], [92], [93]. Because the power required for DSP and analogue circuits

increases with rising values of M, achieving infinite throughput and EE is perceptibly impractical [16], [94]. However, research has consistently demonstrated that infinite EE is possible. Most of the modelling has been evaluated the EE models while not considering the effect of an increasing number of UEs. Simultaneously wireless information and power transfer (SWIPT) has many applications in 5G and IoT by transmitting the maximum power and harvesting the energy per user [54]. It maximizes the EE of the given system and uses a dual inner/outer layer with a resource allocation framework to solve maximization.

Moreover, dual multiple access channels (MAC) are resolved by SWIPT based BC-MAC approach with resource allocation under fixed constraints [55]. Meanwhile, 5G has to deliver ultra-high data rates for high-rate applications such as IoT, and energy augmentation is the solution to extend the lifetime of wireless devices. It also increases the sustainability of the wireless networks by increasing the power of wireless nodes to save energy from the local environment.

2.7 Related Work to Pre-coding Schemes in Spectral Efficiency Augmentation

On the other hand, the UL signal deduction becomes inefficient and complex because of huge amount of atennas. Meanwhile, the proposed algorithm in [95] is efficient and achieves optimal Bit Error rate (BER), which depends on the least-square (LS) channel estimator compared to the traditional UL detection algorithm. Thus, 5G is designed to adjust the high reliability, data traffic and to improve spectral and EE with low latency. At the same time, the Richardson and Neumann series expansion (NSE) method has been used to avoid the matrix inversion. In this regard, the non-linear maximum likelihood (ML) and sphere decoder are illogical due to increased complexity by increasing the number of antennas [96]. Meanwhile, a method in [97] provides a good arrangement between BER and complexity. Thousands of antennas are used in a system for tens of users to offer services simultaneously. The channel is also estimated according to the user's pilot signals to the BS. In contrast, the massive MIMO system provides the advantage of high reliability, high spectral, and EE. ML, minimum mean square MMS method, M-MMSE, S-MMSE, RZF, MR, and ZF deduction for channel estimation are used in the [98], [99], [100], [101] while MMSE is preferred as it can

better SE other than complexity [102]. Although circuit power preference algorithms have been proposed to maximize EE in a multi-cell environment, the precoding techniques for increasing SE in the MIMO system have a better impact. An antenna selection scheme is used to expand the EE of the UL transmissions while it has more power consumption of the mobile antennas [100], [101], [102]. Therefore, pilot reuse techniques are proposed for reducing co-channel interference without increasing the bandwidth, and cell density is also analyzed. Meanwhile, a low complexity in channel estimation is becoming a big concern. MMSE, Element-wise MMSE, and LS estimators compute the complexity with the trade-off of SE. Moreover, the power consumption and EE of the BSs can be improved by using an effective strategy and an efficient DL MIMO system consisting of ZF, BF, and perfect channels in the BS. Unimodal and user data rates increase together for maximum EE, but unimodal has average EE per BS. The linear precoding of channels is an efficient way with DL and UL pre-coders to reduce the effect of inter-user and improper noise. Furthermore, large array and multiplexing gain are used for large spectral and EE. A BS is equipped with a large antenna array to develop the orthogonal channel pairwise among users and BS by using small-scale fading [103]. Besides that, a massive MIMO system reduces the transmitted power of the BS and terminal. The research carries some full-duplex (FD) models that are more suitable for short-range communication like WiFi and small-cell networks than arrangements with realistic parameters proposed by ZF design [104]. Hence, 5G antennas SE and EE are major factors in the designing of 5G antennas. Furthermore, the latest idea of the massive MIMO networks and distributed antennas system improves inter-cell interference and a balanced quality of experience. Therefore, massive MIMO technology gives an impressive SE compared to the conventional co-located MIMO [105]. The achievable SE of precoding and combining structures is getting more attention in analogue-digital implementation, and 5G should support low power consumption [106]. For sustainable development in 5G, it has to improve energy and cost efficiency comparatively by Integrating the massive MIMO with examining the impact of pilot contamination on this new communication scenario. The latest articles claim that it is probable to attain SE by evaluating UL ad DL transmission models with channel estimation, as shown in Table. 2.1.

Table 2.1 *Comparison of related work of SE in Massive MIMO.*

Work	**Cell**	**UL/DL**	**Combining/Precoding scheme**
[95]	Single	UL	LS precoding
[96-98]	Multicell	UL&DL	MMSE, RZF, ZF, MR Precoding
[100]–[102]	Multicell	UL&DL	MMSE precoding and combining
[103]	Multicell	UL&DL	MMSE, RZF, ZF, MR Precoding
[104]	Multicell	UL	MMSE Precoding
[105]	Single	UL&DL	ZF Precoding
[106]	Single	UL&DL	----------

2.8 Energy Efficiency Trade-off with Spectral Efficiency and Throughput

The EE tradeoff with SE and network throughput becomes more essential in massive MIMO systems after the optimal antenna placement, PC of users' equipment, and throughput reduction. In this regard, the PC model is presented in [107] where a model of closed-form approximation for the UL network is proposed, and an ideological approach for EE and SE trade-off is suggested. The work [108] is considered evaluation criteria for the trade-off of EE and SE, and the Rayleigh fading channel has been evaluated with a more generic closed-form approximation. This model optimized the EE gain with SE and antenna selection satisfaction and compared it with a single-input single-output (SISO) network. Moreover, the model indicates that the MIMO systems are EE enhancers and decrease the numbers of antennas at the transmitter side when the PC model is taken into account. Rayleigh fading channel is further considered in [109], and the UL and DL system models for distributed MIMO networks are formulated with various PC models. Generic and accurate low and high-SE approximations drive the expression of trade-offs and optimize the numbers antennas strength by considering PC models. MRC scheme-based approximation for the trade-off of EE and SE is also

computed in [86], [110], [111] having PC models for the antenna selection of transmitter. As other models indicate that the increment in antenna enhances the efficiency but reduces the SE, the optimal value of SE that can maximize the EE is obtained. The model presented in [112] has considered the PC models of transceiver PC and radiated PC, and close form expression is used for the optimal EE-SE trade-off. Pareto optimal set based is a method for computation EE-SE trade-off with the multiple objective optimizations methods presented in [113] where PC and the number of available antennas at the BS are considered. This model was a Cobb-Douglas production model, and it has computed trade-off matric to convert an optimization function into a single objective function. The results have achieved the optimized PC for the maximum available antennas in the network and optimized the trade-off through various priority levels.

The latest trends are CSI at the transmitter, as authors did in [114], [115], [116]. They all formulated the expressions for signal-to-interference noise ratio in transmitting PC, and the number of available antennas then optimized the trade-off. S.M Nimmagadda has contributed to the EE-SE trade-off by providing two algorithms for complex optimization approaches and obtaining optimised results [117]. The initial algorithm is practised by modified grey wolf optimization. The second algorithm, named modified lion algorithm, is formed for improved convergence rate and helps in a better trade-off between the SE and EE. In this regard, a user-centric (UC) access point selection method has been proposed [118] to improve the performance and optimization of EE-SE trade-offs in MIMO systems.

The antenna channel effects on MIMO throughput are computed as spatial multiplexing efficiency, reducing power imbalance [119]. The sum rate of resource allocation is called throughput by [120] and developed a model for maximization of throughput and EE. A model of 400 antennas and several transmitters are taken into account for the throughput analysis in [113] and provided an elaborative background for studying the EE and throughput of wireless networks. Further throughput analysis by considering some approximations and assumptions is proposed in [47].

Table 2.2 *Comparison of related work in Massive MIMO.*

Ref. No	Key Contribution	Approximation Approach	Trade-Off of EE with	Limitations
[107]	Improve the EE and SE trade-off through optimal antenna placement, PC of users' equipment, and throughput reduction.	Closed-form approximation	SE	Throughput is reduced
[108]	RF channel evaluated and optimized the EE-SE trade-off with antenna selection.	More generic closed-form approximation	SE	It mainly focuses on cell-edge communication and small cell advancement.
[109]	RF channel evaluated for distributed MIMO networks for various PC models and optimized the numbers antennas.	Generic and accurate low and high-SE approximations	SE	Only suitable for a specific scenario
[86], [110], [111]	Optimized the EE-SE trade-off with PC models for the antenna selection of transmitter.	MRC scheme-based approximation	SE	Not considered the multiple BS
[20]	Transceiver PC and radiated PC are considered for optimal EE-SE trade-off.	Close form expression	SE	Only applicable for the single-cell scenario.

[114]–[116]	Computed the CSI for the number of available antennas and optimized the EE-SE trade-off.	SIN ratio	SE	Precoding design is very simple.
[117]	Improved convergence rate that helps in a better trade-off between the SE and EE	MGW optimization	SE	Not work well for a selection of multiple antenna and multiple BS
[118]	Improved the performance and optimization of EE-SE trade-off	UC access point selection	SE	Complexity is increased.
[8-9]	The antenna channel effects on throughput are computed by spatial multiplexing efficiency.	---------	Throughput	Fewer PC models are considered.
[23]	Throughput analysis by considering approximation & assumptions is proposed.	-------	Throughput	It is unstable due to immediate re-transmissions
Proposed	EE-SE and EE-Throughput trade-off	Logarithmic Approximation	SE and Throughput	Hardware is not considered.

2.9 Summary

The EE tradeoff with SE and network throughput models are discussed in this chapter. The optimal antenna placement, optimal numbers of PC of users' equipment, and power consumption models are considered essential terms in the proposed work. Moreover, power consumption and EE of the BS can be improved by using an effective strategy including zero-forcing, beamforming, and perfect channel.

CHAPTER 3
PERFORMANCE EVALUATION OF ENERGY EFFICIENCY

3.1 Introduction

BS permits only up to 8 antenna ports in existing 3G and 4G standards. The BS antennas for the 5G System communication, on the other hand, have been enhanced to enable data transmission rates of up to several GBs/second. Strategies (more BS nodes), amplified bandwidth (mm-Wave spectrum), the improvements are expected to be realised, or massive MIMO systems. Each BS is outfitted with M antennas and communicates with N UEs in real-time to achieve channel hardening in this system. Practically, it is not possible to enhance the unbounded EE. It is only impossible to achieve when the system model includes the power consumed by analogue circuits for RF and baseband processing, as well as signal processing, which increases proportionally with M & N. As massive MIMO defined in [121], the ratio of M and N was more than one, whereas in [86], [122], the ratio was assumed to be a small constant value.

All BSs used linear transmit precoding and received combining to process their signals independently. The author evaluated a standard Massive MIMO system model that can be implemented in some applications [86]. So far, efficient modelling of power usage has been a major concern for these systems. Significantly, battery technology in mobile UEs is not advancing due to the exponentially increasing demand for multimedia communication [122]. A key goal is to analyze a massive MIMO network for accurate power consumption models during UL and DL transmissions since this has a greater impact on optimising EE and area throughput.

The followings are the findings of this objective.

- Increasing the number of BS antennas increases total circuit power and transmitted power.
- BS contains hundreds of antennae allowing UE to optimize EE and area throughput.
- By applying the ratio of decreasing cell size, as specified in [123] expression 3.39. The radius and user density values are established in accordance with the expression

cell. Reducing the cell radius reduces the system's network capacity while increasing the EE.

3.2 Uplink and Downlink Model

Besides, the flat-fading channel is examined for transmission constrained by coherence time-frequency blocks as defined by SCB. TDD is employed because the BS and UEs are highly synchronized as shown figure 3.1.

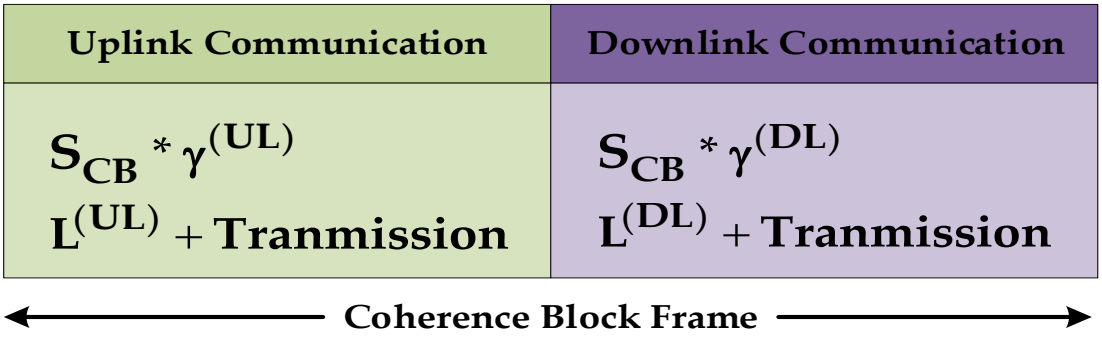

Figure 3. 1 *Coherence block frame: UL/DL transmissions.*

The smaller antenna spacing or the lack of dispersion for large antenna arrays allows for significant antenna correlation [93]. Various antenna configurations for related to this work are presented in the literature, including the cylinder design, linear configuration, and rectangle configuration [91], [92]. The writers considered the conical configuration. Furthermore, all processing schemes and detection algorithms are active in these networks, which greatly minimize power usage. However, the overall circuit power dissipation increases gradually. by increasing M [66]. Received vector at l^{th} BS is denoted with Y_l, $Y_l \in \mathbb{C}^{\mathrm{M}}$ given as

$$Y_l = \sum_{l=1}^{N} \mathrm{G}\sqrt{\rho_l^{Tx}}\, x_l + n_l \tag{3.1}$$

G in equation 3.1 specifies the M x N matrix between BS and UE. The channel coefficients between the lth UE and the ith BS antenna are identified as ($g_{il} \triangleq G_{il}$). The $x_l\sqrt{\rho^{\mathrm{TX}}}$, where ($\rho^{TX}$ Represents the average dispersed power). Moreover, the n_l is an AWGN vector. The g_{il} written as $g_{il} = h_{il}\sqrt{\beta_{il}}$, l ranges from {1, 2… N} and h_{il} is the flat fading coefficient from l^{th} UE and i^{th} BS antenna. It represents signal fading

caused by obstructions like huge buildings and moving cars and signal propagation distance from BS to UE. Where, h_{il} denotes channel vector, which is provided as $h_{il} \sim CN\big(0, (\boldsymbol{\beta}_{il}\boldsymbol{I}_{\mathbf{m}})\big)$. The (h_{il}) are the channel vector entries that define the propagation channel between the *l*th UE and the *i*th BS antenna. The shadow fading and attenuation coefficient is denoted by $\boldsymbol{\beta}_{il}$ while the identity matrix is marked by $\boldsymbol{I}_{\mathbf{m}}$. The three pre-coding techniques, including MMSE, are used to perform UL data identification and data pre-coding activities. The LS-MIMO transmitter decreases inter-user interference by employing spatial signal processing methods similar to pre-coding. The BS is said to be capable of collecting flawless channel information using UL pilot sequences. As a result, ZF results for single-cell cases are obtained. The $Q = [q_1, q_2, \ldots, q_i] \in \mathbb{C}^{M \times N}$ represents the UL linear received matrix as in (3.2) [20]:

$$Q = \begin{cases} H\,(H^H H)^{-1} & ZF \\ H(H^H H\,P^{UL} + \sigma^2 I)^{-1} & MMSE \\ H & MRT \end{cases} \tag{3.2}$$

In (3.2), $(.)^H$ and $(.)^{-1}$ represents the Hermiston matrix and inverse transpose individually. In further, $H = \left[v_{i,1}, v_{i,2}, \ldots, v_{i,N}\right] \in \mathbb{C}^{M \times K}$ include the channel values for all the UEs and power vector for UL is P^{ul} = diag $[p_1^{UL}, p_2^{UL}, \ldots., p_i^{UL}] \in \mathbb{C}^{\mathrm{N} \times \mathrm{N}}$. The ZF pre-coding is capable of increasing the network's efficiency and capacity. If the receiver has excellent CSI for a large number of UEs [91]. ZF requires a significant overhead when addressing the Signal to SNR to obtain the maximum multiplexing advantage. Linear processing techniques for DL communication are defined as V=$[v_1, v_2, \ldots, v_N] \in \mathbb{C}^{\mathrm{M} \times \mathrm{N}}$. V matrix is modelled as in (3.3)

$$\mathrm{V} = \begin{cases} H\,(H^H H)^{-1} & ZF \\ H(H^H H\,P^{UL} + \sigma^2 I)^{-1} & MMSE \\ H & MRC \end{cases} \tag{3.3}$$

To simplify the calculus complexity, Q = V, according to the equation in [124]. It is also known as a pre-detection combining scheme [69]. For self-contained AWGN. It functions as a combiner and restores a signal to its original form. The N(th)user terminal (UE/UTs) is actually positioned on x_N ($x_N \in \mathbb{R}^2$) measured in meters.

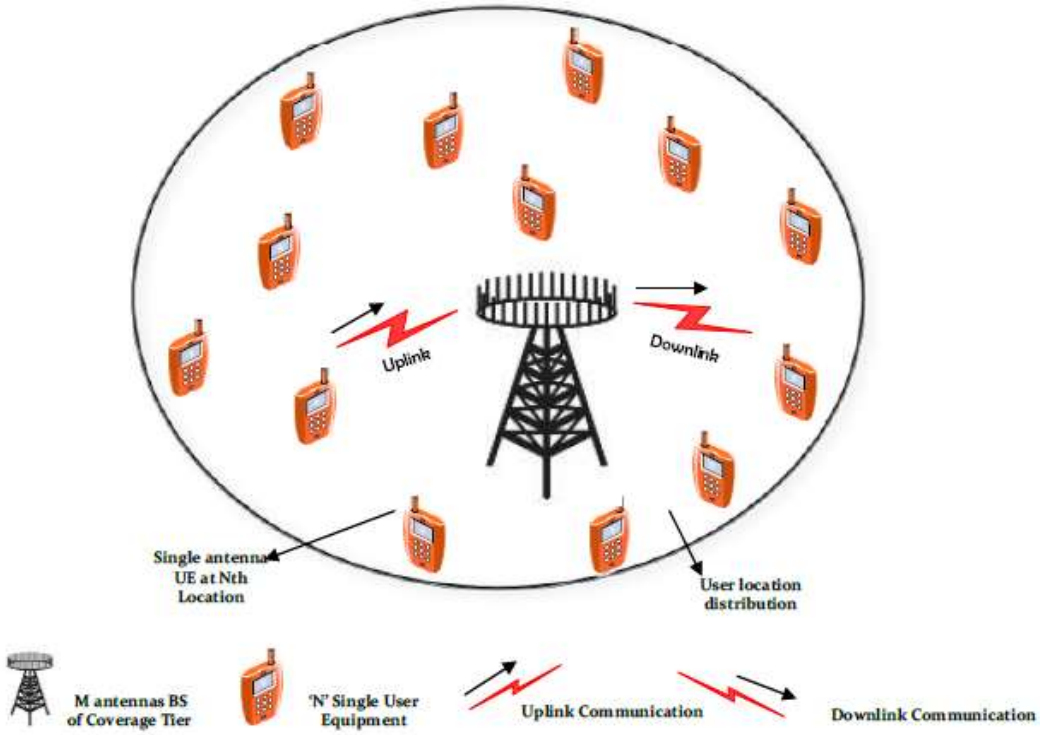

Figure 3. 2 *UL and DL transmission of the proposed single cell scenario*

BS in the coverage layer, with N single-antenna user terminals, are considered. In the cell, all users are distributed at random. The x_N is determined about BS using round-robin (RR) selection. The UEs are carefully chosen for the communication. The UE locations are reserved with arbitrary variables from the user distribution. The distances between BS and UEs are significantly greater than the range between BS antennas in the array configuration. Assume that (r) denotes the maximum distance a UE has from BS and (*dm*) represents the minimum distance a UE has from BS. All UEs are uniformly distributed around the BS. Furthermore, the position of UE is denoted by *f(x),* which is modelled as (3.4) [66].

$$f(x) = \begin{cases} \left(\pi(r^2 - d_m^2)\right)^{-1} & d_m \leq \|x\| \leq r \\ 0 & \text{otherwise} \end{cases} \tag{3.4}$$

ζ represents the large scale fading gave as $\zeta = (\omega/\|x\|^{\varphi})$. φ *is* $(\varphi > 2)$ path loss exponent and constant $\omega > 0$ as an attenuation factor in the channel at d_m. The Inverse channel attenuation is [66]:

$$\mathrm{E} = \mathbb{E}((\zeta)^{-1}) = \left\{ \frac{\left(r^{\varphi+2} - d_m^{\varphi+2}\right)}{\left(\left(1 + (\varphi/2)\right)(r^2 - d_m^2)\omega\right)} \right\} \tag{3.5}$$

3.3 Methodology and Calculations

The main goals of this work are to improve the EE of a massive-MIMO system and to estimate the optimum power consumption using MMSE, ZF, and MRT/C pre-coders. It is realized that the power consumption methodology and energy is saved by installing low power BS according to traffic requirements. It is notable for decreasing power usage by lowering infrastructure costs and efficiently controlling the spectrum [69]. The power consumed by BS is proportional to the multiple transmitting antennas versus the multiple UEs operating concurrently.

Figure 3.3 depicts the results of the calculations done in this section. In the first and second phases, the UL and DL communication data rates are determined. The computations of power consumption by PAs and circuitry at the BS and UEs are shown on the right side of the flow diagram. The data rate is averaged, and the total and power consumption calculations are summed to determine the total power expended.

Finally, the seventh step provides the average data rate to the overall power dissipation ratio, which is utilized to calculate EE. The following section contains the detailed computations shown in Figure 3.3.

3.3.1 Average Data Rate

Figure 3.3's upper left corner shows two stages for calculating the average rate. According to (3.6), the average rate is the feasible data rates in DL and UL communications.

$$R_i^{tot} = R_i^{UL} + R_i^{DL} \tag{3.6}$$

where R_i^{UL} is achievable data rate and R_i^{DL} are the UL&DL data rates. By Gaussian-code books, the achievable UL data rate is given in [122] but the computed term as (3.7) is given as:.

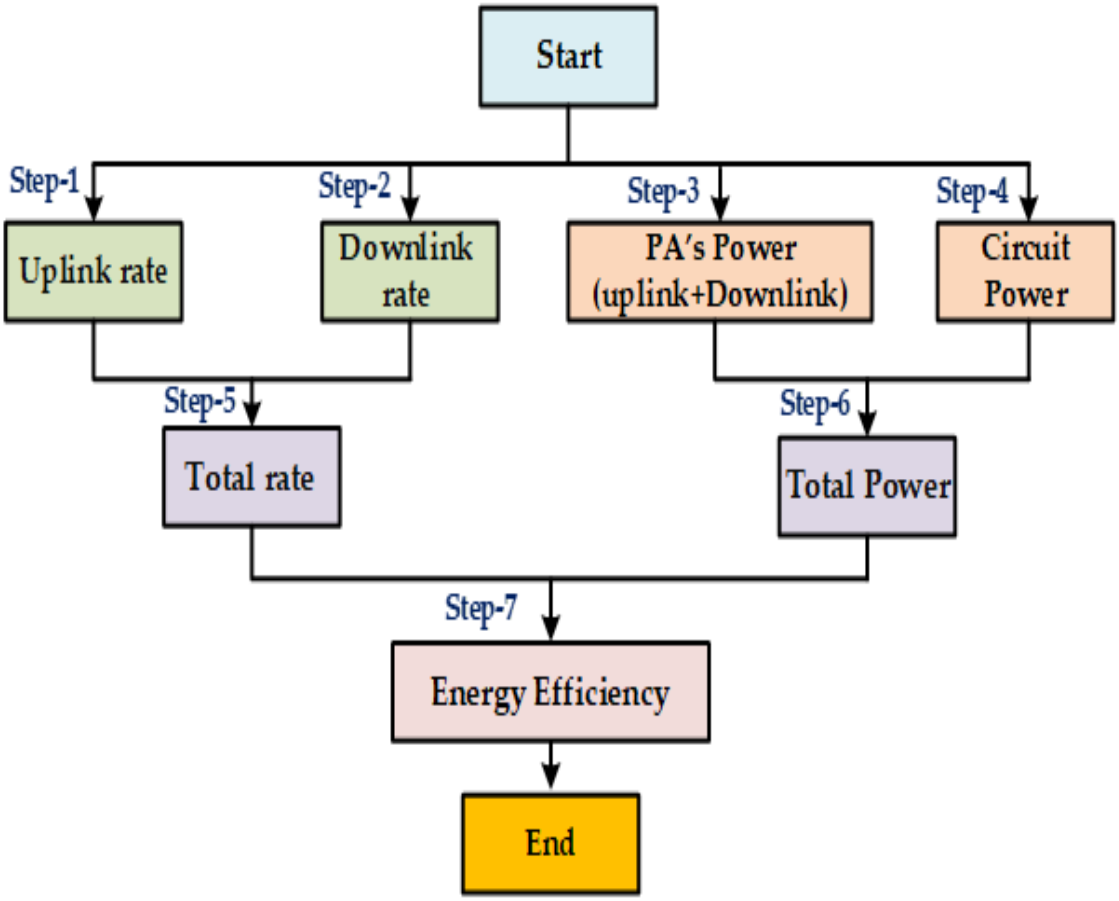

Figure 3.3 *Computational flow of the model.*

$$R_i^{UL} = \overline{R}_{UL}\left(\gamma^{UL}\left(1 - \frac{L^{UL}N}{S_{CB}\,\gamma^{UL}}\right)\right) \tag{3.7}$$

where γ^{UL} is the UL transmission fraction, and L^{UL} represents the UL-pilot length. Moreover, $\left[1 - \left((L^{UL}N)/(S_{CB}\,\gamma^{UL})\right)\right]$ are pilot overhead value and gross-rate is given as $\left[\overline{R}_{UL} = Blog\,(1 + \Phi_1)\right]$, where Φ_1 is calculated as (3.8)

$$\Phi_1 = \frac{\left(p_i^{UL}\left|q_i^H h_i\right|^2\right)}{\sum_{l=1,l\neq i}^{i} p_l^{UL}\left|q_i^H h_l\right|^2 + \sigma^2\|q_i\|^2} \tag{3.8}$$

where σ^2 shows noise power and P^{UL} =$[p_1^{UL}, p_2^{UL}, .., p_i^{UL}]^T$ is UL power allocation. In [93] power distribution vector in UL is p^{UL} =$\sigma^2(Z^{UL})^{-1}1_i$, (I, l) are elements of Z^{ul} $\in C^{N\times N}$ given is (3.9)

$$[Z^{UL}]_{N,l} = \begin{cases} \dfrac{\left(\left|q_i^H h_i\right|^2\right)}{\left(\left(2^{\frac{\overline{R}}{B}-1}\right)\|q_i\|^2\right)} & \text{, for i} < \text{l} \\ -\dfrac{\left(\left|q_i^H h_i\right|^2\right)}{\|q_i\|^2} & , for\ i \neq l \end{cases} \tag{3.9}$$

According to [125] if zero-forcing pre-coder is applied where $M \geq N + 1$, and $gross\ rate = \text{B log}\left(1 + \rho(M - N)\right)$, where ρ is proportional to received SINR. Then R_i^{Dl} becomes:

$$R_i^{Dl} = \overline{R}_{DL}\left(\gamma^{DL} \left(1 - \frac{L^{DL}N}{S_{CB}\,\gamma^{DL}}\right)\right) \tag{3.10}$$

where γ^{DL} is DL transmission fraction L^{DL} is the DL pilot length, the pilot overhead can be modelled as $\left[1 - \left((L^{DL}N)/(S_{CB}\,\gamma^{DL})\right)\right]$ and the gross rate is given as $\left(\overline{R}_{DL}\right)$=$\left[\overline{R}_{DL} = Blog(1 + \Phi_2)\right]$. The value of Φ_2 is (3.11)

$$\Phi_2 = \frac{p_i^{DL}\left(\left(\left|h_i^H v_i\right|^2\right)/(\|v_i\|^2)\right)}{\sum_{l=1,l\neq i}^{N} p_l^{DL}\left(\left(\left|h_i^H v_i\right|^2\right)/(\|v_i\|^2)\right) + \sigma^2} \tag{3.11}$$

$p^{DL} = \sigma^2(Z^{DL})^{-1}$ is DL power vector, (i, l) component of $Z^{DL} \in \mathbb{C}^{N\times N}$. Z^{DL} is computed as cast-off:

$$[Z^{DL}]_{N,l} = \begin{cases} \dfrac{\left(\left|h_i^H v_i\right|^2\right)}{\left(2^{\frac{R}{B}} - 1\right)\|v_k\|^2} & , for\ i < l \\ -\dfrac{\left(\left|h_i^H v_i\right|^2\right)}{(\|v_l\|^2)} & , for\ i \neq l \end{cases} \tag{3.12}$$

The results of (3.7) and (3.8) are plugged in (3.6) to calculate the achievable rate for i^{th} as (3.13), where $\overline{R}$ is considered gross rate, and the achievable data rates for bi-directional communications is:

$$R_i^{tot} = \left(N - \left(\frac{N(L^{UL} + L^{DL})}{S_{CB}}\right)\overline{R}\right) \tag{3.13}$$

3.3.2 Computations of Power Consumptions

The models are presented in [91] [92]. The proposed model including all characteristics of power consumption (3.14):

$$P_{total} = P_{PA} + P_{Cir}^{total} \tag{3.14}$$

In (3.14), P_{PA} is the power consumption by PA and P_{Cir}^{total} is the total power consumption of the circuit. In prior works, total circuit power is computed as (P_{Cir}^{total}=Ps), where the Ps where Ps is a constant amount of power consumption calculated for load-independent backhaul, control signals, system cooling power, and baseband processor [15], [90]. This method of determining circuit power is incorrect. The circuit power grows proportionally with M in a system where M's value. In previous models, the circuit power consumption claims that raising M can lead to limitless EE; however, infinite EE is difficult to achieve. [66] delineates the average power utilised by PA as [66] as, $P_{PA} = \frac{B\gamma}{\eta}\sum_{N=1}^{N}\mathbb{E}\{p_N^{UL}\}$. The power consumption by PA during UL is computed:

$$P_{PA}^{UL} = \frac{\rho KB\sigma^2\,\gamma^{UL}}{\eta^{UL}}\left(\frac{r^{\varphi+2} - d_m^{\varphi+2}}{\omega\left(1+\left(\frac{\varphi}{2}\right)\right)(r^2 - d_m^2)}\right) \tag{3.15}$$

Similarly, the DL PA's power can model as (3.16)

$$P_{PA}^{DL} = \frac{\rho \mathrm{NB}\sigma^2\gamma^{\mathrm{DL}}}{\eta^{\mathrm{DL}}}\left(\frac{r^{\varphi+2} - d_m^{\varphi+2}}{\omega(1+\varphi/2)(r^2 - d_m^2)}\right) \tag{3.16}$$

The total power consumed by PA is calculated as ($P_{PA}^{UL} + P_{PA}^{DL}$) That is the sum of (3.15) and (3.16). The (η_{PA}) represents the efficiency of PA given as $\left(\frac{\gamma^{\mathrm{UL}}}{\eta^{\mathrm{UL}}} + \frac{\gamma^{\mathrm{DL}}}{\eta^{\mathrm{DL}}}\right)^{-1}$.

$$P_{PA}^{ZF} = \left\{\frac{(\rho NB\sigma^2)}{\eta_{PA}}\left(\frac{r^{\varphi+2} - d_m^{\varphi+2}}{\omega\left(1+(\varphi/2)\right)(r^2 - d_m^2)}\right)\right\} \tag{3.17}$$

The P_{Cir}^{total} is the total power as computed in [126]. A proposed mathematical model of P_{Cir}^{total} is given as:

$$P_{Cir}^{total} = P_{\mathrm{t}} + P_{\mathrm{C/d}} + P_{\mathrm{b}} + P_{\mathrm{e}} + P_l + P_{\mathrm{s}} \tag{3.18}$$

In (3.18), P_t denotes the power consumed by transceiver chains and ($P_{C/d}$) can be modeled as:

$$P_b = \left(\sum_{i=1}^{N} \left(\mathbb{E}\left(R_i^{UL} + R_i^{DL} \right) * \left(P_{cod} + P_{dec} \right) \right) \right) \tag{3.19}$$

The P_{bt} is a power required by backhaul traffic power.

$$P_b = \left(\sum_{i=1}^{N} \left(\mathbb{E}(R_i^{tot}) * P_{bt} \right) \right) \tag{3.20}$$

By the help of $\mathrm{P_e}$, the estimation of channel state given as: $[P_e = P_e^{UL} + P_e^{DL}]$ given as:

$$P_e = \left\{ 2BN^2 \left(ML^{UL} + \frac{(2\,L^{UL})}{S_{CB}\Psi_{UE}} \right) \right\} \tag{3.21}$$

Furthermore, P_l is exploited to indicate the power dispersed at BS when linear processing techniques are applied. In linear processing, two types of power are measured: the first is necessary for computing Q and V, and the second is required for matrix-vector multiplication by each data Symbol [66] . The pre-coding/decoding matrices are calculated again in the same coherent block, and its complexity depends on the type of scheme had used. As a result, power usage for MRT/MRC is provided as (3.22).

$$P_l^{MRC/MRT} = \left\{ \frac{2MNB}{\Psi_{BS}} \left(1 - \left(\frac{L^{UL} + L^{DL}}{3S_{CB}} \right) \right) + \left(\frac{3BMN}{S_{CB}\Psi_{BS}} \right) \right\} \tag{3.22}$$

Moreover, in ZF consumed power becomes:

$$P_l^{ZF} = \left\{ \left(\frac{BN^3}{3S_{CB}\Psi_{UE}} \right) + \left(\frac{BM(3N^2 + N)}{\Psi_{BS}} \right) \right\} \tag{3.23}$$

where $\Psi_{\mathrm{LS}} = 12.8 \& \Psi_{\mathrm{UD}} = 5 Gflops/W$ as per [19]. Lastly, in $MMSE$ consumed power becomes as (3.24)

$$P_l^{MMSE} = \left\{\left(\frac{BN^3}{3S_{CB}\Psi_{UE}}\right) + \left(\frac{BM(3N^2+N)}{\Psi_{BS}}\right)\right\} \tag{3.24}$$

where P_s is assumed the power needed by cotrol signals, baseband sinnals and coolong purpose that is fixed.

3.3.3 Optimization of M, N, and ρ

(M^{optim}) and further intended as:

$$M^{optim} = \left\{\frac{(\rho N - 1) + e^{W\left(\rho^2\left(\frac{1}{e}\left(\frac{(P_{PA}+\alpha_1)}{\alpha_2}\right)+(N-1)\right)+1\right)}}{\rho}\right\} \tag{3.25}$$

where the values ($\alpha_1, \alpha_2 > 0$) as P_{PA} is is calculated in (12), where α_1& α_2 are power consumed is given as:

$$\alpha_1 = \frac{\left\{\left(4\,B\,\frac{L^{UL}}{S_{CB}\Psi_{UE}}\right)N^2 + \left(\frac{B}{3S_{CB}\Psi_{BS}}\right)N^3\right\}\left\{\left(P_{fix}+P_{syn}\right) + (P_{UE})\right\}}{N} \tag{3.26}$$

$$\alpha_2 = \frac{\left(\frac{B\left(2+\frac{1}{S_{CB}}\right)}{\Psi_{BS}}\right)N + \left(\frac{B(3-2L^{DL})}{S_{CB}\Psi_{BS}}\right)N^2 + (P_{BS})}{N} \tag{3.27}$$

.The lower bound of optimal M can be calculated as (3.28):

$$M^{optim} \geq \left\{\frac{\frac{P_{PA}}{\alpha_2} + \frac{\alpha_1}{\alpha_2} + N + \frac{1}{\rho}}{\ln(\rho) + \ln\left(\frac{P_{PA}}{\alpha_2} + \frac{\alpha_1}{\alpha_2} + N + \frac{1}{\rho}\right) - 1}\right\} + (N) - \left(\frac{1}{\rho}\right) \tag{3.28}$$

The (ρ^{optim}) is calculated by using Lambert function as:

$$\rho^{optim} = \frac{\left\{e^{W\left(\rho\left(\frac{(M-N)\,(\alpha_1+M\alpha_2)}{e}\left(\frac{N}{P_{PA}}\right)+\frac{1}{e}\right)+1\right)} - (1)\right\}}{M-N} \tag{3.29}$$

where $\alpha_1$and α_2 are given in (3.30) and (3.31), respectively.

$$\alpha_1 = \frac{\left\{\left(4\,B\frac{L^{UL}}{S_{CB}\Psi_{UE}}\right)N^2 + \left(\frac{B}{3S_{CB}\Psi_{BS}}\right)N^3\right\}\left\{\left(P_{fix} + P_{syn}\right) + \left(P_{UE}\right)\right\}}{N} \tag{3.30}$$

$$\alpha_2 = \frac{\left(\frac{B\ (2 + \ 1/S_{CB})}{\Psi_{BS}}\right)N + \left(\frac{B(3 - 2L^{DL})}{S_{CB}\Psi_{BS}}\right)N^2 + (P_{BS})}{N} \tag{3.31}$$

The authors in [63], [127], [128] illustrate that the TDD based system allows a power drop that can be directly proportional to ($1/M$ or$\sqrt{1/M}$ imperfect-CSI), however keeping the non-zero data rates for the value of' that approaches to infinity. The lower bound of ρ^{optim} can be intended as (3.32).

$$\rho^{optim} \geq \left\{\frac{\frac{P_{PA}}{\alpha_2} + \frac{\alpha_1}{\alpha_2} + N + \frac{1}{\rho}}{ln(\rho) + ln\left(\frac{P_{PA}}{\alpha_2} + \frac{\alpha_1}{\alpha_2} + N + \frac{1}{\rho}\right) - 1}\right\} + (N) - \left(\frac{1}{\rho}\right) \tag{3.32}$$

Finding the roots of the following polynomial were the terms in (3.34) [92]. Hence, to provide critical tractability, let's suppose the summation of ('SINRρN' and in that way the power of PA) and the total numbers of BS antennas for each UE, (M/N), retained as constants ($\bar{\rho} = \rho$N) and ($\bar{\mu} = M/N$) with ($\bar{\rho} > 0$) and ($\bar{\mu} > 1$). Therefore, the gross rate value can be taken as $\{\bar{c} = B_{log}(1+\bar{\rho}(\bar{\mu} - 1))\}$ and the optimal value of UEs can be taken as:

$$N^{optim} = \min_i \lfloor N_i^o \rfloor \tag{3.33}$$

$$\left\{N^4 - \left(\frac{2S_{CB}}{(L^{DL} + \ L^{UL})}N^3\right) - N^2\Lambda_2 - 2N\Lambda_1 + \left(\frac{S_{CB}\Lambda_1}{(L^{DL} + \ L^{UL})}\right)\right\} = 0 \tag{3.34}$$

In (3.34), $\lfloor N_i^o \rfloor$describes the positive real roots of (3.35).

$$\Lambda_1 = \left\{\frac{(P_s + P_t) + P_{PA}}{\left(\frac{B}{3S_{CB}\Psi_{BS}} + \left(\frac{MB(3 - 2\tau^{DL})}{S_{CB}N\Psi_{BS}}\right)\right)}\right\} \tag{3.35}$$

$$\Lambda_2 = \left\{ \frac{\frac{S_{CB}}{(L^{DL}+L^{UL})}\left(\frac{4BL^{UL}}{S_{CB}\Psi_{BS}} + \frac{B\left(\frac{2}{N}+\frac{M}{NS_{CB}}\right)}{\Psi_{BS}}\right)}{\frac{B}{3S_{CB}\Psi_{BS}}\left(\frac{MB(3-2\tau^{DL})}{S_{CB}N\Psi_{BS}}\right)} \right\} \tag{3.36}$$

The N^{optim} will become as (3.37).

$$N^{optim} = \left\lfloor \left(\frac{(P_s+P_t)+P_{PA}}{\frac{B}{3S_{CB}\Psi_{BS}} * \left(\frac{MB(3-2\tau^{DL})}{NS_{CB}\Psi_{BS}}\right)} \right) \left(\sqrt{1 + \frac{S_{CB}\left(\frac{B}{3S_{CB}\Psi_{BS}} * \left(\frac{MB(3-2\tau^{DL})}{NS_{CB}\Psi_{BS}}\right)\right)}{(L^{DL}+L^{UL})\left((P_s+P_t)+P_{PA}\right)}} \right) \right\rfloor \tag{3.37}$$

In previous subsection, it provide a modest closed-form formulations of M, N, and ρ that allow us to optimize the throughput as well EE. The objective is to calculate the joint-global optimum. As M and N are numerals [93].

3.3.4 Modeling of Energy Efficiency

This section shows a reduction in the overall power consumed by the system, which can be accomplished by decreasing the system's static power consumption. The presented power consumption model is used to calculate the EE for the pre-arranged system model. The following optimization problem can be used to model EE.

$$\max_{\substack{M,K\in\mathbb{Z} \\ \overline{R}\geq 0}} (EE) = \left\{ \frac{\sum_{i=1}^{M}(R_i^{tot})}{\left(P_{Tx}^{UL}+P_{Tx}^{DL}+P_{Cir}^{total}(M,N,\overline{R})\right)} \right\} \tag{3.38}$$

$$\max_{\substack{M,K\in\mathbb{Z} \\ \rho\geq 0}} (EE) = \left\lfloor \frac{\left(K-(K(L^{UL}+L^{DL})/S_{CB})\overline{R}\right)}{\left(\left(\left(\frac{\rho k B\sigma^2}{\eta_{PA}}\right)\left(\frac{r^{\varphi+2}-d_m^{\varphi+2}}{\omega\left(1+(\varphi/2)\right)(r^2-d_m^2)}\right)\right)+P_{Cir}^{total}\right)} \right\rfloor \tag{3.39}$$

3.4 Results and discussion

[66] has considered a suitable number M for the EE calculations with ZF, MMSE, and MRC/MRT pre-coding schemes. The UEs are dispersed inconstantly; thus the large-scale fading is demonstrated using $\zeta = (\omega / \|x\|^{\varphi})$ Where ω & φ values are given in Table 3.1.

Table 3.1 *Simulation parameters.*

Simulation Parameter	**Values**
Required Bandwidth (B)	20MHz
Coherence Bandwidth (B_{Coh})	180 kHz
Coherence Time (T_{Coh})	10msec
Maximum Distance /cell radius(r)	(200) meters
Minimal Distance (d_m)	(40) meters
Channel attenuation (ω)	$10^{-3.5}$
Path loss exponent (φ)	3.76
$P_s, P_{C/d}, P_b$ & P_t	(15, 1, 3 & 0.25) Watt
σ_c(reuse1, 2, 3)	$(0.528, 0.116, 0.021)$

The efficiency of 0.4 and 0.3 is obtained for PA used at BS and UEs, respectively and rest of the parameters are given in Table3.2 as considered in [66].

3.4.1 Energy Efficiency Performance Comparison

In Figure 3.4, the results of EE verses transmit antennas in the single-cell (MRT/C with different schemas are shown. The results are also compared with [88] and [66], then the proposed model demonstrates improved performance.

Table 3.3 compares all of the possibilities. The peak value of EE vs the number of BS antennas in a single cell scenario (with perfect/imperfect CSI) offers 15% better results with a smaller M.

Table 3.2 *Sequence of Simulation.*

Proposed Algorithm	
Step 1:	According to Table I, Initialize the simulation parameters.
Step 2:	Calculate the orthogonal pilot sequences and inverse channel attenuation
Step 3:	If MRT = true || MMSE = true
Step 4:	For M = 1 : N max; *Calculate RF power; Circuit Power; SINR and opt. EE* end
Step 5:	if ZF algorithm = true *Compute circuit Power; RF Power; opt. EE & SNIR* *M opt, N opt and optimum power* end
Step 6:	Plot of Figures EE for single and multi-cell; RF; antenna Power & Area-throughput

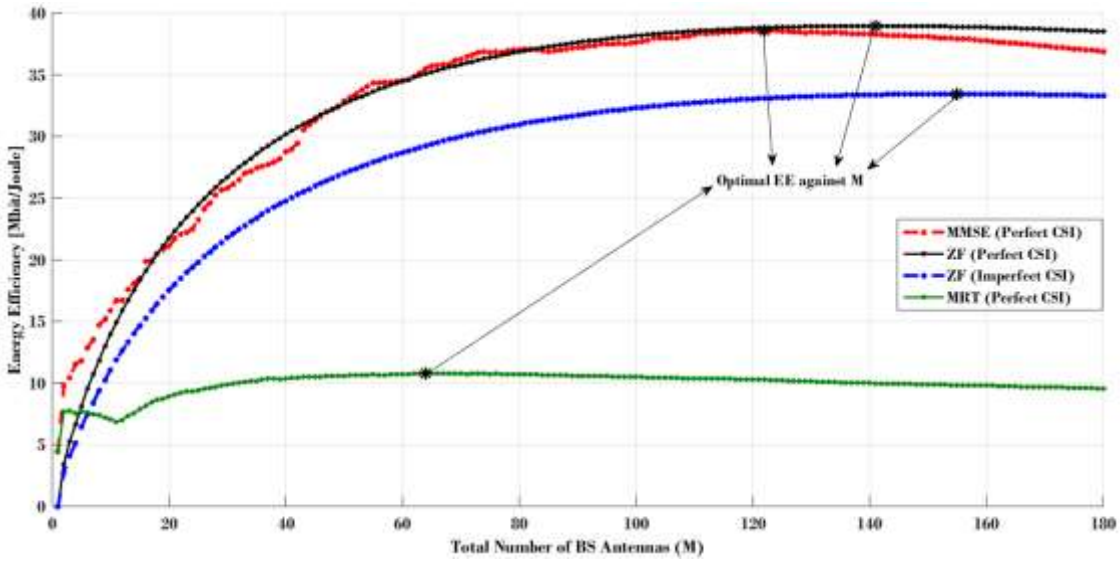

Figure 3.4 EE Performance comparison.

Table 3.3 *Comparison: Results in figure 3.4 and prior works.*

Linear Processing Scheme	**Results (Proposed Model)**		**Results** [87], [94]	
	EE	M	EE	M
MMSE-Perfect CSI	38	122	30	165
ZF-Perfect CSI	39	141	31	165
ZF-Imperfect CSI	31	155	26	185
MRT/C-Perfect CSI	10	82	8.0	85

Moreover, the PA's power dissipation that exploits EE for optimal N with M is given in Figure 3.5. The MMSE has a power dissipation of 50 watts, whereas the ZF with perfect and imperfect CSI has 55 and 70 watts, respectively. Whereas for MRT/MRC, the value is 5 Watt, which is relatively low in comparison to MMSE and ZF.

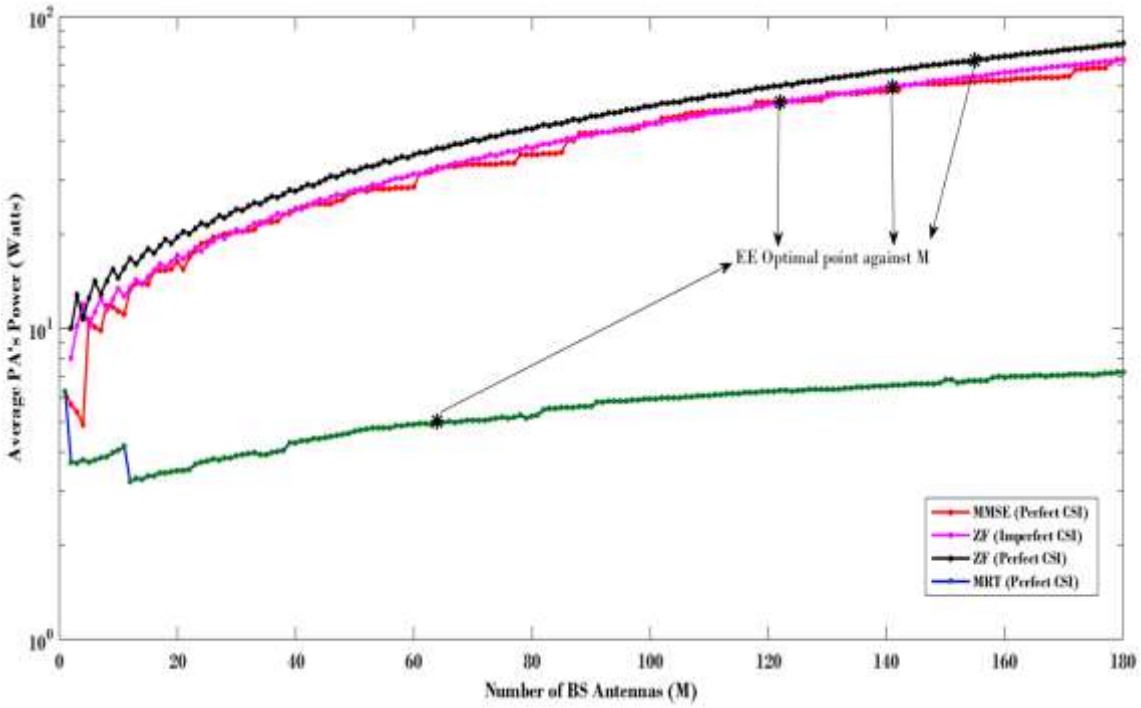

Figure 3.5 *Comparison of PA's power consumption.*

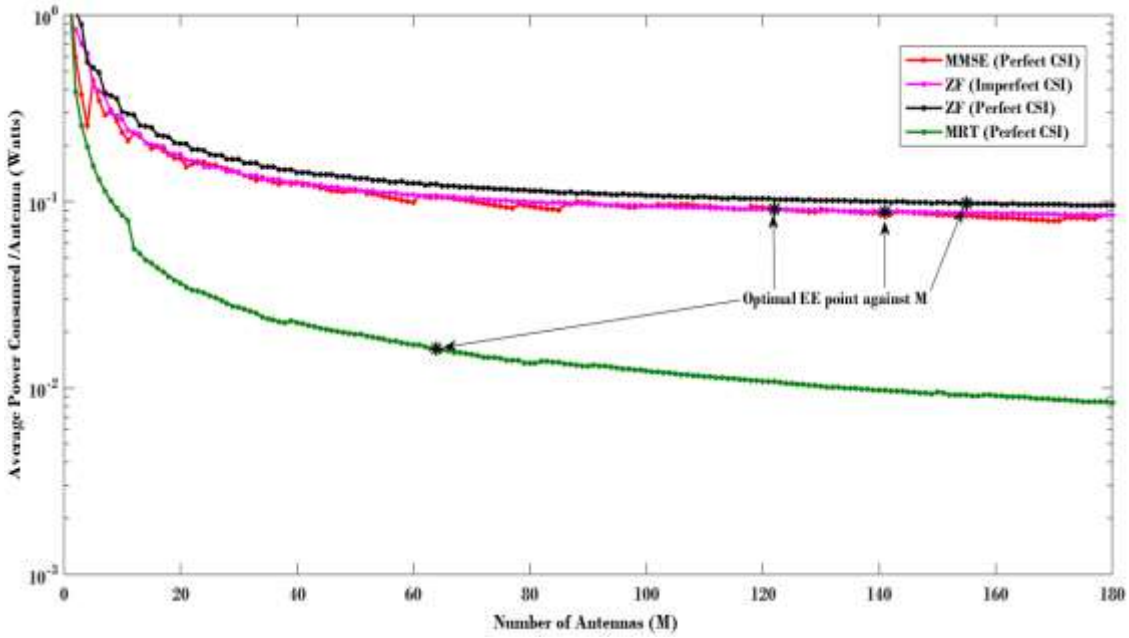

Figure 3.6 *The power consumed by each antenna.*

3.4.2 Results for Area-throughput

Following Figure 3.7 reveals a real-time advancement in the area throughput as compared with existing literature. The maximum improvement is achieved in the case of MMSE and ZF with imperfect CSI.

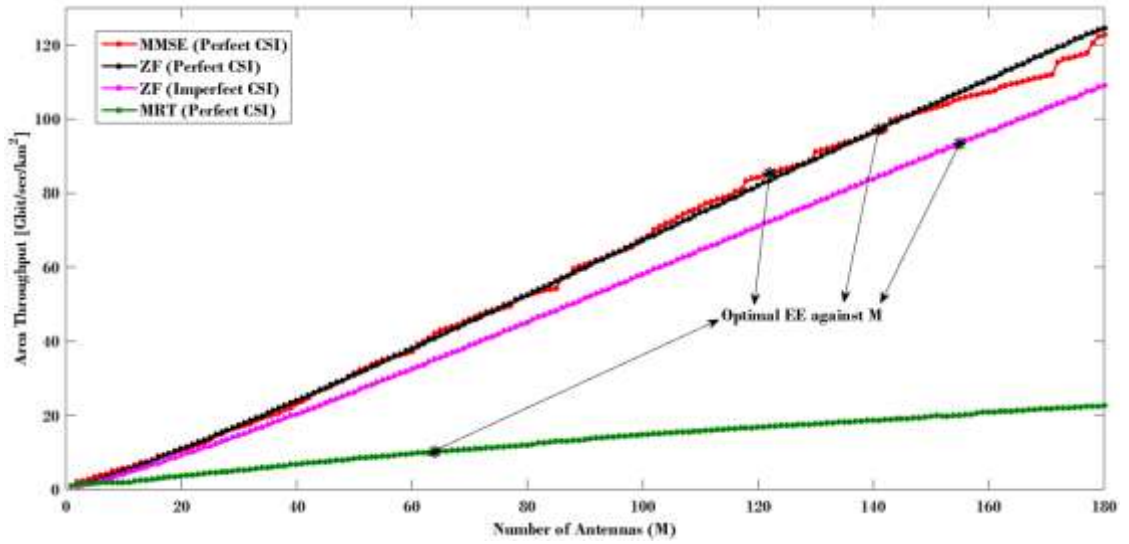

Figure 3.7 *Area-throughput in single-cell setup.*

It verifies that massive MIMO with appropriate interference mitigation linear pre-coding methods can deliver exceptional area throughput and EE. In sharp contrast, big

deployments of transmit antennas while using MRT/C processing significantly limit both jobs, either the EE or the area throughput.

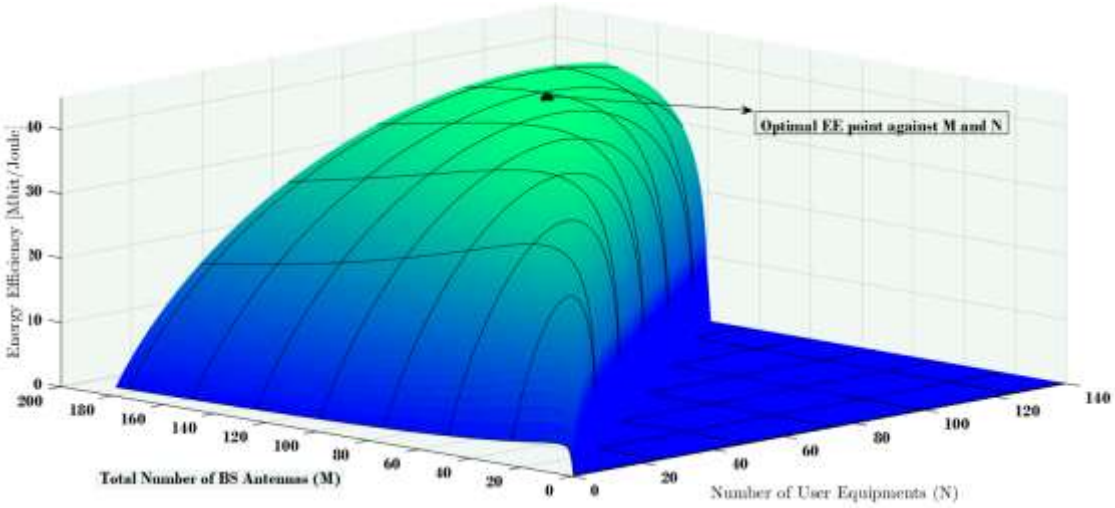

Figure 3.8 *Appropriate number of antennas and users to realize optimal values of EE.*

In comparing the numerical values of plots in Figure 3.7 and the results of previous work, the given plots demonstrate that the proposed model gives noteworthy progress in terms of area throughput. Figure 3.8 provides a 3D plot to show the results of an appropriate number of antennas and user equipment to realize optimal values of EE. The optimal EE is achieved at M=160 that are serving around N=100 UE efficiently. Table 3.4 shows the comparison of area throughput of the literature. The improvement of area throughput can be significantly observed from the generated numerical results.

Table 3.4 *Comparison of area throughput.*

Linear Processing Scheme	**Results (Proposed Model)**	**Results of *[16] ,[116]***
	EE	EE
ZF with Perfect CSI	21.0	15.0
MMSE with Perfect CSI	82.0	60.0
ZF with Imperfect CSI	80.0	62.0
MRT with Perfect CSI	97.0	73.0

3.5 Summary

This chapter examined massive MIMO systems to ensure optimum EE and area throughput gains. The system computed average data rates for UL and DL communications and then proposed an essentially applicable, less complex, and energy-efficient power consumption model. It then investigated an extremely optimal power distribution scheme to produce significant EE and area throughput improvement in a single cell situation. The simulation results have substantial ramifications.

CHAPTER 4
PERFORMANCE EVALUATION OF SPECTRAL EFFICIENCY

4.1 Introduction:

Advancement in Massive MIMO systems is a key factor in encouraging the 5G network as it has high spectral and energy efficiencies having multiple transmitter and receiver antennas [129], [130], [131]. Recently many researchers have been enthusiastic about studying massive MIMO networks, whereas channel estimation, the UL and DL transmission, SE, energy augmentation models have been evaluated in the last decade. The mathematically modelling of the UL and DL signals communication and different channel estimation schemes for the UL transmission are computed for the SE. It is also compared the complexity and SE of the channel mentioned above estimators. The second objective is to provide an accurate MR precoding model for DL transmission for enhancing the SE.

Chapter objectives are well accomplished and summarized.

- A multi-cell scenario is considered where the UL and DL transmission models are considered with inter-cell interference and noises.
- MMSE, EW-MMSE, and LS channel estimators' schemes are modelled to carry the max. SE in UL transmission. However, MMSE is better than EW-MMSE and LS because of high SE and better interference mitigation practice.
- MR precoding model for DL transmission for enhancing the SE is evaluated in the last section.

The computed results of the proposed models are appropriate to endorse the massive MIMO systems that can enhance SE in a 5G cellular network. This chapter is structured as follows. Section 4.2 is an illustration of a massive MIMO system model for both UL and DL communication. In section 4.3.1, the UL SE with the MMSE estimator is compared with EW-MMSE and LS. Section 4.3.2 the MR precoding scheme is modelled for the augmentation of DL SE. Finally, key insinuation conclusions are drawn in Section 4.5. The Table. 4.1 show the symbolic represents used in this chapter.

Table 4. 1 *Symbolic representation.*

Symbols	***Description***
$\mathbb{E}(.)$	Expectation
$\|.\|$ and $\|\|.\|\|$	Absolute values and Euclidean norm
$\boldsymbol{I}_K$	K × K identity matrix
Ψ	Pilot signal sequence
n_j^{dl}	additive receiver noise
B	Bandwidth
$T_{coh}\ and\ B_{coh}$	Coherence Time & Coherence Bandwidth
$w_{lr} \in C^{M_l}$	Assigned as transmit precoding vector
$y_j^{UL} \epsilon\ \mathbb{C}$ and $y_j^{DL} \epsilon\ \mathbb{C}$	Transmission symbols (UL and DL)
$\frac{\tau_{UL}}{\tau_{coh}} and\ \frac{\tau_{DL}}{\tau_{coh}}$	UL transmission and DL transmission pre log factor

4.2 System Model for Uplink and Downlink Massive MIMO

This section includes the specifications of a multicell massive MIMO system covering the UL and DL transmission models, linear processing schemes, and channel models. The systems describe the UL and DL MIMO transmission in cell j and cell l as illustrated in figure.1. Channel vectors h_{lk}^{j} and h_{jk}^{l} are considered in UL and DL respectively between the BS j and UE k. The UL data transmission signal has considered the desired signal, inter-cell interference, and noise. On the other hand, DL data transmission signal has added the part of the intra-cell signal.

On the consideration mentioned above, the following segments are modelled.

4.2.1 Uplink

In this stage, user K transmits the data to one of the correspondence BSs. Let the users K have the transmitted symbol vector in the l cell is $s_l = \left[s_{l,1}\ \ s_{l,2} \dots \dots \dots s_{l,k}\right]$ and the received UL signal $y_j^{UL} \epsilon\ \mathbb{C}^M$ from the users K at BSj can be written as:

$$y_j^{UL} = \sqrt{\rho ul} \sum_{l=1}^{L} \sum_{K=1}^{K_i} \mathrm{h}_{lk}^{j} S_{lk}^{UL} + \mathrm{n}_j^{UL} \tag{4.1}$$

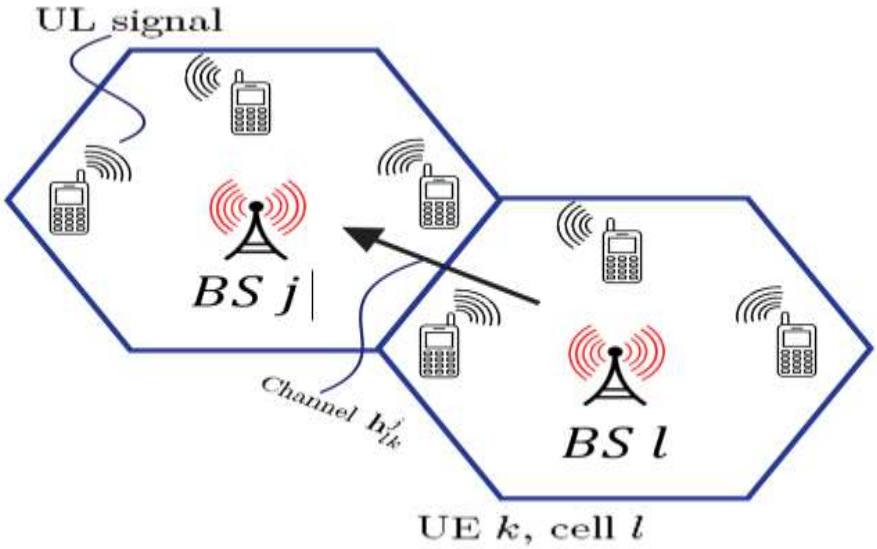

Figure 4.1 Illustration of the UL Massive MIMO transmission in cell j and cell l.

Where n_j^{UL} is an additive receiver noise denotes $n_j^{UL} \sim \mathcal{CN}\left(O_{M_j}, \sigma_{UL}^2 \mathrm{I}_{M_j}\right)$ while O_{M_j} is zero mean and σ_{UL}^2 is variance. Then the UL signal in cell l denote $s_{lk}^{UL} \epsilon\, \mathbb{C}$ has power $p_{UL,lk} = \mathbb{E}\left\{\left|s_{lk}^{UL}\right|^2\right\}$ and $\rho_{UL} > 0$ means the UL SNR and UL signal $y_j^{UL} \epsilon\, \mathbb{C}^M$ is given as:

$$y_j^{UL} = \sqrt{\rho_{UL}} \sum_{K=1}^{K_j} \mathrm{h}_{jk}^{j} S_{jk}^{UL} + \sqrt{\rho_{UL}} \sum_{\substack{l=1 \\ i \neq j}}^{L} \sum_{K=1}^{K_i} \mathrm{h}_{li}^{j} S_{li}^{UL} + \mathrm{n}_j^{UL} \tag{4.2}$$

whereas, $\sqrt{\rho_{UL}} \sum_{K=1}^{K_j} \mathrm{h}_{jk}^{j} S_{jk}^{UL}$ is desired signal and $\sqrt{\rho_{UL}} \sum_{\substack{l=1 \\ i \neq j}}^{L} \sum_{K=1}^{K_i} \mathrm{h}_{li}^{j} S_{li}^{UL}$ is inter-cell interference. The BS as dedicated in cell j selects the receive combining vector $y_j^{UL} \epsilon\, \mathbb{C}^M$ at the time of data transmitting for separating the desired UE signal from the interferences and can be written as:

$$\begin{aligned} V_{jk}^{UL} y_j^{UL} = {} & \sqrt{\rho_{UL}}\, V_{jk}^{UL} \mathrm{h}_{jk}^{j} s_{ji}^{UL} + \sqrt{\rho_{UL}} \sum_{\substack{i=1 \\ i \neq k}}^{K_j} V_{jk}^{UL} \mathrm{h}_{jk}^{j} s_{ji}^{UL} \\ & + \sqrt{\rho_{UL}} \sum_{\substack{i=1 \\ i \neq j}}^{L} \sum_{i=1}^{K_i} V_{jk}^{UL} \mathrm{h}_{jk}^{j} s_{ji}^{UL} + n_j^{UL} \end{aligned} \tag{4.3}$$

Then the desired signal becomes $\sqrt{\rho_{UL}}\, V_{jk}^{UL} \mathrm{h}_{jk}^{j} s_{ji}^{UL}$ with intra-cell signals and inter-cell interference. The selection of combing vector modelling in SE is analyzed with the different combining schemes in the next section.

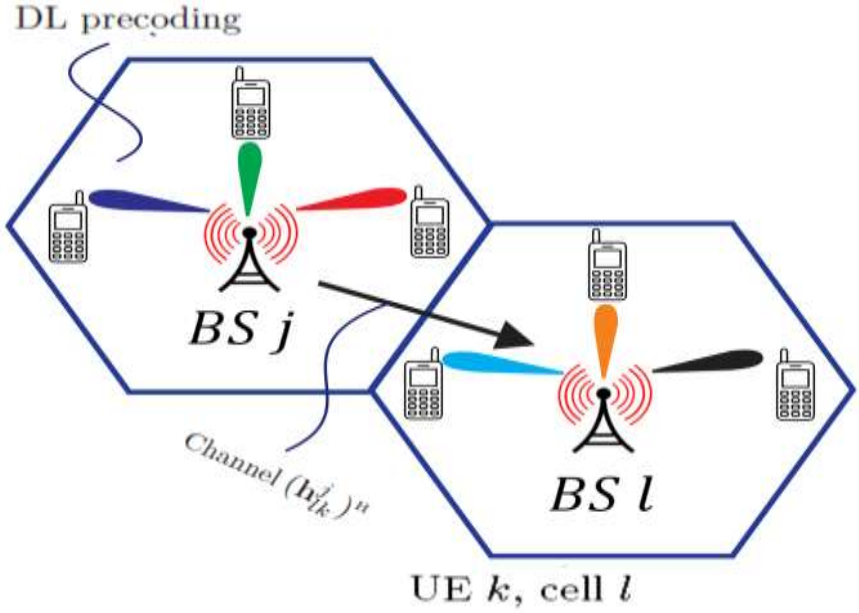

Figure 4.2 *Illustration of the DL Massive MIMO transmission in cell j and cell l.*

4.2.2 Downlink

As per Massive MIMO illustration in Figure 4.2 for dl transmission, BS j transmits the signal in cell l that is written as:

$$x_l = \sum_{i=l}^{k_l} W_{lir_{li}} \tag{4.4}$$

Where $w_{lr} \in C^{M_l}$ is assigned as transmit precoding vector. Then the received signal $y_j^{DL} \epsilon\, \mathbb{C}$ is modelled as:

$$y_j^{DL} = \sqrt{\rho_{DL}} \sum_{l=1}^{L} (h_j^{DL})^H xl + n_j^{DL} \tag{4.5}$$

The symbol vector denoted as $x_l = [x_{l,1} \;\; x_{l,2} \ldots\ldots\ldots x_{l,k}]$ and n_j^{DL} is an additive receiver noise. The term $\sqrt{\rho_{DL}} > 0$ means the SNR of DL. Then y_j^{DL} can be written as:

$$y_j^{DL} = \sqrt{\rho_{DL}} \sum_{l=1}^{L} \sum_{i=1}^{K_l} (h_{jk}^{DL})^H W_{lirli} + n_j^{DL} \tag{4.6}$$

$$y_j^{dl} = \sqrt{\rho_{DL}}\ (h_{jk}^{j})^H w_{jkr_{jk}} + \sqrt{\rho_{DL}}\ \sum_{\substack{i=1 \\ i \neq k}}^{K_j} (h_{jk}^{j})^H W_{jir_{ji}} + \sqrt{\rho_{DL}}\ \sum_{\substack{l=1 \\ l \neq j}}^{L} \sum_{i=1}^{K_l} (h_{jk}^{DL})^H W_{lir_{li}} + n_j^{DL} \tag{4.7}$$

Then the desired signal becomes $\sqrt{\rho_{DL}}\ (h_{jk}^{j})^H w_{jkr_{jk}}$ for the dl with intra-cell signals and inter-cell interference. In the next section, the selection of transmitting precoding vectors in terms of SE is analyzed with the different precoding schemes.

4.3 Methodology and Calculations

M-MMSE, S-MMSE, RZF, ZF, and MR combiner and precoder are used in this model for SE of UL and DL, respectively. The enhancement in SE for the given system and optimized modeling are the main aims of this chapter. The methodology for the SE in MIMO systems in which proposed estimators optimize the SE.

The first comparison of different estimators is made by estimating MMSE, EW-MMSE, and LS channel. Although the LS and EW-MMSE are less complex in computing, the loss in SE incurred by these estimators is not ignorable, as discussed. In contrast, MMSE is preferred as it has better SE than complexity [104]. Proposed numerical equations test different combing and precoding schemes for SE of UL and DL transmissions after selecting MMSE channel estimation. The computational flow of the model is shown in figure 4.3. The UL data and channel estimation are calculated in the first two steps. Steps 3 and 4 are the computation stage of different combing and precoding schemes with the same vectors. The average sum of SE per cell is optimized for UL and DL in step 5 while the data is still not over, then the computation is again

computed. In this way, the average sum of SE per cell is expended as per the following stages:

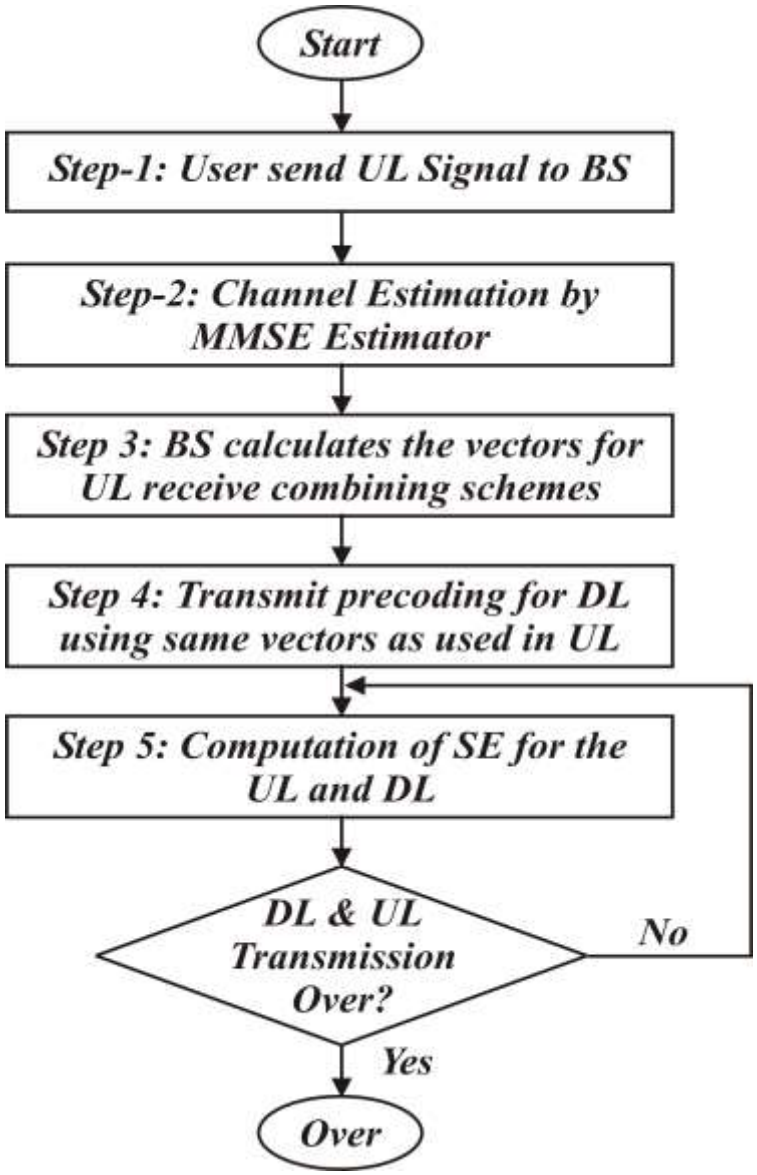

Figure 4.3 *Computational flow chart the model.*

4.3.1 Channel Estimation:

In dedicated UL, each cell transmits a pilot sequence for allowing the BSs to compute H_{jj} of their local channel H_{jj} while the sequence is mutually orthogonal. The channel estimation is based on random variables, and the statistical distribution of variable are taken into account. The received signal correlates the pilot sequence, and MMSE estimate the channel vector $\hat{h}_{li}^{j}$, given as:

$$y_{jk}^{tr} = \hat{h}_{UL}^{j} + \sum_{l \neq j} \hat{h}_{ULi}^{j} + \frac{1}{\sqrt{\rho tr}} n_{jk} \tag{4.8}$$

and

$$\hat{h}_{ULi}^{j} = \sqrt{p_{ULi}} R_{ULi}^{j} \Psi_{ULi}^{j} Y_{jULi}^{p} \tag{4.9}$$

where Y_{jUL}^{p} is the UL pilot transmission and pilot sequence become:

$$\Psi_{ULi}^{j} = \left(\sum_{(v,i') \in p_{UL}} pvi'^{\tau_r} R_{ULl'i'}^{j} + \sigma_{ULi}^{2} I_{M_j} \right)^{-1} \tag{4.10}$$

Where the Estimation error is $\hat{h}_{ULi}^{j} = h_{ULi}^{j} - \hat{h}_{ULi}^{j}$ has correlation matrix $C_{ULi}^{j} = \mathbb{E}\{\hat{h}_{ULi}^{j} (\hat{h}_{ULi}^{j})^{H}\}$ given as:

$$C_{ULi}^{j} = R_{ULi}^{j} - p_{ULi} R_{ULi}^{j} \Psi_{ULi}^{j} R_{ULi}^{j} \tag{4.11}$$

The MMSE is estimated by invoking the orthogonal property, and the estimated error is statistical independent of $\hat{h}_{UL}^{j}$. As per the pilot communication phenomenon, UEs with the same pilot sequence for the transmission can mutually pollute the channel estimation. Although channels are statistically independent, the interference reduces the estimation quality by increasing MSE and making the channel estimation statistically dependent. Above channel, estimation can mitigate the interference of UEs that practice the same pilot. The massive MIMO systems have a considerable influence over conventional networks due to large numbers of UEs having pilot sequences that can easily suppress the interference. Besides, the MMSE estimator minimizes the MSE of the channel estimate, given as:

$$\mathbb{E}\left\{ \left\| \mathrm{h}_{ULi}^{j} - \hat{\mathrm{h}}_{ULi}^{j} \right\|^{2} \right\} = \mathbb{E}\left\{ \left\| \hat{\mathrm{h}}_{ULi}^{j} \right\|^{2} \right\} = \mathbb{E}\left\{ \mathrm{tr}\left(\hat{\mathrm{h}}_{ULi}^{j} \left(\hat{\mathrm{h}}_{ULi}^{j} \right)^{u} \right) \right\} = \mathrm{tr}\left(C_{ULi}^{j} \right) \tag{4.12}$$

The cell j and cell l are used for the $UE\ k$ and ULi for the interference respectively, and the correlation matrix at BS j is:

$$\mathbb{E}\left\{\hat{\mathrm{h}}_{jk}^{j}\left(\hat{\mathrm{h}}_{ULi}^{j}\right)^{u}\right\} = \begin{cases}\sqrt{p_{ULi}P_{jk}}R_{jk}^{j}\Psi_{ULi}^{j}R_{ULi}^{j} & (UL,i)\in\mathcal{P}_{jk}\\ O_{M_j\times M_j} & (UL,i)\notin\mathcal{P}_{jk}\end{cases} \tag{4.13}$$

And the antenna correlation coefficient is written as:

$$\begin{aligned}&\frac{\mathbb{E}\left\{\left(\mathrm{h}_{ULi}^{j}\right)^{u}\mathrm{h}_{ULi}^{j}\right\}}{\sqrt{\mathbb{E}\left\{\left\|\mathrm{h}_{jk}^{j}\right\|^{2}\right\}\mathbb{E}\left\{\left\|\mathrm{h}_{ULi}^{j}\right\|^{2}\right\}}}\\ &=\begin{cases}\dfrac{\mathrm{tr}\left(R_{ULi}^{j}R_{jk}^{j}\Psi_{ULi}^{j}\right)}{\sqrt{\mathrm{tr}\left(R_{jk}^{j}R_{jk}^{j}\Psi_{ULi}^{j}\right)\mathrm{tr}\left(R_{ULi}^{j}R_{ULi}^{j}\Psi_{ULi}^{j}\right)}} & (UL,i)\in\mathcal{P}_{jk}\\ & (UL,i)\notin\mathcal{P}_{jk}\end{cases}\end{aligned} \tag{4.14}$$

Whereas, $\mathbb{E}\left\{\left(\mathrm{h}_{li}^{j}\right)^{u}\mathrm{h}_{li}^{j}\right\}=0$ for all UEs with $(UL,i)\neq(j,k)$. The expression of non-zero expectation is carried out from the UL transmission section and taking into account all the consideration with $(UL,i)\in\mathcal{P}_{jk}$ while channel vector is $y_{jk}^{p}=y_{jULi}^{p}$, written as $\mathbb{E}\{y_{jULi}^{p}\left(y_{jULi}^{p}\right)^{u}\}=\tau_{p}\left(\psi_{ULi}^{j}\right)^{-1}$ and the normalized MSE (NMSE) written as:

$$\mathrm{NMSE}_{UL}^{j}=\frac{\mathrm{tr}\left(C_{UL}^{j}\right)}{\mathrm{tr}\left(R_{UL}^{j}\right)} \tag{15}$$

This expression is used for the comparison of the estimation quality using different estimation schemes in different scenarios. The MMSE estimation provides enough statistical information for the UL data transmission that can help in decoding. This computation has required an inverse matrix of Ψ_{ULi}^{j} and makes the method very complex as attached large antennas with huge numbers of users [132]. This provokes us to solve for the simpler calculations and the estimation that is EW-MMSE. Lemma 1 is an EW-MMSE estimation with the statistics of the estimates. The assumption is made on the correlation matrix R_{ULIi}^{j} that depends on $A_{ULi}^{j}|_{mm}$ diagonal.

Lemma 1. If base l uses an EW-MMSE estimation where the channel is estimated between users k in cell l. Although each element can be estimated by MMSE, the EW-MMSE estimates the vectors with error and vectors without error.

$$A_{ULi}^{j}|_{mm} = \frac{\sqrt{p_{ULi}}|R_{ULIi}^{j}|_{mm}}{\sum_{(l',i')\epsilon p_{li}} p_{UL'i'}\tau_p|R_{l'i'}^{j}|_{mm} + \sigma_{UL}^{2}} \; m = 1, \ldots \ldots .. M \tag{4.16}$$

This is quite simpler in computational compared to MMSE, except in the case of diagonal spatial correlation matrices where each channel element estimates it separately. It is notable that A_{ULi}^{j} reduces the complexity. The EW-MMSE is obtained as:

$$\text{MSE} = \text{tr}\,(R_{ULi}^{j}) - \sum_{m-1}^{M} \frac{p_{ULi\tau_p(|R_{ULi}^{j}|mm)^2}}{\sum_{(UL',i')\epsilon p_{ULi}} p_{UL'i'}\tau_p|R_{UL'i'}^{j}|_{mm}+\sigma_{UL}^{2}} \tag{4.17}$$

In the case of noise-free calculation, then the LS channel estimator is considered [133] as it is very simple and low complexity. The LS channel estimator is estimated in Lemma 2.

Lemma 2. In this model y_{jULi}^{pi} having the desired channel $\sqrt{p_{ULi}}\tau_{pi}\hat{\mathrm{h}}_{ULi}^{j}$ in cell l and $\hat{\mathrm{h}}_{ULi}^{j}$is an LS estimator of h_{ULi}^{j}. MSE deviation is obtained as $\left\|y_{jULi}^{pi} - \sqrt{p_{ULi}}\tau_{pi}\hat{\mathrm{h}}_{ULi}^{j}\right\|^{\mathbf{2}}$, $\hat{\mathrm{h}}_{ULi}^{j}$ is written as:

$$\hat{\mathrm{h}}_{li}^{j} = \frac{1}{\sqrt{p_{ULi}}\tau_{pi}} y_{jULi}^{pi} \tag{4.18}$$

The LS estimators become simple as discussed $\mathbf{A}_{ULi}^{j} = \frac{1}{\sqrt{p_{ULi}}\tau_{pi}}\mathbf{I}_{M_j}$ and the complexity of the LS estimator is proportional to the Mj. As per equations called in Lemma 1, the MSE written as:

$$\text{MSE} = \text{tr}\left(\sum_{(UL',i')\in\frac{\mathcal{P}i_{ULi}}{UL,i}} \frac{p_{UL'i'}}{p_{ULi}} R_{UL'i'}^{j} + \frac{\sigma_{UL}^{2}}{p_{ULi}\tau_{pi}}\mathrm{I}_{M_j}\right) \tag{4.19}$$

4.3.2 Uplink Spectral Efficiency with the Combing Schemes of MMSE Estimator:

In this part, the achievable SE of the UL is analyzed based on the MMSE estimator with different receive combining schemes. As earlier discussed, a signal $y_j^{ul} \epsilon \mathbb{C}^M$ is received at BSj and the UL signal in cell l from UE k is S_{jk}^{ul}s having the power of $p_{ul,lk}$= $\mathbb{E}\left\{\left|s_{lk}^{ul}\right|^2\right\}$ and $\rho ul > 0$, then the total UL capacity of UE k in cell j is written as:

$$\mathrm{V}_{jk}^{\mathrm{UL}}\mathrm{y}_j = \mathrm{V}_{jk}^{\mathrm{UL}}\hat{\mathrm{h}}_{jk}^{j}\mathrm{s}_k + \mathrm{V}_{jk}^{\mathrm{H}}\tilde{\mathrm{h}}_{jk}^{j}\mathrm{s}_{jk} + \sum_{\substack{i=1 \\ i\neq k}}^{K_j}\mathrm{V}_{jk}^{\mathrm{H}}\mathrm{h}_{ji}^{j}\,\mathrm{s}_{jk}\sum_{\substack{l=1 \\ i\neq j}}^{L}\sum_{i=1}^{K_1}\mathrm{V}_{jk}^{\mathrm{UL}}\mathrm{h}_{Uli}^{j}\,\mathrm{s}_{li} + \mathrm{V}_{jk}^{\mathrm{UL}}\mathrm{n}_j \quad (4.20)$$

$$\mathrm{SE}_{jk}^{UL} = \frac{\tau_{ul}}{\tau_{coh}}\mathbb{E}\{\log_2(1+\mathrm{SINR}_{jk}^{\mathrm{L}})\} \quad (4.21)$$

Where $\frac{\tau_{ul}}{\tau_{coh}}$ is a pre-log factor is the ratio of UL data samples per coherence block.

Where the effective SNR becomes:

$$\mathrm{SINR}_{jk}^{\mathrm{UL}} = \frac{p_{jk}\left|\mathrm{v}_{jk}^{\mathrm{H}}\hat{\mathrm{h}}_{jk}^{j}\right|^2}{\sum_{l=1}^{L}\sum_{\substack{i=1 \\ (Ul,i)\neq(j,k)}}^{K_1} p_{Uli}\left|\mathrm{v}_{jk}^{\mathrm{H}}\hat{\mathrm{h}}_{jk}^{j}\right|^2 + \mathrm{v}_{jk}^{\mathrm{H}}\left(\sum_{l=1}^{L}\sum_{ULi=1}^{K_1} p_{Uli}\mathbf{C}_{Uli}^{j} + \sigma_{UL}^2\mathbf{I}_{M_j}\right)\mathrm{v}_{jk}} \quad (4.22)$$

As per $\mathrm{SINR}_{jk}^{\mathrm{UL}}$ used in (4.21) for UE k in cell j is optimized through multicell MMSE (M-MMSE) and M-MMSE combining vector for $k = 1, \ldots, K_j$ and $\mathbf{V}_{jk}^{\mathrm{ULM-MMSE}} = \left[\mathrm{v}_{j1} \ldots \mathrm{v}_j\mathrm{k}_j\right]$ is given as:

$$\mathbf{V}_{jk}^{\mathrm{ULM-MMSE}} = \mathrm{tr} * p_{jk}\left[\sum_{l=1}^{L}\sum_{i=1}^{K_1} p_{Uli}\left(\hat{\mathrm{h}}_{Uli}^{j}\left(\hat{\mathrm{h}}_{Uli}^{j}\right)^{u} + \mathbf{C}_{Uli}^{j}\right) + \sigma_{UL}^2\mathbf{I}_{M_j}\right]^{-1}\hat{\mathrm{h}}_{jk}^{j} \quad (4.23)$$

Which further leads to

$$\mathrm{SINR}_{jk}^{\mathrm{ULM-MMSE}} = \mathrm{tr} * p_{jk}\left(\hat{\mathrm{h}}_{Uli}^{j}\right)^{u}\left[\sum_{l=1}^{L}\sum_{\substack{i=1 \\ (l,i)\neq(j,k)}}^{K_1} p_{Uli}\,\hat{\mathrm{h}}_{Uli}^{j}\left(\hat{\mathrm{h}}_{Uli}^{j}\right)^{u} + \sum_{l=1}^{L}\sum_{i=1}^{K_1} p_{Uli}\mathbf{C}_{Uli}^{j} + \sigma_{UL}^2\mathbf{I}_{M_j}\right]^{-1}\hat{\mathrm{h}}_{jk}^{j} \quad (4.24)$$

This is the case when estimated channels are known, then it not only optimizes the SINR and also minimizes the MSE. The expression in (4.24) provides exact and optimized SINR for the massive MIMO systems. As discussed in the previous section, the reduction in complexity has to pay a reduction in SE, and MMSE has superior SE. In this regard, the different combining schemes of the MMSE channel estimator proposed in the previous section are shown in Table 4.2 with Computing combining vectors Multiplication. SE analysis is discussed in the next section.

Table 4.2 *Computational complexity per coherence block of different combining schemes.*

Scheme	**Reception Multiplication**	**Computing combining vectors Multiplication**
Multicell MMSE	$\tau_{UL}M_jK_j$	$\sum_{l=1}^{L}\frac{(3M_j^2+M_j)K_l}{2}+\frac{M_j^3-M_j}{3}+M_j\tau_p(\tau_p-K_j)$
Single-cell -MMSE	$\tau_{UL}M_jK_j$	$\frac{3M_j^2K_j}{2}+\frac{M_jK_j}{2}+\frac{M_j^3-M_j}{3}$
RZF	$\tau_{UL}M_jK_j$	$\frac{3K_j^2M_j}{2}+\frac{3K_jM_j}{2}+\frac{K_j^3-K_j}{3}$
ZF	$\tau_{UL}M_jK_j$	$\frac{3K_j^2M_j}{2}+\frac{K_jM_j}{2}+\frac{K_j^3-K_j}{3}$
MR	$\tau_{UL}M_jK_j$	----------

4.3.3 Downlink Spectral Efficiency

As related in (4.7), the DL signal received y_{jk}^{DL} in cell l is:

$$y_{jk}^{DL} = \underbrace{E\{\sqrt{\rho_{DL}}(h_{jk}^{DL})^H W_{jk}^{DL}\}r_{jk}^{DL}}+\underbrace{\sqrt{\rho_{DL}}\,((h_{jk}^{DL})^H W_{jk}^{DL}-E\{(h_{jk}^{DL})^H W_{jk}^{DL}\}r_{jk}^{DL})}+ \underbrace{\sqrt{\rho_{DL}}\sum_{\substack{i=1\\ i\neq k}}^{K_j}(h_{jk}^{DL})^H W_{ji}^{DL}r_{ji}^{DL}} + \underbrace{\sqrt{\rho_{DL}}\sum_{\substack{l=1\\ l\neq j}}^{L}\sum_{i=1}^{K_l}(h_{jk}^{l})^H W_{DLi}r_{DLi}}+\underbrace{n_{jk}} \quad (4.25)$$

Then the desired signal becomes $E\{\sqrt{\rho_{DL}}(h_{jk}^{DL})^H W_{jk}^{DL}\}r_{jk}^{DL}$ with average pre-coded channel $E\{(h_{jk}^{DL})^H W_{jk}^{DL}\}$ having the third and fourth terms as intra-cell interference and

inter-cell interference, respectively. The second term is also desired for the unknown channel. The Selection of transmitting precoding vectors in terms of SE is based on hardening bounding which can take any type of pro coding vector and channel estimation. The DL channel capacity in term of the SE of UE k in cell j as lower bound is:

$$\underline{SE}_{jk}^{DL} = \frac{\tau_{DL}}{\tau_{coh}} log_2\left(1 + \underline{SINR}_{jk}^{DL}\right) \text{ bit/Hz} \tag{4.26}$$

Where $\frac{\tau_{DL}}{\tau_{coh}}$ is a pre log factor ratio of samples of DL data and samples per coherent block and then $\underline{SINR}_{jk}^{DL}$ is:

$$\underline{SINR}_{jk}^{DL} = \frac{\rho_{jk}|E\{W_{jk}^H h_{jk}^{DL}\}|^2}{\sum_{l=1}^{L}\sum_{i=1}^{K_l}\rho_{DLi}E\{|W_{DLi}^H h_{jk}^l|^2\} - \rho_{jk}|E\{W_{jk}^H h_{jk}^{DL}\}|^2 + \sigma_{DL}^2} \tag{4.27}$$

In (4.26), $\underline{SE}_{jk}^{DL}$ refers $\underline{SINR}_{jk}^{DL}$ as effective SINR of fading channel related to UE k in cell j. $\rho_{jk}|E\{W_{jk}^H h_{jk}^{DL}\}|^2$is the gain of the desired signal by the average precoded channel. $\rho_{DLi}E\{|W_{DLi}^H h_{jk}^l|^2\}$ is donates as the total power of all signals and $\rho_{jk}|E\{W_{jk}^H h_{jk}^{DL}\}|^2$is the power of the desired signal. The SE expression in (4.26) is computed for precoding based on the MMSE channel estimation computed in the previous section. If $W_{jk} = \frac{\hat{h}_{jk}^{DL}}{\sqrt{E\{t||\hat{h}_{jk}^{DL}||^2\}}}$ then $\underline{SINR}_{jk}^{DL}$ for MR precoding based on MMSE channel estimation is:

$$\underline{SINR}_{jk}^{DL} = \frac{\rho_{jk}^{DL} tr\left(R_{jk}^{DL}\Psi_{jk}^{DL}R_{jk}^{jDL}\right)p_{jk}^{DL}}{\underbrace{\sum_{l=1}^{L}\sum_{i=1}^{K_l}\frac{\rho_{DLi}tr\left(R_{lk}^l\Psi_{lk}^lR_{lk}^l\right)}{tr\left(R_{lk}^l\Psi_{lk}^lR_{lk}^l\right)}}_{} + \underbrace{\sum_{(l,i)\epsilon p_{jk}\setminus(j,k)}\frac{\rho_{DLi}p_{jk}\tau_p\left(R_{jk}^l\Psi_{lk}^lR_{lk}^l\right)}{tr\left(R_{lk}^l\Psi_{lk}^lR_{lk}^l\right)}}_{} + (} \tag{4.28}$$

Where $\Psi_{jk}^{DL}\Psi_{li}^{DL}$ define in (4.9) and (4.10) for UL as similar is here. In the denominator, the first term is non-coherent interference, and the second term is coherent interference having spatially uncorrelated factor $R_{li}^j = \beta_{li}^j I_{M_j}$. The SE of DL is analyzed in the next

section by taking the same combing vectors $\mathbf{V}_{jk}^{\mathrm{ULM-MMSE}} = \left[\mathrm{v}_{j1} \ldots \mathrm{v}_j \mathrm{k}_j\right]$ in precoding schemes based on MMSE channel are:

$$\mathbf{V}_{jk}^{\mathrm{DLM-MMSE}} = \left[\mathrm{v}_{j1} \ldots \mathrm{v}_j \mathrm{k}_j\right]$$

$$= \begin{cases} V_{JK}^{M-MMSE} & of\ \ M - MMSE\ precoding \\ V_{JK}^{S-MMSE} & of\ S - MMSE\ precoding \\ V_{jk}^{RZF} & of\ RZF\ precoding \\ V_{JK}^{ZF} & of\ \ ZF\ precoding \\ V_{JK}^{MR} & of\ \ MR\ precoding \end{cases} \tag{4.29}$$

4.4 RESULTS AND DISCUSSION

In this section, SE expression for UL and DL evaluated in previous sections are simulated and validated of a proposed scenario for the massive MIMO cellular network. The calculation of SE with M-MMSE, S-MMSE, RZF, ZF, MR combining and precoding schemes by taking M number of antennas having simulation parameters of Table 4.3.

In the first step, the two-cell network composed of $cell\ j\ and\ cell\ l$ assumes the Wyner model of interface signals and desired signals during inter-cell and intra-cell interferences. The ratio of inert-cell and intra-cell channel gain is formed and UL and DL sequences for the cell are computed. The second step generates random estimated channel vectors of desired UE in a cell, and BS is given by H_{lk}^{l}€ C^M up to k=1 to k=K for UL transmission. Same as UL, the DL channel response $(H_{lk}^{l})^H$ is generated by active and BS while the SE, SNR, and channels gain are also taken into account as computed. In the third step, the SE-EE relation is computed for the selection of M number of antennas by considering P_{CC}, and CP as computed. Fourth step computes the SE-EE relation for the selection of multiple UEs as formulated where MP_{CC}, CP_l, and K time UEs are considered. The change of EE concerning change in SE computes tradeoff scenario, and EE's derivate is taken by logarithm function-based approximation. The fifth step computes the combining schemes as multicell MMSE,

single-cell MMSE, RZF, ZF, and MR with their power consumption for the UL signal are driven. In the next step, the DL signal for computing the precoding vector uses the same vector as used in UL. The power consumed by the transmission of the UL and DL signals through the pilot sequence is computed. Step.7 computes the power consumption-based combing and precoding vectors by considering the P_{fix} consumed by transceiver (P_{tran}), P_{ch} consumed power by coder/decoder ($P_{c,d}$), load-dependent consumption ($P_{L,bH}$), and digital signal processing power (P_{DSP}). The last step of the simulation sequence generates the plots of different figures for SE-EE tradeoff with logarithm-based function approximation.

Table 4.3 *Simulation parameters.*

Simulation Parameter	**Values**
Required Bandwidth (B)	20MHz
Coherence Time (T_{Coh})	10msec
Maximum Distance /cell radius(r)	(200) meters
Maximum Antennas (M)	500
Channel attenuation (ω)	$10^{-3.5}$
UEs (K)	18
The effective SNR	−10 dB to 20 dB
Network layout	Square pattern
Receiver noise power	−94dBm
Samples per coherence block	$\tau_{coh} = 200$

The SE of UL and DL for BS and UEs according to listed parameters in Table 4.3 is simulated as per table sequence. Simulations are based on Figure 4.1, Tables 4.3 and 4.4, and the optimized result is discussed in the next section.

Table 4.4 *Sequence of simulation.*

Proposed Algorithm	
Step 1:	According to Table 4.3, Adjust the simulation parameters.
Step 2:	Randomly drop UEs in each cell and compute UL sequence
Step 3:	Generate random estimated channel vectors $\hat{h}_{jk}^{j}\left(\hat{h}_{ULi}^{j}\right)^{u}$
Step 4:	Compute receive combining vectors $\mathbf{V}_{jk}^{\mathrm{ULM-MMSE}} = \left[v_{j1} \ldots v_{j}k_{j}\right]$
Step 5:	compute DL sequence for precoding
Step 6:	Compute precoding vectors $\mathbf{V}_{jk}^{\mathrm{DLM-MMSE}} = \left[v_{j1} \ldots v_{j}k_{j}\right]$
Step 7:	if MMSE algorithm = true and resulting SINRUL as eq.22 and eq. 27 End
Step 8:	Compute SE for $\mathrm{SE}_{jk}^{UL} = \frac{\tau_{ul}}{\tau_{coh}}\mathbb{E}\{\log_2(1+\mathrm{SINR}_{jk}^{L})\}$ & $\underline{\mathrm{SE}}_{jk}^{DL} = \frac{\tau_{DL}}{\tau_{coh}}\log_2(1+\underline{\mathrm{SINR}}_{jk}^{DL})$ bit/Hz
Step 9:	Plot of Figures SE for multi-cell combining & Precoding schemes; M-MMSE, S-MMSE, RZF, ZF, MR

4.4.1 Channel Estimators Comparison

The full potential of massive MIMO systems cannot be achieved without selecting the best suitable channel estimation at the time of UL pilot transmission. As per the proposed scenario, BS j estimates, the channel of UE k and another cell transmits the same pilot signal. The effective SNR as per Table 4.3 is taken as it varied from −10 dB to 20 dB. Figures 4.4 and 4.5 show the number of complex multiplication and MMSE numbers versus the number of antennas in the multi-cell scenario with MMSE, EW-MMSE, and LS channel estimators. These estimators are numerically computed in section A of the methodology segment, while Lemma 1 and Lemma 2 are considered for the EW-MMSE and LS, respectively. As mentioned in [104], the MMSE channel estimator has superior SE compared to other estimators with greater computation

complexity. The statistical characteristics obtained from the MMSE estimator are fine as the Minimum means square error decreases gradually with the increment in effective SNR, as shown in Figure 4.5. It is tested in this model of channel estimation and found the same patron as termed in [104]. Meanwhile, this model is based on SE and required minimum MMMSE other than the complexity. In this regard, the result publicized in Figure 4.5 also depicts that can compute better SE for the proposed model while ignoring Figure 4.4 as the MMSE estimator is complex.

4.4.2 Results for SE of UL Combining Schemes

The results of SE with different combining schemes are shown in Figure 4.6. The proposed model has better improvement in SE as compared to previous work done in [104]. The SE of a system is gradually increased with the number of antennas and cells. Figure 4.6 demonstrates that multicell M-MMSE has greater SE than single-cell S-MMSE, increasing SE by increasing antennas. As literature highlights, the SE of UL massive MIMO systems intends to channel estimation instead of combing schemes. Meanwhile, the proposed model results are compared with the MMSE combining scheme of [104] after comprehensive numerical computation of channel estimation. The summary of improvement in SE with previous work is given in Table. 4.5, where the proposed MMSE estimator for multicell M-MMSE has great augmentation in SE compared to given combing schemes and M-MMSE given in [104].

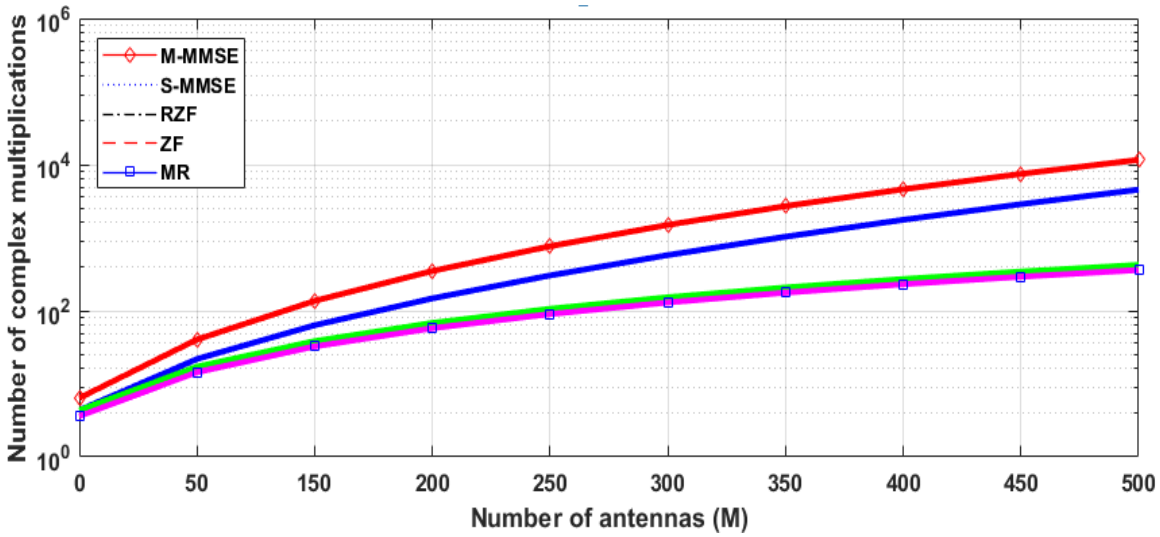

Figure 4. 4 *Results of numbers of complex multiplication versus numbers of antennas.*

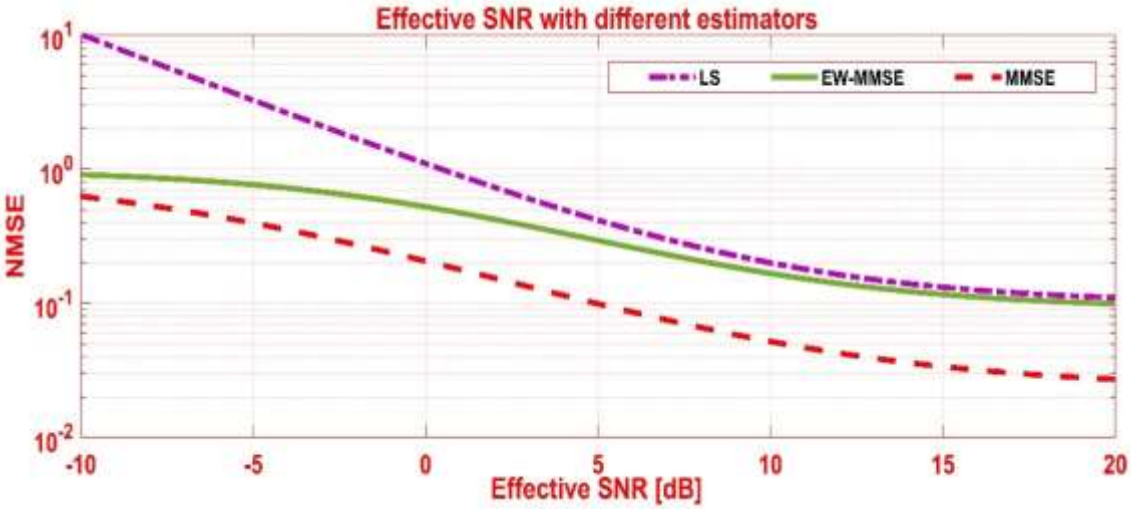

Figure 4. 5 *Results of MMSE versus numbers of antennas.*

Table 4.5 *Comparison: Results in Figure. 4.3 and past works.*

Combining Schemes	**Results (Proposed Model)**		**Results [104]**	
	EE bit/Hz per cell	M	EE bit/Hz per cell	M
M-MMSE	140	500	33	100
S-MMSE	105	500	------	----
RZF	90	500	-----	----
RF	90	500	-----	----
MR	52	500		----

4.4.3 Results for Spectral Efficiency of Downlink Precoding Schemes

Figure 4.7 illustrates the achievable average sum of SE per cell against the proposed massive MIMO system for five precoding schemes. As per K user and effective SNR is given in Table 4.3; the average SE per cell increases with the number of antennas grows. It indorses the dramatic benefits of implantation in large-scale antennas in BS. It is also observed that the desired average SE rate with MMSE precoding is approximately doubled with the MR scheme at the same configuration. The comparison of past work in Table 4.6 also shows that the MMSE precoding scheme is always better than other schemes and, ultimately, a top choice for a massive MIMO system.

To evaluate the performance (as per figure 4.7) of the proposed massive MIMO system precoder over the rest of the schemes, the simulation result of M-MMSE matched with from [125], [132], RZF with from [104], [125], RF with from [125], [104], and MR with from [104], [125], [132] are provided in Table 4.6. The numerical expression and simulation results show the achievable average sum of SE per cell is increased as compared to past work done [104], [125], [132] after considering the proposed numerical expression.

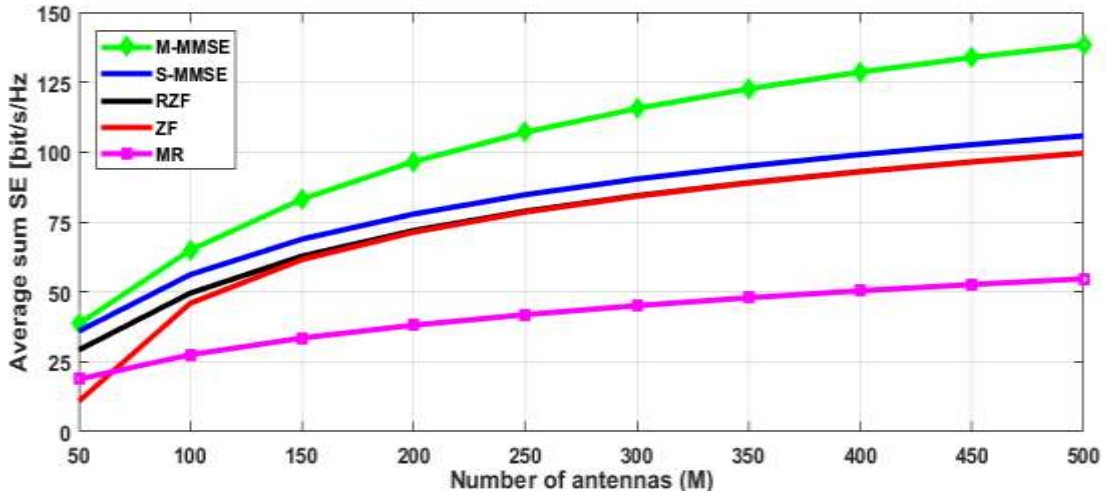

Figure 4. 6 *Desired Spectral Efficiency: Interference from other cell and noise added to the signal during UL Transmission.*

Table 4. 6 *Comparison: Results in figure 4.4 and past works.*

Precoding Schemes	***Results*** [104], [125], [132]		***Results*** [104], [125], [132]		***Results*** [104], [125], [132]		***Results (Proposed Model)***	
	EE bit/Hz per cell	M	EE bit/Hz per cell	M	EE bit/Hz per cell	M	EE bit/Hz per cell	M
M-MMSE	105	500	110	500	------	128	125	500
S-MMSE	----	500	------	500	------	128	110	500
RZF	------	500	108	500	110	128	105	500
RF	103	500	------	500	110	128	105	500
MR	58	500	45	500	85	128	65	500

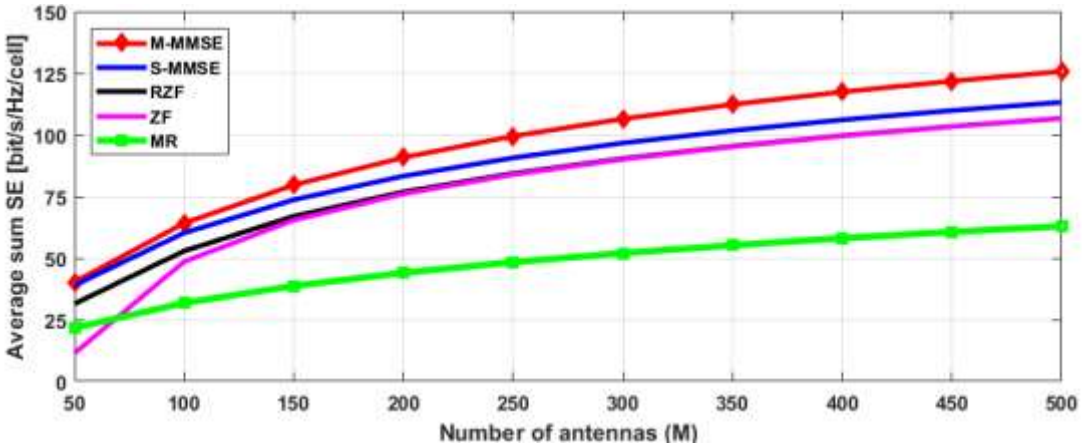

***Figure 4.** 7 Desired SE: Interference from other cells and noise added to the signal.*

4.5 Summary

This chapter has augmented an optimal SE per cell in the proposed massive MIMO system and computed MMSE channel estimation with different combining and precoding schemes. The first step is to figure out a multi-cell scenario, compute the expressions for UL and DL transmission, and then recommend a realistic, efficient, and applicable model. The computation of an MMSE channel estimator instead of EW-MMSE and LS is adopted to enhance the achievable average SE per cell based on the schemes mentioned above. The simulation results have revealed remarkable implications.

CHAPTER 5
Optimal Energy Efficiency Trade-Off with Spectral Efficiency and Throughput

5.1 Introduction

With the current revolution in the 5G wireless cellular network and its accomplishment with massive MIMO systems, the networks are ten times optimized for efficiency, SE , and throughput. The existing standards of 3G and 4G mobile networks are not meeting the challenging data rates, and large numbers of the antenna allow only up to 8 antenna ports [130]. The Massive MIMO has capabilities to handle the vibrant growth of applications having high data rate, the BS_s with massive numbers of antennas, and highly efficient services to users. The developments and advancements in this emerging technology shows that Massive MIMO has become a gold mine of research progressions in wireless communication sector [134]. Moreover, it provides a heightened efficiency, SE and throughput although managing a large number of antennas at the BS having a much complex system [135]. On the other hand, the average data rate for wireless data transmission has been doubling every 18 months since the last 30 years, while 5G mobile network standards are under consideration. The rapid advancement and hurried demand encourage the 33-46 GHz frequency band in the testing phase, where 5G is practising a 28 GHz frequency that has not yet been completed the standard [136]. At the same time, the old-fashioned wireless network systems have been facing complications such as meagre reliability, poor connection, less efficiency, low EE, low SE, and low throughput. An exponential raised in mobile-connected smart devices and smartphone users already exploited the existing cellular networks. Keeping in view the facts as mentioned above and Martin cooper's law states (both data and voice doubled every 2.5 years), there is a desperate need for high-quality services and optimized wireless networks to increase the capacity and connectivity as future necessitated [100]. In this regard, the EE of massive MIMO systems becomes a perilous consideration in 5G as it concerns large numbers of antennas and increments in-circuit PC. Massive MIMO systems can cater to all the technical aspects to optimize the EE by handling more antennas and reasonable circuit power conumption [137].

As multimedia applications increased and rapid demand for data rate in the last decade, researchers have focused on improving the SE of wireless networks and throughput caused by SE. Meanwhile, MIMO technology achieved more attention in 5G wireless communication networks by having a vast potential of achieving optimize SE in terms of magnitude [128], [138], [139]. As BS_s are equiped with several antennas and high data rate of fast trafic caused the power conusmptin more then the SE can be optimized by magnitude and acomplish all related concerns. A tradoff between SE and EE has been considerd a eesntial factor and there is a need of balancing between this combination. The different UL-DL models are developed to obtain optimal trade off through antenna selction approches, beamforming, and hndleing BSs well [140]. As already mentioned, the massive MIMO is the gifted model for 5G [141], and it gives higher ES and EE having thousands of antennas. Still, each antenna has assigned a dedicated frequency that includes digital-analogue and analogue-digital converters, noise amplifiers, etc. In this affection, large numbers of enabled antennas have been instigated more PC and increased the hardware cost in BS. Although there is a significant improvement in SE by providing more antennas for many users in the same radio channel frequency, the PC declines the EE. It has been experienced in previous systems that the depreciation of PC triggered low resolution in converters that are not beneficial. Therefore SE and EE are to be optimized so that optimal antennas can be attached with minimum PC. Massive MIMO has been recently discussed as a potential technique to empower network throughput and EE [120]. The throughput is pigeonholed a spatial multiplexing efficiency based on antennas' channel effects [119]. The use of more efficient hardware and the low-cost circuit has been reduced the throughput of the network due to the concerns of PC and hardware cost by large numbers of antenna. On the other hand, the EE of a network depends on less PC; therefore, a need for a tradeoff between throughput and EE becomes a critical concern.

The following are the main objectives of this chapter:

- A multi-cell scenario is considered where the UL and DL transmission models are computed based on the Wyner model.
- Optimized parameters are computed to select multiple antennas and multiple users by logarithm function-based approximation method and validate the optimized relation of SE-EE.

- The expression is formed in a massive MIMO network for the UL and DL models while combining and computed precoding schemes.
- Different combining and precoding schemes are used for total circuit power consumption as they optimize throughput-EE's relation.

The rest of the chapter is organized as follows: section. 5.1 highlights the complete work of the trade-off. Section.5.2 is based on the proposed system model for UL and DL, where the Wyner model is considered for the approximation. Section. 5.3 investigates EE-SE tradeoff by keeping in view the Wyner model for two cell scenarios and computed optimized relation to select multiple antennas and UEs. Section. 5.4 computes the complete realistic power and examines the combining and precoding schemes for UL and DL networks; ultimately, it refers to the optimized tradeoff between EE and throughput. Section. 5.5 and 5.6 are the results discussion with model validation and conclusion, respectively.

Table 5. 1 *Symbolic Representation.*

Symbols	Description
β_r	Ratio of inert cell and intra cell channels gain
$H_l^l \in \mathbb{C}$	Channel response
n_l^{UL}	Noise in UL
O_{M_j} and σ_{UL}^2	zero means and variance
n_j^{dl}	Additive receiver noise in DL
ρ_{UL}	Transmit power
σ_{UL}^2	Noise power
$p_{UL}\beta_l^l$, $p_{UL}\beta_j^l$	Signal power and interference power
CP_l	Circuit power
μ	PA efficiency
P_{fix}	Fix power consumed
P_{tran}	Transceiver power consumed
P_{ch}	Channel estimator power
$P_{c,d}$	Consumed power by coder/decoder
$P_{L,bH}$	Load dependent consumption
P_{DSP}	Digital signal processing power

5.2 System Model

The system model designates the UL and DL transmission models where the multicell scenario is taken into consideration. The Wyner model is assumed to model UL and DL transmission as analytical and straightforward tractable [142]. The two-cell network consisting Cell j and cell l as shown in Figure 1 describe the system model for the interfacing and desired signals while inter-cell and intra-cell interferences, and noise are also taken as weighty parameters. The notations are used in this network are β_l^l, $\beta_l^l, \beta_l^j, \beta_j^j, and\ \beta_j^l$ and each UE in cell l preserves the same average channel gain β_l^l from BS that is to be served. Similarly, average channel gain β_l^j is also similar for the BS of the cell j while each UE in cell j has same average gain as β_j^l and β_j^j are illustrated in figure. 1. Wyner model specifies that intra cell gain and inter cell gain are equal as assumed i.e. $\beta_l^l = \beta_j^j$ and β_l^j=β_j^l. The ratio of inert cell and intra cell channels gain are formed as.

$$\beta_r = \frac{\beta_j^l}{\beta_l^l} = \frac{\beta_j^l}{\beta_l^l} = \frac{\beta_j^l}{\beta_j^j} = \frac{\beta_j^l}{\beta_j^j} \tag{5.1}$$

The ratio of average gain used in the modeling β_r varies between 0-1 where β_r a value near 0 means weak intercell interference and β_r a value near to 1 means is strong. The channel response notations are used in this chapter are $H_l^l \in \mathbb{C}$ and $H_j^l \in \mathbb{C}$ and the relation with channel gain is written as:

$$H_n^l = \sqrt{\beta_n^l} \qquad \text{for n} = j\ , l \tag{5.2}$$

The following are the modeling of UL and DL transmission signals as per the facts mentioned earlier.

5.2.1 Uplink

The UL network is analyzed by assuming that k is the active UEs in each cell and then the channel response of k^{th} desired UE in a cell l and BS is given by $H_{lk}^l \in C^M$ up to $k = 1$ to $k = K$ and the channel response is:

$$y_l^{UL} = \sqrt{\rho ul}\left[\sum_{k=1}^{K} H_{lk}^{l} S_l^{UL} + \sum_{K=1}^{K} H_{jk}^{l} S_{jk}^{UL}\right] + \mathrm{n}_l^{UL} \tag{5.3}$$

Where S_{jk}^{UL} is the k^{th} UE signal in cell l and the receiver noise denotes $n_l^{UL} \sim \mathcal{CN}\left(O_{M_j}, \sigma_{UL}^2 \mathrm{I}_{M_l}\right)$. The terms O_{M_j} and σ_{UL}^2 are zero means and variance, respectively. $\rho_{UL} > 0$ is used for the UL SNR. The BS if cell l receives a signal transmitted by the desired UEs as K and UL signal $y_{lk}^{UL} \epsilon\, \mathbb{C}^M$ is given as:

$$\begin{aligned} V_{lk}^{UL} y_l^{UL} = \sqrt{\rho_{UL}}\, V_{lk}^{UL} H_{lk}^{l} s_{li}^{UL} + \sqrt{\rho_{UL}} \sum_{\substack{i=1 \\ i \neq k}}^{K_l} V_{lk}^{UL} H_{ln}^{l} s_{ln}^{UL} \\ + \sqrt{\rho_{UL}} \sum_{n=1}^{K_n} V_{lk}^{UL} H_{li}^{l} s_{jn}^{UL} + n_l^{UL} \end{aligned} \tag{5.4}$$

Where $\sqrt{\rho_{UL}}\, V_{lk}^{UL} H_{lk}^{l} s_{li}^{UL}$ considered as the desired signal, $\sqrt{\rho_{UL}} \sum_{\substack{i=1 \\ i \neq k}}^{K_l} V_{lk}^{UL} H_{ln}^{l} s_{ln}^{UL}$ term formed as intra cell interference, $\sqrt{\rho_{UL}} \sum_{n=1}^{K_n} V_{lk}^{UL} H_{li}^{l} s_{jn}^{UL}$ given as intercell interference, and n_l^{UL} is noise.

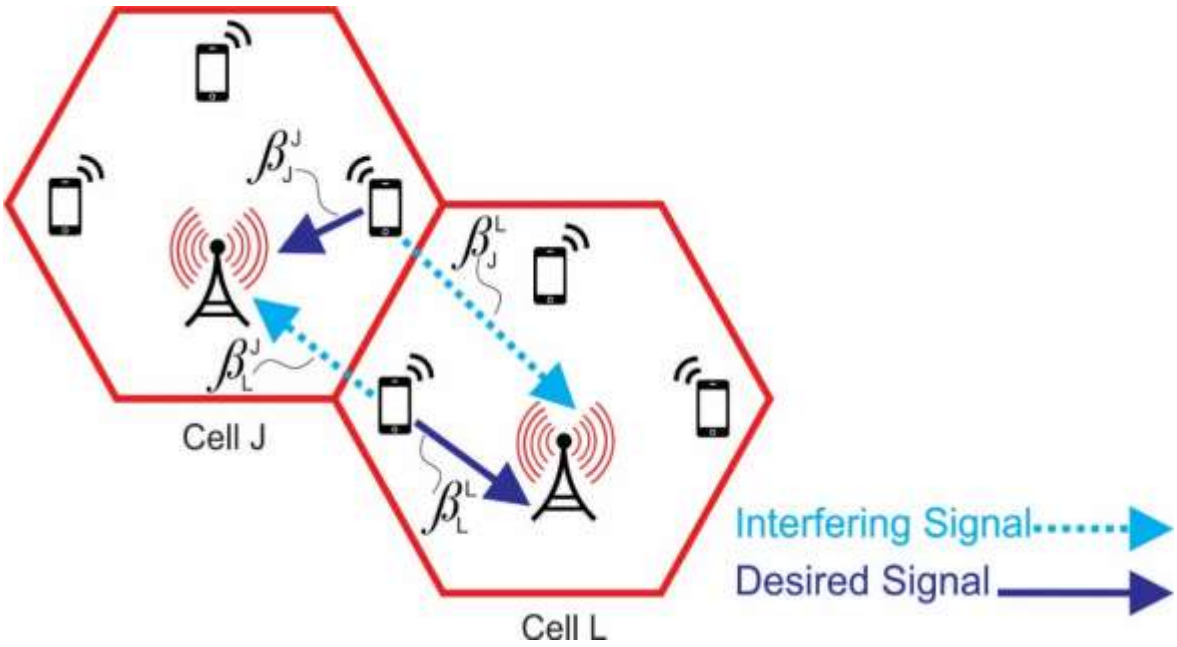

Figure 5. 1 *Illustration of desired and interfering signals for the UL transmission in cell l and cell j.*

Let the BS of cell l has channel response and SE of UL for the UE is:

$$SE_l = log_2\left[1 + \frac{1}{\beta_r + \frac{1}{SNR_l}}\right] \tag{5.5}$$

Where β_r is defined in Equation (5.1) and SNR_l is given as:

$$SNR_l = \frac{\rho_{UL}}{\sigma_{UL}^2}\beta_l^l \tag{5.6}$$

ρ_{UL} is used for transmitting power and σ_{UL}^2 is noise power. Considered Equations (5.1) and (5.6) for $\beta_r \neq 1$ then SE is formulated as:

$$SE_l = \mathbb{E}\left\{log_2\left(1 + \frac{p_l\left|H_l^l\right|^2}{p_l\sum_{k=1}^{k}\left|H_{jk}^l S_{jk}^{UL}\right|^2 + \sigma_{UL}^2}\right)\right\} \tag{5.7}$$

The Equation (5.5) is linked with power-related terms; then the equation is formed as:

$$1 + \frac{1}{\beta_r + \frac{1}{SNR_l}} = \frac{p_{UL}\beta_l^l}{p_{UL}\beta_j^l + \sigma_{UL}^2} \tag{5.8}$$

Where $p_{UL}\beta_l^l$, $p_{UL}\beta_j^l$, and σ_{UL}^2 are signal power, interference power, and noise power, respectively.

5.2.2 Downlink

As UL model is developed in the previous section based on the Wyner model as illustrated in Figure. 5.1 and this section defines the DL model for the enhancement of SE. Desired and interfering signals of DL in two cell scenarios are discussed, as shown in Figure 5.2, while the Wyner model is considered. The illustration average channel gain is discussed in the previous section. In the DL model, the K^{th} active UEs of each cell receives a signal send by serving BS using linear precoding schemes. Same as UL, the DL channel response of K^{th} active UEs of each cell receives a signal sent by serving BS is $(H_{lk}^l)^H$ and received DL signal in cell l is modelled as.

$$y_j^{dl}=\sqrt{\rho_{DL}}H_{lk}^{l})^{H}w_{lkr_{lk}}S_{lk}+\sqrt{\rho_{DL}}\sum_{\substack{i=1\\ i\neq k}}^{K_l}(H_{lk}^{j})^{H}W_{lir_{ji}}S_{li}+\sqrt{\rho_{DL}}\sum_{\substack{j=1\\ j\neq l}}^{L}\sum_{i=1}^{K_l}(H_{lk}^{DL})^{H}W_{lir_{li}}s_{ji}+n_l^{DL} \quad (5.9)$$

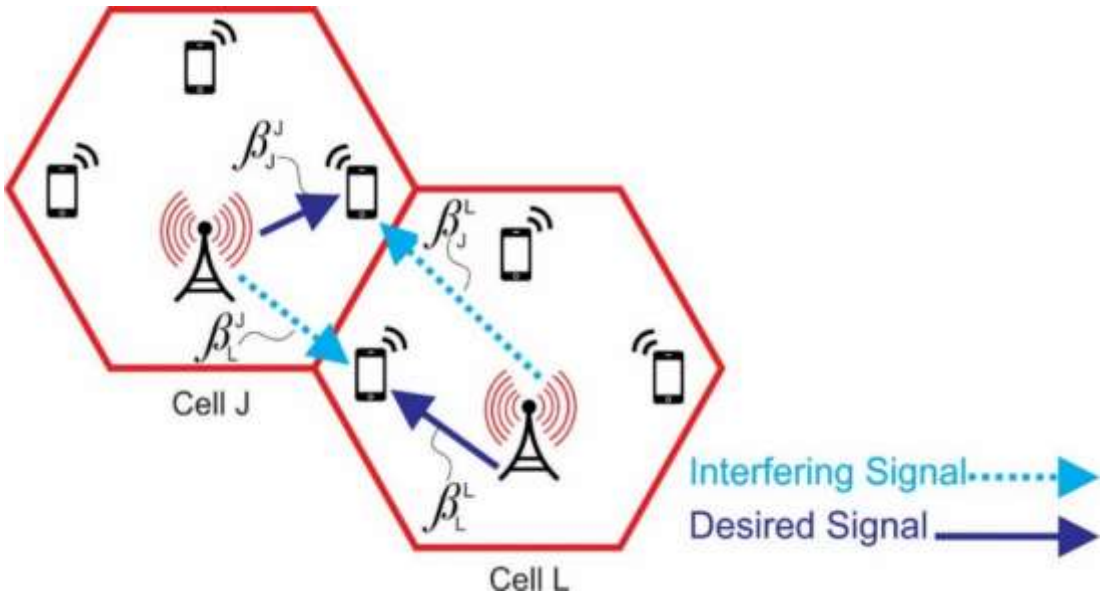

Figure 5. 2 Illustration of desired and interfering signals for the DL transmission in cell l and cell j.

Where $\sqrt{\rho_{DL}}H_{lk}^{l})^{H}w_{lkr_{lk}}s_{lk}$ is desired signal, with intra cell interference, intercell interference, and noise signals respectively. Moreover, $w_{lkr_{lk}} and\ s_{lk}$ are precoding vector and DL transmitted signal. As per Wyner model discussed in Equation (5.1) and Figure. 5.2 the β_r relation with SE becomes:

$$SE_l=\sum_{k=1}^{k}Log_2\left(1+\frac{M}{\sum_{\substack{i=1\\ i\neq k}}^{k}G(\varphi_{li}^{l})+\beta_r\sum_{i=1}^{k}G\left(\varphi_{ji}^{j}\right)+\frac{1}{SNR_l}}\right) \quad (5.10)$$

With precoding channels, a DL SE $[bit/s/Hz/cell]$ is formed as:

$$SE_l=\sum_{k=1}^{K}\mathbb{E}\left\{Log_2\left(1+\frac{p_l\left|H_l^l\right|^2}{p_l\sum_{\substack{k=1\\ i\neq k}}^{k}\frac{\left|H_{lk}^{l}H_{li}^{l}\right|^2}{\left|H_{li}^{l}\right|^2}+p_l\sum_{i=1}^{k}\frac{\left|H_{jk}^{l}S_{jk}^{UL}\right|^2}{\left|H_l^l\right|^2}+\sigma_{DL}^2}\right)\right\} \quad (5.11)$$

5.3 Energy Efficiency and Spectral Efficiency Trade off

As discussed in the literature, the SE increases with installing more BS antennas and several UEs in a cell, while this SE increment causes the raise in PC. This phenomenon decreases the overall EE; therefore a mechanism that can jointly increase the SE and EE is required. This section investigates the EE-SE tradeoff by keeping in view the Wyner model for two cell scenarios as illustrated in Figures. 5.1 and 5.2. The selection of multiple antennas and UEs for optimizing the tradeoff of EE-SE is discussed below.

5.3.1 Selection of Multiple BS Antennas

The first step in antenna selection is an assumption of active UE in cell l and having no interfering signal then SE in cell l is given as:

$$SE_l = log_2\left(1 + (M-1)\frac{\rho_{UL}}{\sigma_{UL}^2}\beta_l^l\right) = \log_2(1 + (M-1)SNR_l) \tag{5.12}$$

Where ρ_{UL} is a transmit power, σ_{UL}^2 is a noise power. To select numbers of the antenna (M) for the optimizing of EE, the circuit power (CP) is also evaluated as it increases when multiple antennas have been selected. In this case, the cell l is chosen to have circuit power CP_l then EE relation with M becomes with logarithm function-based approximation:

$$EE_l = \frac{B\log_2\left(1 + (M-1)\frac{\rho_{UL}}{\sigma_{UL}^2}\beta_l^l\right)}{\frac{1}{\mu}ETP + CP_l} \tag{5.13}$$

Where ETP is effective in transmitting power, and μ has a range of $0 < \mu \leq 1$ for the PA efficiency with bandwidth B.

$$EE_l = B\left(\frac{SE_l}{\frac{1}{\mu}ETP + CP_l}\right) \tag{5.14}$$

The expression below provides a link between EE and SE.

$$v_o = \frac{\sigma^2}{\mu\beta_0^0} \tag{5.15}$$

Equations. (5.13), (5.14), and (5.15), yields:

$$EE_l = B\left(\frac{SE_l}{(2^{SE_l}-1)\frac{\nu_0}{M-1}}\right) \tag{5.16}$$

Total power consumption also has M times the power consumption of circuit components (P_{CC}) power, where expression becomes.

$$EE_l = B\left(\frac{SE_l}{(2^{SE_l}-1)\frac{\nu_0}{M-1} + CP_l + MP_{CC}}\right) \tag{5.17}$$

By taking M number of antennas, P_{CC} circuit consumption, CP circuit power taken into account and given as:

$$EE_l \approx \frac{\mathrm{e}B}{(1+\mathrm{e})}\left(\frac{\log_2(M\,CP_l + MP_{CC})}{(CP_l + MP_{CC})}\right) \tag{5.18}$$

Where $\log_2(M\,CP_l + MP_{CC})$ is SE. The final expression of selection for multiple antennas is:

$$EE_l \approx \frac{\mathrm{e}B}{(1+\mathrm{e})}\left(\frac{SE_l}{(CP_l + MP_{CC})}\right) \tag{5.19}$$

5.3.2 Selection of Multiple User Equipment's

Similarly, as the numbers of UEs increased the same as the numbers of antennas, the SE increased with raises in power consumption that caused the reduction in EE. A Wyner model is shown in Figure. 5.1 with K antenna in both cells having relative channel gain in Equation (5.1), the SE of cell l is given as:

$$SE_l = \log_2\left(1 + \frac{M-1}{(K-1) + K\beta_r + \frac{\sigma_{UL}^2}{\rho_{UL}\beta_l^l}}\right) \tag{5.20}$$

As SE formed in Equations. (5.5,5.6,and 5.8) the expressions become:

$$p_{UL} = \left(\frac{M-1}{(2^{SE_l}-1)} - K\beta_r + 1 - K\right)^{-1}\frac{\sigma_{UL}^2}{\beta_l^l\beta_0^0} \tag{5.21}$$

The tradeoff relation of EE-SE is formed in the below equation.

$$EE_l = B\frac{KSE_l}{K\left(\frac{M-1}{(2^{SE_l}-1)} - K\beta_r + 1 - K\right)^{-1} v_0 + CP_l + MP_{CC} + KP_{UE}} \tag{5.22}$$

The power consumption of M times BS (MP_{CC}), CP_l, and K time users UEs are considered in (5.22). Thus, the change of EE concerning change in SE can show the tradeoff scenario and, in this regard, the derivate of EE with respect to SE is taken by logarithm function-based approximation as:

$$\begin{aligned} &K\left(\frac{M-1}{(2^{SE_l}-1)} - K\beta_r + 1 - K\right)^{-1} v_0 + CP_l + MP_{CC} + KP_{UE} \\ &\quad = K\,SE_l\left(1 - \left(\frac{2^{SE_l}-1}{M-1}\right)K\beta_r - 1 + K\right)^{-2} \frac{v_0 \log_e(2)}{M-1} 2^{SE_l} \end{aligned} \tag{5.23}$$

Insert the Equation (5.23) into Equation (5.22) and expression forms as:

$$EE_l = B\frac{1}{\left(1 - \left(\frac{2^{SE_l}-1}{M-1}\right)K\beta_r - 1 + K\right)^{-2} \frac{v_0}{M-1} 2^{SE_l}} \tag{5.24}$$

5.4 Energy Efficiency and Throughput Tradeoff

In the previous section, the tradeoff between EE and SE is optimized, and only three power consumption terms are evaluated as $CP_l, MP_{CC},$ and KP_{UE} in (5.23). In this section, the trade-off of SE and throughput is formulated while the circuit power consumption Model and DL&DL models are taken into account. In the circuit power consumption model for evaluating the tradeoff between EE and throughput, the transmit power, circuit power consumed by hardware at the BS side, coding/decoding power, and digital signal processing power are considered. In this regard, the expression formed for the BS l in massive MIMO network as.

$$\mathrm{CP}_l = P_{\mathrm{fix}} + P_{tran} + P_{ch} + P_{c,d} + P_{L,bH} + P_{DSP} \tag{5.25}$$

The CP model considers the fixed power **(**P_{fix}), consumed by transceiver (P_{tran}), channel estimator power (P_{ch}), consumed power by coder/decoder ($P_{c,d}$), load-dependent consumption ($P_{L,bH}$), and digital signal processing power (P_{DSP}). The overall power consumed by $BS\ l$ for the $UL\ and\ DL$ combined the expression is given as.

$$P_{Sig} = P_{R,T} + P_{Com}^{UL} + P_{Pre}^{DL} \tag{5.26}$$

Where P_{Sig} is an overall power consumed in transmission and receiving of signal and $P_{R,T}$, P_{Com}^{UL}, and P_{Pre}^{DL} are transmitter/Receiver power, combining vectors, and precoding vectors consumed power, respectively. P_{Com}^{UL} and P_{Pre}^{DL} are further computed for combining and precoding vector respectively as elaborated in section.5.3 and written as.

$$P_{Com}^{UL} = \frac{7B}{\tau_{UL}L} K_l \tag{5.27}$$

$$P_{Pre}^{DL} = \frac{4B}{\tau_{DL}L} M_l K_l \tag{5.28}$$

Table 5. 2 *Illustration of Power consumed by BS for the signal processing with different combining/precoding vector computations.*

Scheme	**Transmitter & receiver Consumed power** $\boldsymbol{P_{R,T}}$	**Power consumed by Computing combining vectors** $\boldsymbol{P_{Com}^{UL}}$	**Power consumed by Computing precoding vector** $\boldsymbol{P_{Pre}^{DL}}$
Multicell MMSE	$\tau_c M_j K_j$	$\frac{7B}{\tau_{UL}L}\left[\sum_{l=1}^{L}\frac{\left(3M_j^2+M_j\right)K_l}{2}+\frac{M_j^3-M_j}{3}+M_j\tau_p\left(\tau_p-K_j\right)\right]$	$\frac{4B}{\tau_{DL}L} M_j K_j$
Single-cell -MMSE	$\tau_c M_j K_j$	$\frac{7B}{\tau_{UL}L}\left(\frac{3M_j^2K_j}{2}+\frac{M_jK_j}{2}+\frac{M_j^3-M_j}{3}\right)$	$\frac{4B}{\tau_{DL}L} M_j K_j$
RZF	$\tau_c M_j K_j$	$\frac{7B}{\tau_{UL}L}\left(\frac{3K_j^2M_j}{2}+\frac{3K_jM_j}{2}+\frac{K_j^3-K_j}{3}\right)$	$\frac{4B}{\tau_{DL}L} M_j K_j$
ZF	$\tau_c M_j K_j$	$\frac{7B}{\tau_{UL}L}\left(\frac{3K_j^2M_j}{2}+\frac{K_jM_j}{2}+\frac{K_j^3-K_j}{3}\right)$	$\frac{4B}{\tau_{DL}L} M_j K_j$
MR	$\tau_c M_j K_j$	$\frac{7B}{\tau_{UL}L} K_j$	$\frac{4B}{\tau_{DL}L} M_j K_j$

The illustration of combining schemes as multicell MMSE, single-cell MMSE, RZF, ZF, and MR with their power consumption for the UL signal is computed in Table.5.2 The same vectors are used for the precoding vector in the DL signal, where consumed power is also figured and written in Table. 5.2. The primary purpose of this section is

to compute a model for optimizing the tradeoff between EE and throughput while considering the power as mentioned above consumption model in all aspects. The power consumed in UL and DL signals by transmitting the pilot sequence can be written as.

$$TTP_l = \frac{\tau_{pi_l}}{\tau_{coh}} \sum_{k=1}^{k_l} \frac{1}{uUE_l} p_l + \frac{\tau_{UL}}{\tau_{coh}} \sum_{k=1}^{k_l} \frac{1}{uUE_l} p_l + \frac{\tau_{DL}}{\tau_{coh}} \sum_{k=1}^{k_l} \frac{1}{uUE_l} p_l \tag{5.29}$$

The total transmit power consist of the total transmit power of the pilot signal $\frac{\tau_{pi_l}}{\tau_{coh}} \sum_{k=1}^{k_l} \frac{1}{uUE_l} p_l$, total transmit power of UL signal $\frac{\tau_{UL}}{\tau_{coh}} \sum_{k=1}^{k_l} \frac{1}{uUE_l} p_l$, and total transmit power of DL signal $\frac{\tau_{DL}}{\tau_{coh}} \sum_{k=1}^{k_l} \frac{1}{uUE_l} p_l$. The simulation parameters and results are discussed in the next section.

5.5 Results and Discussions

This section simulates and evaluates SE, EE, and Throughput expression for UL and DL. The calculation of throughput with M-MMSE, S-MMSE, RZF, ZF, MR combining and precoding schemes by taking M number of antennas, K numbers of UEs are considered. The optimal tradeoff of EE with SE and throughput is discussed in detail. The model is simulated in MATLAB, and the simulation sequence is illustrated in Table. 5.3.

5.5.1 Energy Efficiency and Spectral Efficiency Tradeoff

As computed in Equation (5.16), the CP_l increases with M times in the selection of multiple antennas and Figure. 5.3 illustrates the SE-EE tradeoff. The x-axis represents the SE in $Bit\ /s/Hz$ and the y-axis represents the EE in $bit/joule$. The results of Figure 5.3 are elaborated in Table.5.4 where $CP_l = 0,5,10,15$ Watts are considered, numbers of antennas are 10 with a bandwidth of 200 KHz, $\frac{\sigma^2}{\beta_0^0}$= -3dBm, and μ=0.5. As shown in Figure. 5.3 and concluded in Table 5.4, for the optimal tradeoff, the SE increases from 0 to 10 $[Bit\ /s/Hz]$ when CP_l wattage increased up to 15 watts but decreased the EE from 2×10^7 to 2.5×10^5 as [115] expresses this fact. The optimal points for the trade-off of SE-EE are shown in Figure 5.3 that is improved compared to [115], where the proposed model has less effect of a decline in EE at given parameters.

Table 5. 3 *Sequence of simulation.*

Proposed Algorithm	
Step 1:	Based on the Wyner model compute UL and DL sequence for the *cell l*
Step 2:	Generate random estimated channel vectors $H_l^l \in \mathbb{C}$ for UL and DL
Step 3:	Compute SE-EE relation for the selection of multiple M as Eq. (5.17-5.19)
Step 4	Compute SE-EE relation for the selection of multiple UEs as Eq. (5.22-5.24)
Step 5:	Compute receive combining vectors for UL as in Table. 5.3.
Step 6:	Compute DL sequence for precoding for DL as in Table. 5.3.
Step 7:	Compute power consumption-based combing and precoding vectors as Eq. (5.25-5.28)
Step 8:	Plot of Figures SE-EE tradeoff with logarithm-based function approximation; Throughput-EE tradeoff for considering power consumption model, combining, and precoding schemes.

Table 5. 4 *Simulation parameters and results for the selection of multiple antennas and M is fixed.*

Parameters	$\boldsymbol{CP_l = 0\ W}$	$\boldsymbol{CP_l = 5\ W}$	$\boldsymbol{CP_l = 10\ W}$	$\boldsymbol{CP_l = 15\ W}$
M	10	10	10	10
B [KHZ]	200	200	200	200
$\boldsymbol{\frac{\sigma^2}{\beta_0^0}}$	-3dBm	-3dBm	-3dBm	-3dBm
$\boldsymbol{\mu}$	0.5	0.5	0.5	0.5
SE [$\boldsymbol{Bit/s/Hz}$]	0	5	8	10
EE [$\boldsymbol{bit/joule}$]	2×10^7	2×10^6	3×10^5	2.5×10^5

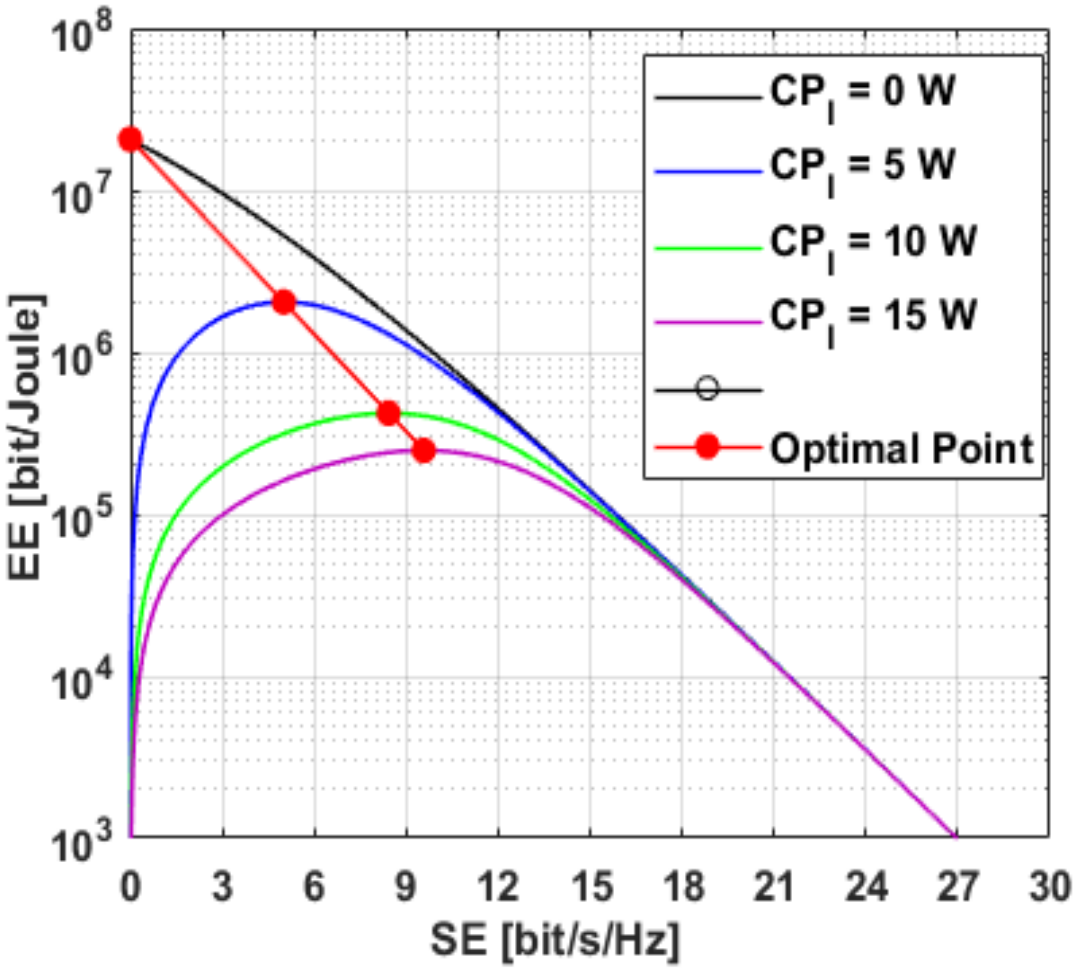

Figure 5. 3 *Illustration of EE-SE tradeoff for different CP_l in case of multiple antenna selections.*

As computed in Equations (5.18 and 5.19), the CP_l +ETP are fixed as $15\ w\ and\ 2\ watt\ with$ Multiple M for optimizing the tradeoff of SE-EE illustrated in Figure. 5.4. The x-axis represents the SE in $Bit\ /s/Hz$, and the y-axis represents the EE in $bit/joule$. The results of Figure 5.4 are elaborated in Table. 5.6 where $M = 5, 20, 100, 1000$ are considered with a bandwidth of 200 KHz, $\frac{\sigma^2}{\beta_0^0}$= -3dBm, and μ=0.5.

As shown in Figure. 5.4 and concluded in Table 5.5, for the optimal trade-off the SE increases from 2 to 10.5 $[Bit\ /s/Hz]$ with several multiple antennas and $CP_l + ETP$ wattages are fixed while it decreases the EE from 2×10^5 to 1.8×10^4. The optimal points for the tradeoff of SE-EE are shown in Figure. 5.4 that is improved as compared to [23].

Table 5. 5 *Simulation parameters and results for the selection of multiple antennas and CP is fixed.*

Parameters	**M = 5**	**M = 20**	**M = 100**	**M = 1000**
$\mathbf{CP_l}[Watt]$	15	15	15	15
$\boldsymbol{ETP}\ [\boldsymbol{Watt}]$	2	2	2	2
B [KHZ]	200	200	200	200
$\boldsymbol{\sigma^2}$	-3dBm	-3dBm	-3dBm	-3dBm
$\overline{\boldsymbol{\beta_0^0}}$				
$\boldsymbol{\mu}$	0.5	0.5	0.5	0.5
SE $[\boldsymbol{Bit\ /s/Hz}]$	2	4	7	10.5
EE $[\boldsymbol{bit/joule}]$	2×10^5	2.5×10^5	9×10^4	1.8×10^4

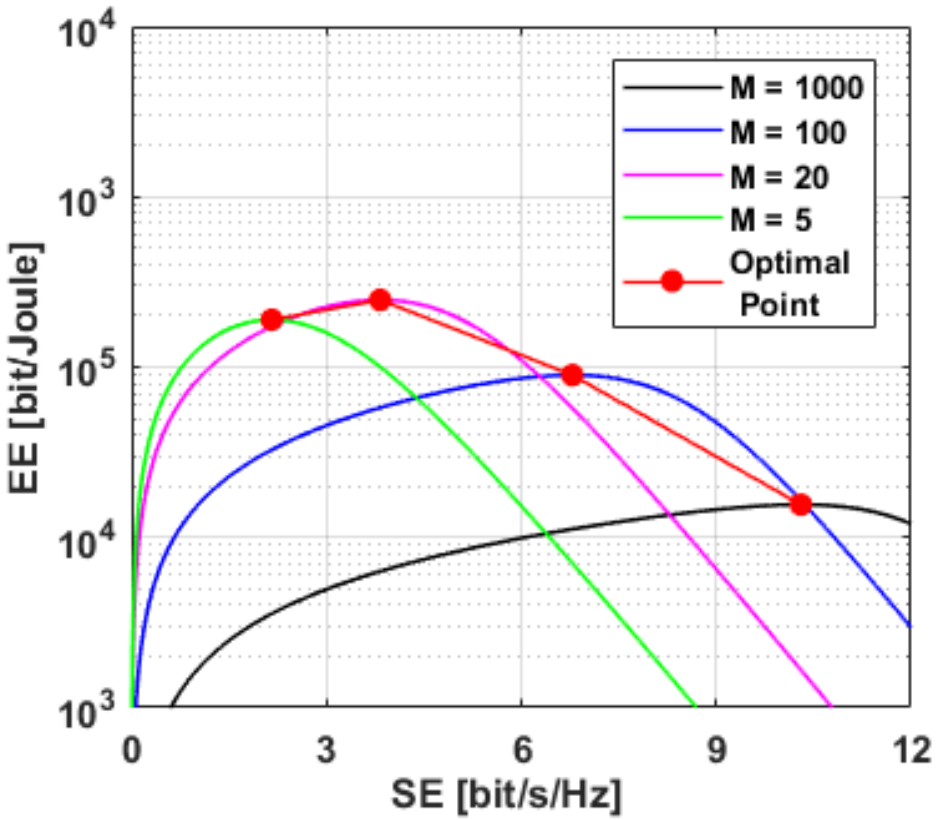

Figure 5. 4 *Illustration of EE-SE tradeoff for different M in case of multiple antenna selections.*

As computed in Equations (5.23 and 5.24), different M/K ratio is taken into account for optimizing the tradeoff of SE-EE illustrated in Figure 5.5. The x-axis represents the SE in $Bit\ /s/Hz$ and the y-axis represents the EE in $bit/joule$. The results of Figure. 5.5 are elaborated in Table. 4.7 where $M/k = 2, 4, 8, 16$ are considered with the same

bandwidth, $\frac{\sigma^2}{\beta_0^0}$, and μ used in multiple antenna selections. As shown in Figure 5.5 and concluded in Table 5.6, for the optimal tradeoff, the SE increases from 14 to 48 $[Bit\ /s/Hz]$ as it increases with several multiple antennas while the notable parameter is that there is not much decrement in EE as it only decreases $3 \times 10^5\ to\ 4 \times 10^5$. The optimal points for the tradeoff of SE-EE are shown in Figure. 5.5 that are improved as compared to [23].

Table 5. 6 *Simulation parameters and results for the selection of multiple UEs and CP is fixed.*

Parameters	$\frac{\mathbf{M}}{\mathbf{K}} = \mathbf{2}$	$\frac{\mathbf{M}}{\mathbf{K}} = \mathbf{4}$	$\frac{\mathbf{M}}{\mathbf{K}} = \mathbf{8}$	$\frac{\mathbf{M}}{\mathbf{K}} = \mathbf{16}$
$\mathbf{CP_l}[Watt]$	15	15	15	15
K	20	20	20	20
M	40	80	160	320
$\boldsymbol{ETP}\ [Watt]$	2	2	2	2
B [KHZ]	200	200	200	200
$\boldsymbol{\sigma^2}$	-3dBm	-3dBm	-3dBm	-3dBm
$\boldsymbol{\frac{\sigma^2}{\beta_0^0}}$				
μ	0.5	0.5	0.5	0.5
SE $[Bit\ /s/Hz]$	14	23	30	48
EE $[bit/joule]$	3×10^5	4×10^5	4×10^5	3×10^5

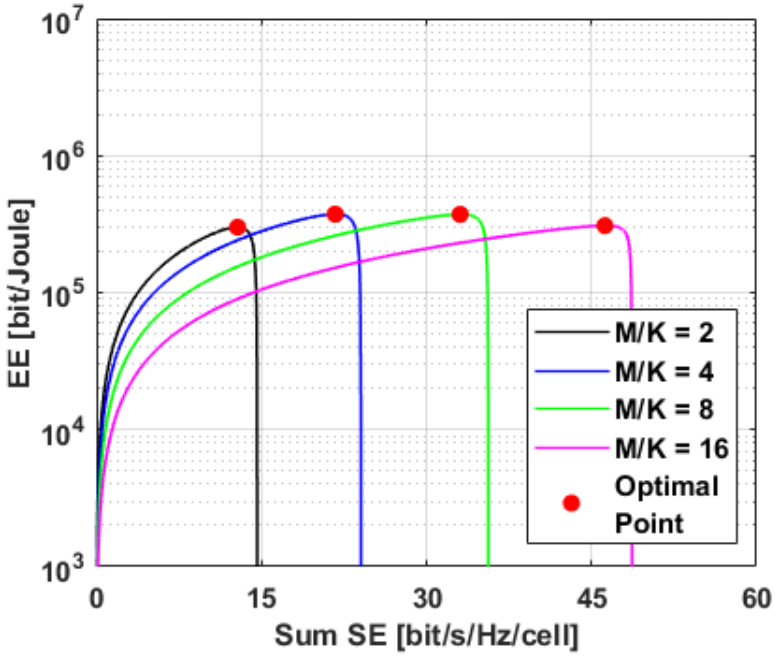

Figure 5. 5 *Illustration of EE-SE tradeoff for different M/K in case of multiple UEs selection.*

5.5.2 Energy Efficiency and Throughput Tradeoff

The tradeoff between EE and throughput is slightly different. It caters to all power consumption models with different combining and precoding schemes for UL and DL separately, as shown in Table 5.2. The final expression is given in Equation (5.29), and two setting values are considered for the optimal tradeoff of EE-Throughput. Multiple antennas are taken into account for finding the total power consumption of all models computed in the next section, and the results are shown in Figure. 5.6. The x-axis represents the varying numbers of antennas, and the y-axis represents the TTP in dBm. The optimal tradeoff needs total transmit power for all combing and precoding vectors such as 41.8, 41.2, 40.9, 40.9, and 40.9 dBm for M-MMSE, S-MMSE, RZF, ZF, and MR, respectively, for the setting value-I as shown in Figure 5.6. The figure also expresses that the dBm for the multiple M does reduce to 39.5, 39.45, 39.40, 39.40, and 39.40 for ZF, RZF, M-MMSE, S-MMSE, and MR respectively after setting the power consumption values to half as setting value-II taken in Table 5.7.

The optimized results of the tradeoff between EE and through results are shown in Table. 5.9 after considering all power consumption models with different combining and precoding schemes for UL and DL separately. The final expression is given in. (5.29), and two setting values are considered for the optimal tradeoff of EE-Throughput. The x-axis represents the throughput values in $Mbit/s/km^2$ and the y-axis represents the EE in $Mbit/Joule/cell$. The power consumption model values in setting value-II are half of the setting value-I, as shown in Table. 5.8 ultimately, the EE is almost doubled as 27 is 52, 26 is 47, 24.5 is 43, 23.5 is 42, and 15 is 23 for M-MMSE, S-MMSE, RZF, ZF, and MR, respectively. The values as mentioned earlier of EE are optimized value at throughput ($Mbit/s/km^2$) of 890, 880, 850, 845, and 450 for different schemes. The proposed model indicates that reducing the total power consumption increases the EE but does not affect the throughput as [27] does.

Table 5. 7 *Simulation parameters for the selecting multiple CP models of different setting values.*

Parameters	**Setting Value-I**	**Setting Value-II**
Fix Power	$8\ W$	$0.4\ W$
Power consumed by each BS	$0.3\ W$	$0.15\ W$
Power consumed by each UE	$0.1\ W$	$0.05\ W$
ETP	$0.4\ W$	$0.04\ W$
Power consumed for encoding	$0.09\ W/(Gbit/S)$	$0.009\ W/(Gbit/S)$
Power consumed for decoding	$0.8\ W/(Gbit/S)$	$0.08\ W/(Gbit/S)$

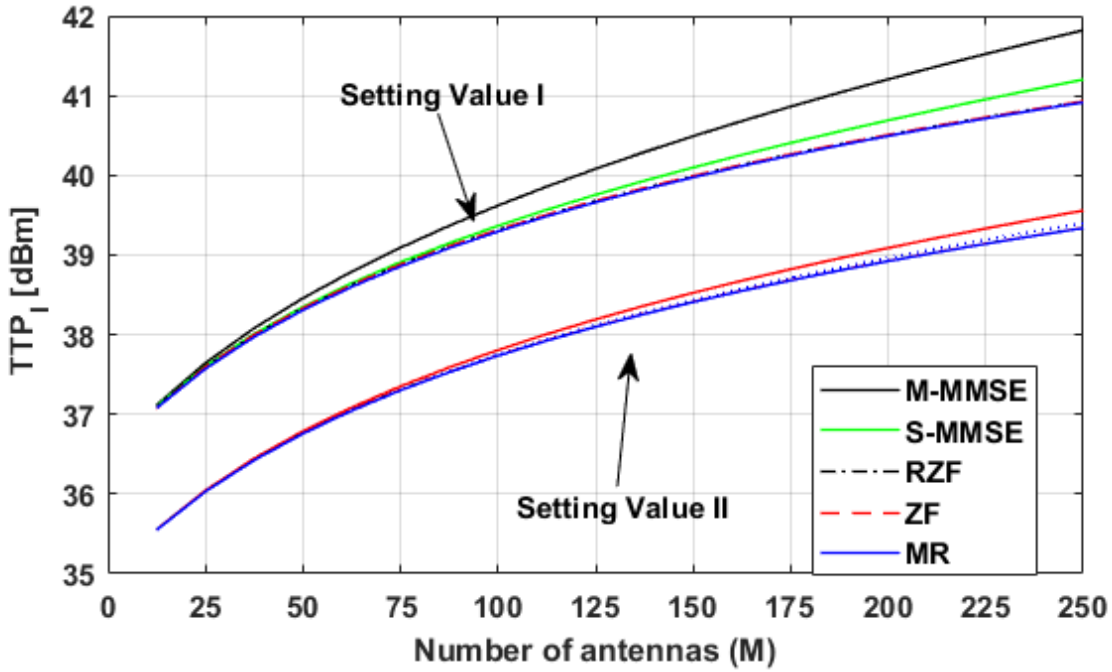

Figure 5. 6 *Results of multiple CP models of different setting values.*

Table 5. 8 *Simulation parameters for the selection of multiple CP models of different setting values.*

Scheme	**EE for Setting Value-I** $Mbit/Joule/cell$	**EE for Setting Value-I** $Mbit/Joule/cell$	**Area Throughput** $Mbit/s/km^2$
M − MMSE	27	52	890
S − MMSE	26	47	880
RZF	24.5	43	850
ZF	23.5	42	845
MR	15	23	450

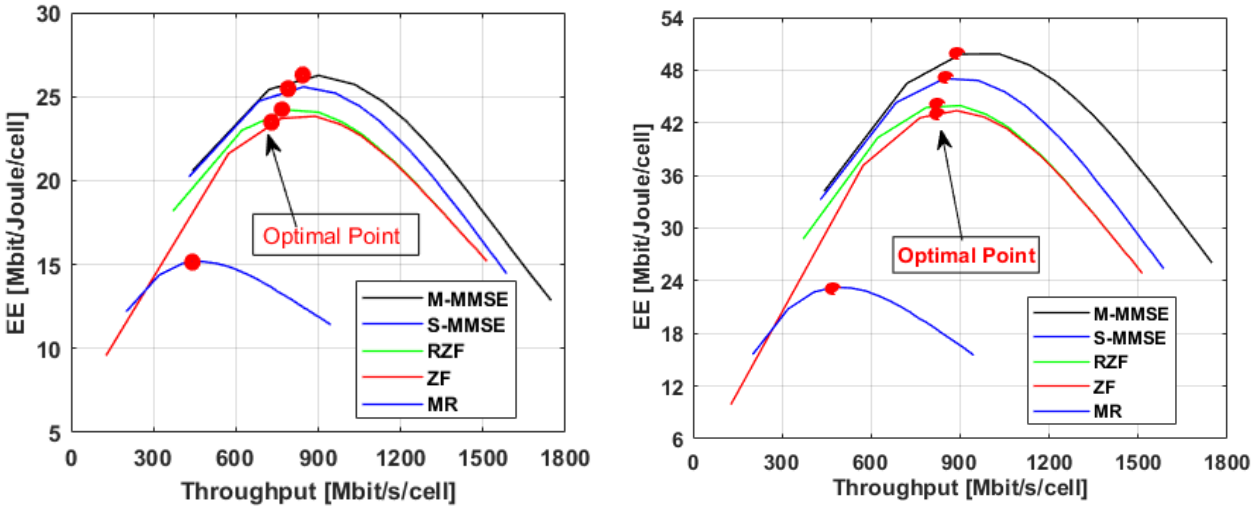

***Figure 5.** 7 Illustration of throughput-EE trade-off, (a) for the setting value-I and (b) for the setting value-II.*

5.6 Summary

In this chapter, the tradeoff of EE with SE and throughput are optimized in the proposed massive MIMO system. The UL and DL systems are modelled with the Wyner model. In the first step, two cell scenarios are considered and computed the expressions for UL. DL transmission based on the Wyner model then recommended an optimized model for both tradeoffs. The optimized parameters are calculated for selecting multiple antennas and the selection of multiple users as these effects enhance the SE and reduce the EE. This model validates the optimized relation of SE-EE with logarithm function-based approximation and revealed remarkable implications in results. Finally, the circuit power consumption model is modelled for evaluating the tradeoff between EE and throughput. In contrast, the transmit power, circuit power consumed by hardware at the BS side, coding/decoding power, and digital signal processing power are considered.

CHAPTER 6
CONCLUSIONS AND FUTURE RECOMMENDATIONS

The author explored massive MIMO systems to obtain optimal EE and area throughput in the first half of this research. The simulation results have significant ramifications. The study was based on uncorrelated fading, which allows each user to have their channel covariance matrix. Monte Carlo simulations produce the MMSE and MRT/MRC results. Although the MMSE delivers the best throughput gain, and ZF processing provides a more considerable efficiency gain. The performance of ZF pre-coding (with poor CSI) is comparable to that of MMSE and ZF (with perfect CSI). The findings with MRT/MRC are not particularly impressive, but it operates at a high IUI, which explains why the rate/UE is lower. For the same values of M and N, the signal processing complexity in this scheme is also lower than in the other methods; however, the power savings are insufficient to compensate for the poor data rates. To achieve the same rates as ZF, the MRT/MRC requires a system with M values substantially bigger than N (M>>N). It will, on the other hand, significantly increase the circuit power dissipation. It is expected that circuit consumption will decrease over time, indicating that better EE can be obtained by using fewer UEs, fewer BS antennas, lower power, and progressive processing techniques. The results of this study show that a massive MIMO system can be developed using low power transceiver (consumer-grade) gear at the coverage layer. The reduction in power dissipation improves results, and it is possible by shortening the circuit. The findings of power usage are shown in Figure 3.4. Reducing the cell radius minimizes the system's network capacity while increasing the EE.

As the 2nd part of this research, the optimal SE is augmented per cell in the proposed massive MIMO system and computed MMSE channel estimation with different combining and precoding schemes. The study originated from MMSE channel estimation after examining EW-MMSE and LS estimators, where MMSE found the more complex but exceptionally improved estimator to enhance the SE per cell. Monte Carlo simulations produce the results of MMSE combining and precoding schemes in MATLAB. Although the MMSE was the optimum channel estimator among all, it was

also observed that MR was less complex. In this regard, the complex computations of MMSE are considered because the variance in results is relatively small and improvement in SE is big. M-MMSE, S-MMSE, RZF, ZF, MR combing, and precoding schemes for UL and DL are tested with the proposed numerical expressions by taking the same vectors where M-MMSE has found the best option to deal with SE. The results with MR precoding are not much good, but it can operate under intercell interference with less complexity in the computation of channel estimation. The findings of this work specify that the massive MIMO system can develop by optimize channel estimation for the augmentation of SE in UL and DL transmissions. Conclusively, it can summarize that some complex computations of MMSE channel estimators can enhance the average sum of SE per cell as results verified in this model.

As the 3rd part of this study, the trade-off between EE and SE and throughput is optimized in the proposed massive MIMO system and modelled the UL and DL systems using the Wyner model. The two cell scenarios are adopted and calculated for uplink and downlink transmission based on the Wyner model in the first step. An optimization model is proposed for these two for both tradeoffs. The optimized parameters for selecting multiple antennas and selecting multiple users are calculated because these terms enhance SE and lower EE. The model verifies the optimization relationship of SE-EE through the approximation based on logarithmic function and finds significant enlightenment to the results. The circuit power consumption is modelled to evaluate the trade-off between EE and throughput while considering transmit power, circuit power consumed by the BS side hardware, encoding/decoding power, and digital signal processing power. In this regard, the UL and DL models for different combining and precoding schemes are used to formulate expressions for the BS in the massive MIMO network and calculate the total power consumption. The M antennas and K UEs are taken to calculate the throughput of M-MMSE, S-MMSE, RZF, ZF, MR combining, and precoding schemes. The EE throughput trade-off result of the power consumption model through the combining and precoding scheme is optimized.

Moreover, it also has received the ability to fix the throughput by reducing power consumption. The optimized trade-off results are verified in the proposed model. The findings of this work assume that by optimizing EE to enhance SE and throughput in UL and DL transmissions, massive MIMO systems can be developed. It finally

improves the EE. The choice of antenna and UE is optimized by evaluating actual power consumption.

The future work of energy-efficient MIMO systems are listed below:

- The uplink and downlink are considered both while hardware and singular processing could be included to optimize the energy efficiency of massive MIMO systems in the future.
- However, the optimized selection of multiple antennas and UEs are studied. These studies focus on energy and spectral efficiency enhancement over 6G Hz frequencies as future aspects.
- We can summarize that some complex computations of MMSE channel estimators can enhance the average sum of SE per cell, as verified in our model.
- To increase the performance of SE, the joint optimal analysis of BS antennas, resolution of ADC, and oversampling parameters with one or more than one receiver can also be an excellent future research topic.
- The complexity analysis of non-linear precoders such as Tomlinson-Harashima Precoder (THP) should also be studied in future.
- The pilot contamination is considered a significant drawback that affects the massive MIMO system's efficiency. The efficiency and performance deprivation is caused by cells interference during channel estimation. This interference is difficult to detect and solve. To mitigate these problems, analysis on cell size, selection of proper frequency reuse parameters and receiver's parameters is still an open topic for future study.
- However, massive MIMO encourages ultra-high frequency, so improving EE and SE still opens areas for further research.

REFERENCES

[1] E. G. Larsson, 'Massive MIMO for 5G: Overview and the road ahead', in *2017 51st Annual Conference on Information Sciences and Systems (CISS)*, 2017, p. 1, doi: 10.1109/CISS.2017.7926182.

[2] P. K. Choudhury and M. A. El-Nasr, 'Massive MIMO toward 5G', *Journal of Electromagnetic Waves and Applications*, vol. 34, no. 9, pp. 1091–1094, 2020, doi: 10.1080/09205071.2020.1783825.

[3] R. Chataut and R. Akl, 'Massive MIMO Systems for 5G and beyond Networks—Overview, Recent Trends, Challenges, and Future Research Direction', *Sensors*, vol. 20, no. 10, 2020, doi: 10.3390/s20102753.

[4] G. Wu, C. Yang, S. Li, and G. Y. Li, 'Recent advances in energy-efficient networks and their application in 5G systems', *IEEE Wireless Communications*, vol. 22, no. 2, pp. 145–151, 2015, doi: 10.1109/MWC.2015.7096297.

[5] M. Arisaka and S. Sugiura, 'Energy-Versus-Bandwidth-Efficiency Tradeoff in Spatially Modulated Massive MIMO DL', *IEEE Wireless Communications Letters*, vol. 8, no. 1, pp. 197–200, 2019, doi: 10.1109/LWC.2018.2866470.

[6] L. Zhao, K. Li, K. Zheng, and M. Omair Ahmad, 'An Analysis of the Tradeoff Between the Energy and Spectrum Efficiencies in an UL Massive MIMO-OFDM System', *IEEE Transactions on Circuits and Systems II: Express Briefs*, vol. 62, no. 3, pp. 291–295, 2015, doi: 10.1109/TCSII.2014.2368351.

[7] J. Li *et al.*, 'Measurement-Based Characterizations of Indoor Massive MIMO Channels at 2 GHz, 4 GHz, and 6 GHz Frequency Bands', in *2016 IEEE 83rd Vehicular Technology Conference (VTC Spring)*, 2016, pp. 1–5, doi: 10.1109/VTCSpring.2016.7504341.

[8] J. Zhang, E. Björnson, M. Matthaiou, D. W. K. Ng, H. Yang, and D. J. Love, 'Guest Editorial Special Issue on Multiple Antenna Technologies for B5G-Part II', *IEEE Journal on Selected Areas in Communications*, vol. 38, no. 9, pp. 1941–1944, 2020, doi: 10.1109/JSAC.2020.3000890.

[9] D. Tsilimantos, J.-M. Gorce, K. Jaffrès-Runser, and H. Vincent Poor, 'Spectral and EE Trade-offs in Cellular Networks', *IEEE Transactions on Wireless Communications*, vol.

15, no. 1, pp. 54–66, 2016, doi: 10.1109/TWC.2015.2466541.

[10] K. N. R. S. V. Prasad, E. Hossain, and V. K. Bhargava, 'EE in Massive MIMO-Based 5G Networks: Opportunities and Challenges', *IEEE Wireless Communications*, vol. 24, no. 3, pp. 86–94, 2017, doi: 10.1109/MWC.2016.1500374WC.

[11] A. Zappone, E. Björnson, L. Sanguinetti, and E. Jorswieck, 'Globally Optimal Energy-Efficient Power Control and Receiver Design in Wireless Networks', *IEEE Transactions on Signal Processing*, vol. 65, no. 11, pp. 2844–2859, 2017, doi: 10.1109/TSP.2017.2673813.

[12] T. Liu, 'Energy-Efficient Massive MIMO Systems for 5G Wireless Communication', 2019.

[13] T. L. Marzetta, 'Noncooperative Cellular Wireless with Unlimited Numbers of BS Antennas', *IEEE Transactions on Wireless Communications*, vol. 9, no. 11, pp. 3590–3600, 2010, doi: 10.1109/TWC.2010.092810.091092.

[14] A. Goldsmith, S. A. Jafar, N. Jindal, and S. Vishwanath, 'Capacity limits of MIMO channels', *IEEE Journal on Selected Areas in Communications*, vol. 21, no. 5, pp. 684–702, 2003, doi: 10.1109/JSAC.2003.810294.

[15] G. Auer, O. Blume, and V. Giannini, 'EE analysis of the reference systems, areas of improvements and target breakdown'. pp. 1–68, 2010.

[16] T. Younas, J. Li, J. Arshad, M. Mekonnen, and H. Munir, 'New Framework for analysis Of EE in massive MIMO With Hardware Impairments', 2018, pp. 1–3, doi: 10.1109/ATNAC.2018.8615215.

[17] W. Liu, S. Han, C. Yang, and C. Sun, 'Massive MIMO or small cell network: Who is more energy efficient?', in *2013 IEEE Wireless Communications and Networking Conference Workshops (WCNCW)*, 2013, pp. 24–29, doi: 10.1109/WCNCW.2013.6533309.

[18] D. Ha, K. Lee, and J. Kang, 'EE analysis with circuit power consumption in massive MIMO systems', 2013, pp. 938–942, doi: 10.1109/PIMRC.2013.6666272.

[19] G. Interdonato, E. Björnson, H. Quoc Ngo, P. Frenger, and E. G. Larsson, 'Ubiquitous cell-free Massive MIMO communications', *EURASIP Journal on Wireless*

Communications and Networking, vol. 2019, no. 1, p. 197, 2019, doi: 10.1186/s13638-019-1507-0.

[20] L. D. Nguyen, H. D. Tuan, T. Q. Duong, O. A. Dobre, and H. V. Poor, 'DL Beamforming for Energy-Efficient Heterogeneous Networks With Massive MIMO and Small Cells', *IEEE Transactions on Wireless Communications*, vol. 17, no. 5, pp. 3386–3400, 2018, doi: 10.1109/TWC.2018.2811472.

[21] A. H. Ahmed, A. Thair Al-Heety, B. Al-Khateeb, and A. H. Mohammed, 'EE in 5G Massive MIMO for Mobile Wireless Network', in *2020 International Congress on Human-Computer Interaction, Optimization and Robotic Applications (HORA)*, 2020, pp. 1–6, doi: 10.1109/HORA49412.2020.9152847.

[22] S. F. Jilani, Q. H. Abassi, and A. Alomainy, 'Millimetre-Wave MIMO Array of a Compact Grid Antenna for 5G Wireless Networks and Beyond', in *2020 International Conference on UK-China Emerging Technologies (UCET)*, 2020, pp. 1–4, doi: 10.1109/UCET51115.2020.9205326.

[23] Y. Fu *et al.*, 'End-to-End EE Evaluation for B5G Ultra Dense Networks', in *2020 IEEE 91st Vehicular Technology Conference (VTC2020-Spring)*, 2020, pp. 1–6, doi: 10.1109/VTC2020-Spring48590.2020.9129481.

[24] Y. Zhou, D. Li, H. Wang, A. Yang, and S. Guo, 'QoS-aware energy-efficient optimization for massive MIMO systems in 5G', in *2014 Sixth International Conference on Wireless Communications and Signal Processing (WCSP)*, 2014, pp. 1–5, doi: 10.1109/WCSP.2014.6992089.

[25] M. Bashar *et al.*, 'UL Spectral and EE of Cell-Free Massive MIMO With Optimal Uniform Quantization', *IEEE Transactions on Communications*, vol. 69, no. 1, pp. 223–245, 2021, doi: 10.1109/TCOMM.2020.3028305.

[26] X. Yu, J.-C. Shen, J. Zhang, and K. B. Letaief, 'Alternating Minimization Algorithms for Hybrid Precoding in Millimeter Wave MIMO Systems', *IEEE Journal of Selected Topics in Signal Processing*, vol. 10, no. 3, pp. 485–500, 2016, doi: 10.1109/JSTSP.2016.2523903.

[27] Q. Ding, Y. Deng, and X. Gao, 'Spectral and EE of Hybrid Precoding for mmWave Massive MIMO With Low-Resolution ADCs/DACs', *IEEE Access*, vol. 7, pp. 186529–186537, 2019, doi: 10.1109/ACCESS.2019.2959612.

[28] Z. Xiao, J. Zhao, T. Liu, L. Geng, F. Zhang, and J. Tong, 'On the EE of Massive MIMO Systems With Low-Resolution ADCs and Lattice Reduction Aided Detectors', *Symmetry*, vol. 12, no. 3, 2020, doi: 10.3390/sym12030406.

[29] M. Hayajneh, M. Ndong, N. A. Ali, and H. Tembine, 'Non-Asymptotic Linear Growth of EE in Distributed Autonomous D2D MIMO Wireless Communications', *IEEE Access*, vol. 8, pp. 105914–105921, 2020, doi: 10.1109/ACCESS.2020.2999021.

[30] S. E. Hajri and M. Assaad, 'An exclusion zone for massive MIMO with underlay D2D communication', in *2015 International Symposium on Wireless Communication Systems (ISWCS)*, 2015, pp. 471–475, doi: 10.1109/ISWCS.2015.7454388.

[31] F. Héliot and R. Tafazolli, 'Optimal Energy-Efficient Source and Relay Precoder Design for Two-Way MIMO-AF Relay Systems', *IEEE Transactions on Green Communications and Networking*, vol. 4, no. 3, pp. 759–773, 2020, doi: 10.1109/TGCN.2020.2984213.

[32] L. Jiang and H. Jafarkhani, 'mmWave Amplify-and-Forward MIMO Relay Networks With Hybrid Precoding/Combining Design', *IEEE Transactions on Wireless Communications*, vol. 19, no. 2, pp. 1333–1346, 2020, doi: 10.1109/TWC.2019.2953032.

[33] T. F. Wong, M. Bloch, and J. M. Shea, 'Secret Sharing over Fast-Fading MIMO Wiretap Channels', *EURASIP Journal on Wireless Communications and Networking*, vol. 2009, no. 1, p. 506973, 2009, doi: 10.1155/2009/506973.

[34] A. Zappone, P.-H. Lin, and E. A. Jorswieck, 'EE in Secure Multi-Antenna Systems', pp. 1–13, 2015, [Online]. Available: http://arxiv.org/abs/1505.02385.

[35] J. Xu, P. Zhu, J. Li, X. Wang, and X. You, 'Secrecy EE Optimization for Multi-User Distributed Massive MIMO Systems', *IEEE Transactions on Communications*, vol. 68, no. 2, pp. 915–929, 2020, doi: 10.1109/TCOMM.2019.2955488.

[36] T. Hossain, M. M. Mowla, and M. Yeakub Ali, 'EE Investigation in Massive MIMO 5G System using Nakagami-m Fading Channel', in *2019 22nd International Conference on Computer and Information Technology (ICCIT)*, 2019, pp. 1–5, doi: 10.1109/ICCIT48885.2019.9038180.

[37] A. T. Abebe and C. G. Kang, 'MIMO-Based Reliable Grant-Free Massive Access With

QoS Differentiation for 5G and Beyond', *IEEE Journal on Selected Areas in Communications*, vol. 39, no. 3, pp. 773–787, 2021, doi: 10.1109/JSAC.2020.3018963.

[38] M. Matalatala, M. Deruyck, E. Tanghe, L. Martens, and W. Joseph, 'Optimal Low-Power Design of a Multicell Multiuser Massive MIMO System at 3.7 GHz for 5G Wireless Networks', *Wireless Communications and Mobile Computing*, vol. 2018, p. 9796784, 2018, doi: 10.1155/2018/9796784.

[39] F. Riera-Palou and G. Femenias, 'Decentralization Issues in Cell-free Massive MIMO Networks with Zero-Forcing Precoding'. 2019.

[40] M. Chiang, 'GP for Communication Systems', *Foundations and Trends® in Communications and Information Theory*, vol. 2, no. 1–2, pp. 1–154, 2005, doi: 10.1561/0100000005.

[41] A. Liu, X. Chen, W. Yu, V. K. N. Lau, and M.-J. Zhao, 'Two-Timescale Hybrid Compression and Forward for Massive MIMO Aided C-RAN', *IEEE Transactions on Signal Processing*, vol. 67, no. 9, pp. 2484–2498, 2019, doi: 10.1109/TSP.2019.2905813.

[42] S. Park, H. Lee, C.-B. Chae, and S. Bahk, 'Massive MIMO operation in partially centralized cloud RANs', *Computer Networks*, vol. 115, pp. 54–64, 2017, doi: https://doi.org/10.1016/j.comnet.2017.01.013.

[43] A. Salh, N. S. M. Shah, L. Audah, Q. Abdullah, W. A. Jabbar, and M. Mohamad, 'Energy-Efficient Power Allocation and Joint User Association in Multiuser-DL Massive MIMO System', *IEEE Access*, vol. 8, pp. 1314–1326, 2020, doi: 10.1109/ACCESS.2019.2958640.

[44] M. R. Sadeghifar, H. Bengtsson, and J. J. Wikner, 'A voltage-mode RF DAC for massive MIMO system-on-chip digital transmitters', *Analog Integrated Circuits and Signal Processing*, vol. 100, no. 3, pp. 683–692, 2019, doi: 10.1007/s10470-019-01497-9.

[45] F. Tan, H. Chen, F. Zhao, and X. Li, 'Energy-efficient power allocation for massive MIMO-enabled multi-way AF relay networks with channel aging', *EURASIP Journal on Wireless Communications and Networking*, vol. 2018, no. 1, p. 206, 2018, doi: 10.1186/s13638-018-1222-2.

[46] M. Sarajlić, L. Liu, and O. Edfors, 'When Are Low Resolution ADCs Energy Efficient in Massive MIMO?', *IEEE Access*, vol. 5, pp. 14837–14853, 2017, doi: 10.1109/ACCESS.2017.2731420.

[47] J. Choi, 'On throughput improvement using immediate re-transmission in grant-free random access with massive mimo', *IEEE Transactions on Wireless Communications*, vol. 19, no. 12, pp. 8341–8350, 2020, doi: 10.1109/TWC.2020.3021622.

[48] C. Mollén, J. Choi, E. G. Larsson, and R. W. Heath, 'Achievable UL rates for massive MIMO with coarse quantization', *ICASSP, IEEE International Conference on Acoustics, Speech and Signal Processing - Proceedings*, no. May, pp. 6488–6492, 2017, doi: 10.1109/ICASSP.2017.7953406.

[49] S. Boovarahan and K. Umapathy, 'Power Allocation Based on CSI in Massive MIMO System', *IOP Conference Series: Materials Science and Engineering*, vol. 925, no. 1, 2020, doi: 10.1088/1757-899X/925/1/012002.

[50] A. L. Imoize, A. E. Ibhaze, A. A. Atayero, and K. V. N. Kavitha, 'Standard Propagation Channel Models for MIMO Communication Systems', *Wireless Communications and Mobile Computing*, vol. 2021, p. 8838792, 2021, doi: 10.1155/2021/8838792.

[51] J. Bai and A. Sabharwal, 'Vector bin-and-cancel for MIMO distributed full-duplex', *EURASIP Journal on Wireless Communications and Networking*, vol. 2017, no. 1, p. 136, 2017, doi: 10.1186/s13638-017-0919-y.

[52] R. Dilli, 'Performance analysis of multi user massive MIMO hybrid beamforming systems at millimeter wave frequency bands', *Wireless Networks*, vol. 27, no. 3, pp. 1925–1939, 2021, doi: 10.1007/s11276-021-02546-w.

[53] K. M. Humadi, A. I. Sulyman, and A. Alsanie, 'SMConcept for Massive Multiuser MIMO Systems', *International Journal of Antennas and Propagation*, vol. 2014, p. 563273, 2014, doi: 10.1155/2014/563273.

[54] M. Alageli, A. Ikhlef, and J. Chambers, 'SWIPT Massive MIMO Systems With Active Eavesdropping', *IEEE Journal on Selected Areas in Communications*, vol. 37, no. 1, pp. 233–247, 2019, doi: 10.1109/JSAC.2018.2872370.

[55] D. Park, 'Sum rate maximisation with transmit antenna selection in massive MIMO broadcast channels', *Electronics Letters*, vol. 54, no. 21, pp. 1245–1247, 2018, doi:

https://doi.org/10.1049/el.2018.5823.

[56] J. Beiranvand and H. Meghdadi, ‘Analytical Performance Evaluation of MRC Receivers in Massive MIMO Systems’, *IEEE Access*, vol. 6, pp. 53226–53234, 2018, doi: 10.1109/ACCESS.2018.2866795.

[57] Y. Zhang, M. Zhou, X. Qiao, H. Cao, and L. Yang, ‘On the Performance of Cell-Free Massive MIMO With Low-Resolution ADCs’, *IEEE Access*, vol. 7, pp. 117968–117977, 2019, doi: 10.1109/ACCESS.2019.2937094.

[58] Q. Ding and Y. Jing, ‘Receiver EE and Resolution Profile Design for Massive MIMO UL With Mixed ADC’, *IEEE Transactions on Vehicular Technology*, vol. 67, no. 2, pp. 1840–1844, 2018, doi: 10.1109/TVT.2017.2763825.

[59] S. Wang, Y. Li, M. Zhao, and J. Wang, ‘Energy-Efficient and Low-Complexity UL Transceiver for Massive SMMIMO’, *IEEE Transactions on Vehicular Technology*, vol. 64, no. 10, pp. 4617–4632, 2015, doi: 10.1109/TVT.2014.2373364.

[60] Q. Bai and J. A. Nossek, ‘EE maximization for 5G multi-antenna receivers’, *Transactions on Emerging Telecommunications Technologies*, vol. 26, no. 1, pp. 3–14, 2015.

[61] N. Liang and W. Zhang, ‘A mixed-ADC receiver architecture for massive MIMO systems’, in *2015 IEEE Information Theory Workshop - Fall (ITW)*, 2015, pp. 229–233, doi: 10.1109/ITWF.2015.7360769.

[62] T. V. K. Chaitanya and T. Le-Ngoc, ‘Energy-Efficient Adaptive Power Allocation for Incremental MIMO Systems’, *IEEE Transactions on Vehicular Technology*, vol. 65, no. 4, pp. 2820–2827, 2016, doi: 10.1109/TVT.2015.2417500.

[63] T. Chien, E. Björnson, and E. Larsson, ‘Joint Power Allocation and Load Balancing Optimization for Energy-Efficient Cell-Free Massive MIMO Networks’, *IEEE Transactions on Wireless Communications*, vol. PP, p. 1, 2020, doi: 10.1109/TWC.2020.3006083.

[64] J. Chen, H. Chen, and F. Zhao, ‘Energy-Efficient Joint User Association and Power Allocation in Relay-Aided Massive MIMO Systems’, *Journal of Communications and Information Networks*, vol. 3, no. 2, pp. 58–65, 2018, doi: 10.1007/s41650-018-0015-4.

[65] A. Stavridis, S. Sinanovic, M. Di Renzo, and H. Haas, 'Energy Evaluation of SMat a Multi-Antenna BS', in *2013 IEEE 78th Vehicular Technology Conference (VTC Fall)*, 2013, pp. 1–5, doi: 10.1109/VTCFall.2013.6692187.

[66] E. Björnson, L. Sanguinetti, J. Hoydis, and M. Debbah, 'Optimal design of energy-efficient multi-user MIMO systems: Is massive MIMO the answer?', *IEEE Transactions on Wireless Communications*, vol. 14, no. 6, pp. 3059–3075, 2015, doi: 10.1109/TWC.2015.2400437.

[67] L. Fan, S. Jin, C.-K. Wen, and H. Zhang, 'UL Achievable Rate for Massive MIMO Systems With Low-Resolution ADC', *IEEE Communications Letters*, vol. 19, no. 12, pp. 2186–2189, 2015, doi: 10.1109/LCOMM.2015.2494600.

[68] Z. Liu, J. Li, and D. Sun, 'Circuit Power Consumption-Unaware EE Optimization for Massive MIMO Systems', *IEEE Wireless Communications Letters*, vol. 6, no. 3, pp. 370–373, 2017, doi: 10.1109/LWC.2017.2693373.

[69] K. ~N. ~R. Surya Vara Prasad, E. Hossain, and V. K. Bhargava, 'EE in Massive MIMO-Based 5G Networks: Opportunities and Challenges', *arXiv e-prints*, p. arXiv:1511.08689, Nov. 2015.

[70] D. C. Araújo, T. Maksymyuk, A. L. F. de Almeida, T. Maciel, J. C. M. Mota, and M. Jo, 'Massive MIMO: survey and future research topics', *IET Communications*, vol. 10, no. 15, pp. 1938–1946, 2016, doi: https://doi.org/10.1049/iet-com.2015.1091.

[71] L. Shao and Y. Zu, 'Approaches of approximating matrix inversion for zero-forcing pre-coding in DL massive MIMO systems', *Wireless Networks*, vol. 24, no. 7, pp. 2699–2704, 2018, doi: 10.1007/s11276-017-1496-z.

[72] X. Gao, O. Edfors, F. Rusek, and F. Tufvesson, 'Linear Pre-Coding Performance in Measured Very-Large MIMO Channels', in *2011 IEEE Vehicular Technology Conference (VTC Fall)*, 2011, pp. 1–5, doi: 10.1109/VETECF.2011.6093291.

[73] H. Wang, G. Li, G. Wang, J. Peng, H. Jiang, and Y. Liu, 'Deep learning based ensemble approach for probabilistic wind power forecasting', *Applied Energy*, vol. 188, pp. 56–70, 2017, doi: https://doi.org/10.1016/j.apenergy.2016.11.111.

[74] P. Zhang, L. Gan, C. Ling, and S. Sun, 'Atomic Norm Denoising-Based Joint Channel Estimation and Faulty Antenna Detection for Massive MIMO', *IEEE Transactions on*

Vehicular Technology, vol. 67, no. 2, pp. 1389–1403, 2018, doi: 10.1109/TVT.2017.2758024.

[75] Y. Man, Z. Li, F. Yan, S. Xing, and L. Shen, 'Massive MIMO pre-coding algorithm based on truncated Kapteyn series expansion', in *2016 IEEE International Conference on Communication Systems (ICCS)*, 2016, pp. 1–5, doi: 10.1109/ICCS.2016.7833644.

[76] N. Fatema, G. Hua, Y. Xiang, D. Peng, and I. Natgunanathan, 'Massive MIMO linear precoding: A survey', *IEEE systems journal*, vol. 12, no. 4, pp. 3920–3931, 2017.

[77] C. Zhang, Y. Jing, Y. Huang, and L. Yang, 'Performance analysis for massive MIMO DL with low complexity approximate zero-forcing precoding', *IEEE Transactions on Communications*, vol. 66, no. 9, pp. 3848–3864, 2018.

[78] M. Zhuang, 'Effects of Erroneous CSI on the Performance of Multiple-Transmit Antenna Selection', *International Journal of Antennas and Propagation*, vol. 2015, p. 281386, 2015, doi: 10.1155/2015/281386.

[79] N. Liang, W. Zhang, and C. Shen, 'An UL interference analysis for massive MIMO systems with MRC and ZF receivers', in *2015 IEEE Wireless Communications and Networking Conference (WCNC)*, 2015, pp. 310–315.

[80] S. Malik *et al.*, 'Design and Analysis of Novel Precoding Scheme for LSAS Using Power Allocation', *Wireless Personal Communications*, vol. 91, no. 2, pp. 811–828, 2016, doi: 10.1007/s11277-016-3498-z.

[81] X. Sun, K. Xu, W. Ma, Y. Xu, X. Xia, and D. Zhang, 'Multi-Pair Two-Way Massive MIMO AF Full-Duplex Relaying With Imperfect CSI Over Ricean Fading Channels', *IEEE Access*, vol. 4, pp. 4933–4945, 2016, doi: 10.1109/ACCESS.2016.2595590.

[82] T.-W. Chiang and J.-H. Lee, 'Lower Bound for Finite-SNR DMT With Position Estimation Errors in MIMO Channels', *IEEE Communications Letters*, vol. 20, no. 8, pp. 1691–1694, 2016, doi: 10.1109/LCOMM.2016.2578926.

[83] J. Zhang, Y. Zhu, S. Ma, X. Li, and K.-K. Wong, 'Large System Analysis of DL MISO-NOMA System via Regularized Zero-Forcing Precoding With Imperfect CSIT', *IEEE Communications Letters*, vol. 24, no. 11, pp. 2454–2458, 2020, doi: 10.1109/LCOMM.2020.3010422.

[84] F. Rusek *et al.*, 'Scaling Up MIMO: Opportunities and Challenges with Very Large Arrays', *IEEE Signal Processing Magazine*, vol. 30, no. 1, pp. 40–60, 2013, doi: 10.1109/MSP.2011.2178495.

[85] T. Van Chien, E. Björnson, and E. G. Larsson, 'Joint Power Allocation and User Association Optimization for Massive MIMO Systems', *IEEE Transactions on Wireless Communications*, vol. 15, no. 9, pp. 6384–6399, 2016, doi: 10.1109/TWC.2016.2583436.

[86] H. Q. Ngo, E. G. Larsson, and T. L. Marzetta, 'Energy and SE of very large multiuser MIMO systems', *IEEE Transactions on Communications*, vol. 61, no. 4, pp. 1436–1449, 2013, doi: 10.1109/TCOMM.2013.020413.110848.

[87] G. Miao, 'Energy-Efficient UL Multi-User MIMO', *IEEE Transactions on Wireless Communications*, vol. 12, no. 5, pp. 2302–2313, 2013, doi: 10.1109/TWC.2013.040213.120942.

[88] H. Yang and T. Marzetta, 'Total EE of cellular large scale antenna system multiple access mobile networks', 2013, pp. 27–32, doi: 10.1109/OnlineGreenCom.2013.6731024.

[89] O. Waqar and R. Adve, 'On the Throughput of Wireless Powered Communication Systems with a Multiple Antenna Bidirectional Relay', *IEEE Wireless Communications Letters*, vol. 8, no. 3, pp. 941–944, 2019, doi: 10.1109/LWC.2019.2900654.

[90] H. Khammari, I. Ahmed, G. Bhatti, and M. Alajmi, 'Spatio-Radio Resource Management and Hybrid Beamforming for Limited Feedback Massive MIMO Systems', *Electronics*, vol. 8, p. 1061, 2019, doi: 10.3390/electronics8101061.

[91] Q. Zhang, S. Jin, M. McKay, D. Morales-Jimenez, and H. Zhu, 'Power Allocation Schemes for Multicell Massive MIMO Systems', *IEEE Transactions on Wireless Communications*, vol. 14, no. 11, pp. 5941–5955, 2015, doi: 10.1109/TWC.2015.2444856.

[92] D. Zhang, K. Yu, Z. Zhou, and T. Sato, 'EE Scheme with Cellular Partition Zooming for Massive MIMO Systems', in *2015 IEEE Twelfth International Symposium on Autonomous Decentralized Systems*, 2015, pp. 266–271, doi: 10.1109/ISADS.2015.21.

[93] S. U. Pillai, T. Suel, and S. Cha, 'The Perron-Frobenius theorem: some of its

applications', *IEEE Signal Processing Magazine*, vol. 22, no. 2, pp. 62–75, 2005, doi: 10.1109/MSP.2005.1406483.

[94] H. Q. Ngo, E. G. Larsson, and T. L. Marzetta, 'Energy and SE of Very Large Multiuser MIMO Systems', *IEEE Transactions on Communications*, vol. 61, no. 4, pp. 1436–1449, 2013, doi: 10.1109/TCOMM.2013.020413.110848.

[95] R. Chataut, R. Akl, and U. K. Dey, 'LSRegressor Selection Based Detection for UL 5G Massive MIMO Systems', in *2019 IEEE 20th Wireless and Microwave Technology Conference (WAMICON)*, 2019, pp. 1–6, doi: 10.1109/WAMICON.2019.8765469.

[96] B. Kang, J.-H. Yoon, and J. Park, 'Low-Complexity Massive MIMO Detectors Based on Richardson Method', *ETRI Journal*, vol. 39, no. 3, pp. 326–335, 2017, doi: https://doi.org/10.4218/etrij.17.0116.0732.

[97] L. Fang, L. Xu, and D. D. Huang, 'Low Complexity Iterative MMSE-PIC Detection for Medium-Size Massive MIMO', *IEEE Wireless Communications Letters*, vol. 5, no. 1, pp. 108–111, 2016, doi: 10.1109/LWC.2015.2504366.

[98] E. Björnson, J. Hoydis, and L. Sanguinetti, 'Massive MIMO Has Unlimited Capacity', *IEEE Transactions on Wireless Communications*, vol. 17, no. 1, pp. 574–590, 2018, doi: 10.1109/TWC.2017.2768423.

[99] J. Singh and D. Kedia, 'Spectral Efficient Precoding Design for Multi-cell Large MU-MIMO System', *IETE Journal of Research*, vol. 0, no. 0, pp. 1–16, 2020, doi: 10.1080/03772063.2020.1791745.

[100] J. Arshad, A. Rehman, A. U. Rehman, R. Ullah, and S. O. Hwang, 'SE augmentation in UL massive mimo systems by increasing transmit power and uniform linear array gain', *Sensors (Switzerland)*, vol. 20, no. 17, pp. 1–15, 2020, doi: 10.3390/s20174982.

[101] H. Yang and T. L. Marzetta, 'Performance of Conjugate and Zero-Forcing Beamforming in Large-Scale Antenna Systems', *IEEE Journal on Selected Areas in Communications*, vol. 31, no. 2, pp. 172–179, 2013, doi: 10.1109/JSAC.2013.130206.

[102] S. Zarei, W. Gerstacker, and R. Schober, 'Low-Complexity Widely-Linear Precoding for DL Large-Scale MU-MISO Systems', *IEEE Communications Letters*, vol. 19, no. 4, pp. 665–668, 2015, doi: 10.1109/LCOMM.2015.2392751.

[103] Z. Zhang, Z. Chen, M. Shen, and B. Xia, 'Spectral and EE of Multipair Two-Way Full-Duplex Relay Systems With Massive MIMO', *IEEE Journal on Selected Areas in Communications*, vol. 34, no. 4, pp. 848–863, 2016, doi: 10.1109/JSAC.2016.2544458.

[104] H. V Nguyen *et al.*, 'On the Spectral and Energy Efficiencies of Full-Duplex Cell-Free Massive MIMO'. 2020.

[105] H. B. Almelah and K. A. Hamdi, 'SE of Distributed Large-Scale MIMO Systems With ZF Receivers', *IEEE Transactions on Vehicular Technology*, vol. 66, no. 6, pp. 4834–4844, 2017, doi: 10.1109/TVT.2016.2616173.

[106] S. Buzzi and C. D'Andrea, 'EE and Asymptotic Performance Evaluation of Beamforming Structures in Doubly Massive MIMO mmWave Systems', *IEEE Transactions on Green Communications and Networking*, vol. 2, no. 2, pp. 385–396, Jun. 2018, doi: 10.1109/tgcn.2018.2800537.

[107] O. Onireti, F. Héliot, and M. A. Imran, 'On the EE-SE trade-off in the UL of CoMP system', *IEEE Transactions on Wireless Communications*, vol. 11, no. 2, pp. 556–561, 2012, doi: 10.1109/TWC.2011.120911.111494.

[108] F. Héliot, M. A. Imran, and R. Tafazolli, 'On the EE-SE trade-off over the MIMO rayleigh fading channel', *IEEE Transactions on Communications*, vol. 60, no. 5, pp. 1345–1356, 2012, doi: 10.1109/TCOMM.2012.031712.110215.

[109] O. Onireti, F. Heliot, and M. A. Imran, 'On the EE-SE trade-off of distributed MIMO systems', *IEEE Transactions on Communications*, vol. 61, no. 9, pp. 3741–3753, 2013, doi: 10.1109/TCOMM.2013.071813.120823.

[110] O. K. Rayel, G. Brante, J. L. Rebelatto, R. D. Souza, and M. A. Imran, 'EE-SE trade-off of transmit antenna selection', *IEEE Transactions on Communications*, vol. 62, no. 12, pp. 4293–4303, 2014, doi: 10.1109/TCOMM.2014.2364040.

[111] S. Mukherjee and S. K. Mohammed, 'On the Energy-SE Trade-off of the MRC Receiver in Massive MIMO Systems with Transceiver Power Consumption', 2014, [Online]. Available: http://arxiv.org/abs/1404.3010.

[112] S. Mukherjee and S. K. Mohammed, 'Energy-SE trade-off for a massive SU-MIMO system with transceiver power consumption', *IEEE International Conference on Communications*, vol. 2015-Septe, no. June, pp. 1938–1944, 2015, doi:

10.1109/ICC.2015.7248609.

[113] N. Achir, M. Debbah, and P. Muhlethaler, 'Massive MIMO cooperative communications for wireless sensor networks: Throughput and EE analysis', *IEEE International Symposium on Personal, Indoor and Mobile Radio Communications, PIMRC*, vol. 2014-June, pp. 590–594, 2014, doi: 10.1109/PIMRC.2014.7136234.

[114] A. Salh, L. Audah, N. S. M. Shah, and S. A. Hamzah, 'Trade-Off Energy and SE in a DL Massive MIMO System', *Wireless Personal Communications*, vol. 106, no. 2, pp. 897–910, 2019, doi: 10.1007/s11277-019-06194-4.

[115] B. Jiang, B. Ren, Y. Huang, T. Chen, L. You, and W. Wang, 'EE and SE tradeoff in massive MIMO multicast transmission with statistical CSI', *Entropy*, vol. 22, no. 9, pp. 1–13, 2020, doi: 10.3390/E22091045.

[116] L. You, J. Xiong, A. Zappone, W. Wang, and X. Gao, 'SE and EE Tradeoff in Massive MIMO DL Transmission with Statistical CSIT', *IEEE Transactions on Signal Processing*, vol. 68, no. c, pp. 2645–2659, 2020, doi: 10.1109/TSP.2020.2986391.

[117] S. M. Nimmagadda, 'Optimal spectral and EE trade-off for massive MIMO technology: analysis on modified lion and grey wolf optimization', *Soft Computing*, vol. 24, no. 16, pp. 12523–12539, 2020, doi: 10.1007/s00500-020-04690-5.

[118] N. Li, Y. Gao, and K. Xu, 'On the Optimal EE and SE Trade-Off of CF Massive MIMO SWIPT System', pp. 1–10.

[119] X. Chen, 'Throughput multiplexing efficiency for mimo antenna characterization', *IEEE Antennas and Wireless Propagation Letters*, vol. 12, no. 1, pp. 1208–1211, 2013, doi: 10.1109/LAWP.2013.2282952.

[120] T. M. Nguyen and L. B. Le, 'Joint pilot assignment and resource allocation in multicell massive MIMO network: Throughput and EE maximization', *2015 IEEE Wireless Communications and Networking Conference, WCNC 2015*, no. Wcnc, pp. 393–398, 2015, doi: 10.1109/WCNC.2015.7127502.

[121] J. Arshad, J. Li, and T. Younas, 'Analysis and implementation of a LS-MIMO system with optimal power allocation', in *2017 IEEE 9th International Conference on Communication Software and Networks (ICCSN)*, 2017, pp. 223–227, doi: 10.1109/ICCSN.2017.8230110.

[122] J. Hoydis, S. ten Brink, and M. Debbah, 'Massive MIMO in the UL/DL of Cellular Networks: How Many Antennas Do We Need?', *IEEE Journal on Selected Areas in Communications*, vol. 31, no. 2, pp. 160–171, 2013, doi: 10.1109/JSAC.2013.130205.

[123] A. Kazerouni, F. J. Lopez-Martinez, and A. Goldsmith, 'Increasing capacity in massive MIMO cellular networks via small cells', in *2014 IEEE Globecom Workshops (GC Wkshps)*, 2014, pp. 358–363, doi: 10.1109/GLOCOMW.2014.7063457.

[124] J. Li, E. Bjornson, T. Svensson, T. Eriksson, and M. Debbah, 'Optimal design of energy-efficient HetNets: Joint precoding and load balancing', *IEEE International Conference on Communications*, vol. 2015-Septe, pp. 4664–4669, 2015, doi: 10.1109/ICC.2015.7249059.

[125] X. Li, E. Björnson, E. G. Larsson, S. Zhou, and J. Wang, 'Massive MIMO with multi-cell MMSE processing: exploiting all pilots for interference suppression', *Eurasip Journal on Wireless Communications and Networking*, vol. 2017, no. 1, pp. 1–15, 2017, doi: 10.1186/s13638-017-0879-2.

[126] M. M. A. Hossain, C. Cavdar, E. Bjornson, and R. Jantti, 'Energy-Efficient Load-Adaptive Massive MIMO', in *2015 IEEE Globecom Workshops (GC Wkshps)*, 2015, pp. 1–6, doi: 10.1109/GLOCOMW.2015.7414181.

[127] W. Wang, Y. Huang, L. You, J. Xiong, J. Li, and X. Gao, 'EE Optimization for Massive MIMO Non-Orthogonal Unicast and Multicast Transmission with Statistical CSI', *Electronics*, vol. 8, no. 8, 2019, doi: 10.3390/electronics8080857.

[128] O. E. F. Rusek, D. Persson, B. K. Lau, E. Larsson, T. Marzetta and and F. Tufvesson, 'Scaling up MIMO: Opportunities and challenges with very large arrays', *IEEE Signal Processing Magazine*, vol. 30, no. 1, pp. 40–60, 2013.

[129] Y. Liu, C.-X. Wang, J. Huang, J. Sun, and W. Zhang, 'Novel 3-D Nonstationary MmWave Massive MIMO Channel Models for 5G High-Speed Train Wireless Communications', *IEEE Transactions on Vehicular Technology*, vol. 68, no. 3, pp. 2077–2086, 2019, doi: 10.1109/TVT.2018.2866414.

[130] R. M. Asif, J. Arshad, M. Shakir, S. M. Noman, and A. U. Rehman, 'EE Augmentation in Massive MIMO Systems through Linear Precoding Schemes and Power Consumption Modeling', *Wireless Communications and Mobile Computing*, vol. 2020, 2020, doi: 10.1155/2020/8839088.

[131] S. K. Goudos, P. D. Diamantoulakis, and G. K. Karagiannidis, 'Multi-Objective Optimization in 5G Wireless Networks With Massive MIMO', *IEEE Communications Letters*, vol. 22, no. 11, pp. 2346–2349, 2018, doi: 10.1109/LCOMM.2018.2868663.

[132] W. Tan, W. Huang, X. Yang, Z. Shi, W. Liu, and L. Fan, 'Multiuser precoding scheme and achievable rate analysis for massive MIMO system', *EURASIP Journal on Wireless Communications and Networking*, vol. 2018, 2018, doi: 10.1186/s13638-018-1223-1.

[133] X. Li, E. Bjornson, E. G. Larsson, S. Zhou, and J. Wang, 'A Multi-Cell MMSE Detector for Massive MIMO Systems and New Large System Analysis', in *2015 IEEE Global Communications Conference (GLOBECOM)*, 2015, pp. 1–6, doi: 10.1109/GLOCOM.2015.7417112.

[134] E. G. Larsson, O. Edfors, F. Tufvesson, and T. L. Marzetta, 'Massive MIMO for next generation wireless systems', *IEEE Communications Magazine*, vol. 52, no. 2, pp. 186–195, 2014, doi: 10.1109/MCOM.2014.6736761.

[135] J. Y. Jang, W. S. Lee, J. H. Ro, Y. H. You, and H. K. Song, 'Weighted gauss-seidel precoder for DL massive mimo systems', *Computers, Materials and Continua*, vol. 67, no. 2, pp. 1729–1745, 2021, doi: 10.32604/cmc.2021.015424.

[136] S. Bashir *et al.*, 'Mimo-terahertz in 6g nano-communications: Channel modeling and analysis', *Computers, Materials and Continua*, vol. 66, no. 1, pp. 263–274, 2021, doi: 10.32604/cmc.2020.012404.

[137] A. Salh *et al.*, 'EELCA in 5G Massive MIMO Systems', *Computers, Materials and Continua*, vol. 67, no. 3, pp. 3189–3214, 2021, doi: 10.32604/cmc.2021.014746.

[138] and R. Z. L. Lu, G. Y. Li, A. L. Swindlehurst, A. Ashikhmin, 'An overview of massive MIMO: Benefits and challengesle', *IEEE Journal of Selected Topics in Signal Processing*, vol. 8, no. 5, pp. 742–758, 2014.

[139] Y. Li, C. Tao, A. Mezghani, A. L. Swindlehurst, G. Seco-Granados, and L. Liu, 'Optimal Design of Energy and SE Tradeoff in One-Bit Massive MIMO Systems', pp. 1–12, 2016, [Online]. Available: http://arxiv.org/abs/1612.03271.

[140] Y. Huang, S. He, J. Wang, and J. Zhu, 'Spectral and EE Tradeoff for Massive MIMO', *IEEE Transactions on Vehicular Technology*, vol. 67, no. 8, pp. 6991–7002, 2018, doi: 10.1109/TVT.2018.2824311.

[141] P. Chan-Yeob, H. R. Jae, J. Y. Jang, and S. Hyoung-Kyu, ‘An Enhanced Jacobi Precoder for DL Massive MIMO Systems’, *Computers, Materials and Continua*, vol. 68, no. 1, pp. 137–148, 2021, doi: 10.32604/cmc.2021.016108.

[142] J. Xu, J. Zhang, and J. G. Andrews, ‘On the accuracy of the wyner model in cellular networks’, *IEEE Transactions on Wireless Communications*, vol. 10, no. 9, pp. 3098–3109, 2011, doi: 10.1109/TWC.2011.062911.100481.